(2)

DOT/FAA/CT-90/24

FAA Technical Center
Atlantic City International Airport
N.J. 08405

A Literature Survey of Airborne Vehicles Impacting with Water and Soil: Head Injury Criteria and Severity Index Development of Computer Program KRASH

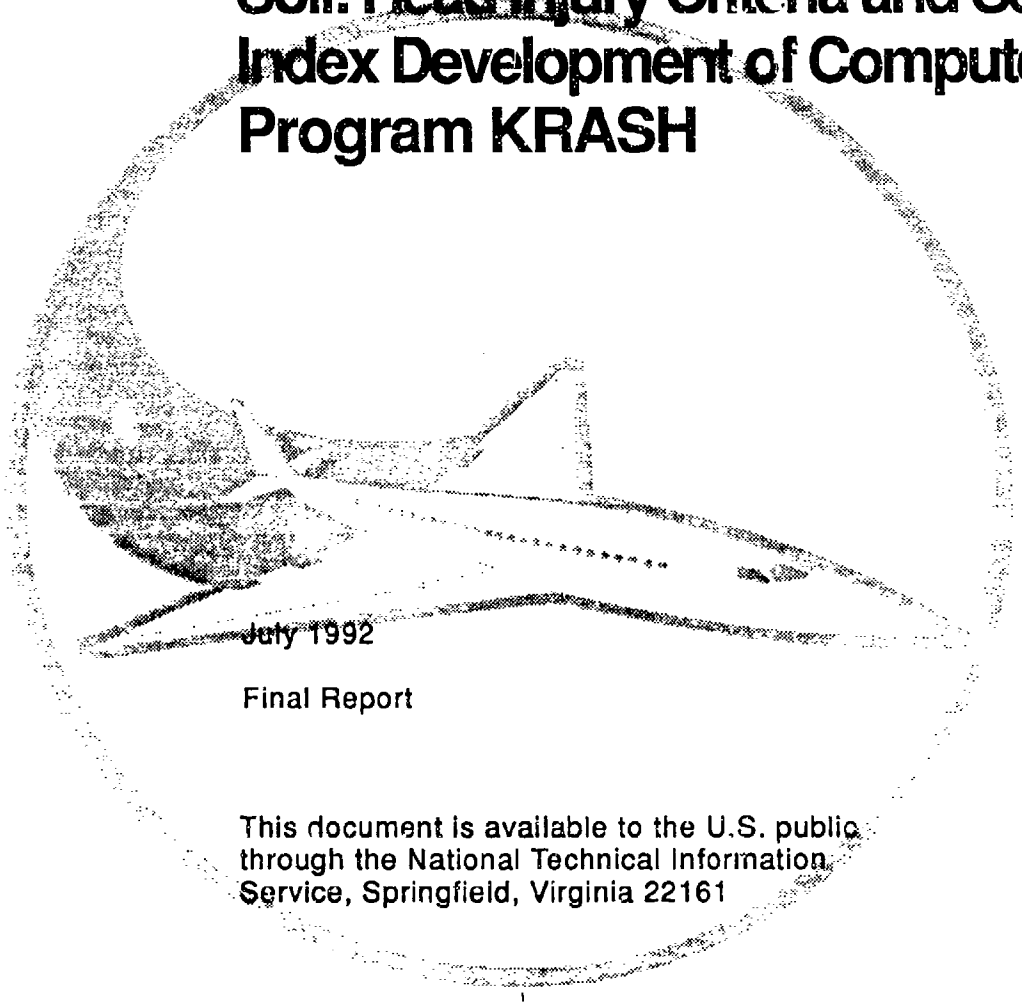

July 1992

Final Report

U.S. Department of Transportation
Federal Aviation Administration

NOTICE

This document is disseminated under the sponsorship of the U. S. Department of Transportation in the interest of information exchange. The United States Government assumes no liability for the contents or use thereof.

The United States Government does not endorse products or manufacturers. Trade or manufacturers' names appear herein solely because they are considered essential to the objective of this report.

Technical Report Documentation Page

1. Report No.	2. Government Accession No.	3. Recipient's Catalog No.
DOT/FAA/CT-90/24		

4. Title and Subtitle	5. Report Date
A LITERATURE SURVEY OF AIRBORNE VEHICLES IMPACTING WITH WATER AND SOIL; HEAD INJURY CRITERIA AND SEVERITY INDEX DEVELOPMENT OF COMPUTER PROGRAM KRASH	July 1992
	6. Performing Organization Code
	8. Performing Organization Report No.
7. Author(s) G. Wittlin, M.A. Gamon	
9. Performing Organization Name and Address Lockheed-Aeronautical Systems Company Burbank, CA 91520	10. Work Unit No. (TRAIS)
	11. Contract or Grant No. DTFA03-84-C-00004
12. Sponsoring Agency Name and Address U.S. Department of Transportation Federal Aviation Administration Technical Center Atlantic City International Airport, NJ 08405	13. Type of Report and Period Covered Final Nov. 1987 - May 1989
	14. Sponsoring Agency Code ACD-210

15. Supplementary Notes

Lawrence Neri, FAA Program Manager
Anthony Wilson, FAA Project Manager

16. Abstract

This report describes a two part study to identify KRASH code requirements for analyses of:

- Structure/terrain interaction
- Head/structure interaction

The literature survey of water and soil impact methodology is presented. The reports are reviewed with regard to incorporation of code modifications to program KRASH. A total of 28 water impact reports were reviewed. In the area of water impact, the representation of a transport airplane lower fuselage as a wedge-shaped planing surfaced is discussed. A relationship is developed between vertical force and depth of fuselage penetration.

Forty soil impact related reports were reviewed in the survey. For soil impact the two potential approaches described include:

1. Empirical definition of soil pressure versus depth.
2. Theoretical definition of soil as a viscoelastic medium.

For the head/structure impact assessment, the Head Injury Criteria (HIC) and Severity Index (SI) calculations are added to program KRASH. The approach, equations, and flow diagrams associated with a simple, single degree-of-freedom model of a mass impacting a surface with a given velocity is described.

17. Key Words	18. Distribution Statement
Occupant Injury Assessment HIC, SI, Water Impact Soil Impact, Analysis KRASH	This document is available to the public through the National Technical Information Services, Springfield, Virginia 22161

19. Security Classif. (of this report)	20. Security Classif. (of this page)	21. No. of Pages	22. Price
Unclassified	Unclassified	72	

Form DOT F 1700.7 (8-72) Reproduction of completed page authorized

TABLE OF CONTENTS

LIST OF ILLUSTRATIONS

LIST OF TABLES

EXECUTIVE SUMMARY

This study is divided into two areas:

1. Structure and terrain inceraction
2. Head and structure interaction

The literature survey of water and soil impact methodology for incorporation into program KRASH is presented. A review of twenty-eight (28) water impact and forty (40) soil impact related reports is included. The reports were reviewed with regard to prospects for modifying the program KRASH code. For water impacts the representation of a transport airplane lower fuselage as a wedge shaped planing surface is discussed. A relationship is developed between vertical force and depth of fuselage penetration. For soil impact the two potential approaches include:

Empirical definition of soil pressure versus depth
Theoretical definition of soil as a viscoelastic medium

For the head/structure impact assessment the Head Injury Criteria (HIC) and Severity Index (SI) calculations are added to program KRASH. This report describes the approach, equations, and flow diagrams associated with a simple, single degree-of-freedom model of a mass impacting a yielding surface with a given velocity.

SECTION 1
INTRODUCTION

Current analyses of airplane crash impacts are performed assuming the impact surface is rigid and unyielding. The primary reason for this approach is simplicity, since the influence of the terrain on the aircraft structure's crashing behavior is not a factor. However, helicopters and light aircraft often crash in terrain which varies from water to mud. Table 1-1 (reference 1), shows the frequency distribution of accidents for civil and military rotorcraft. Over 40 percent of all accidents occur in soft sand and plowed fields. Also, nearly 40 percent of Navy rotorcraft accidents occur in water. A 1971-73 accident review (reference 2) of light, fixed wing airplanes showed 46 percent of the accidents occurred on level, flat terrain. A detailed Federal Aviation Administration - Civil Aeromedical Institute (FAA-CAMI) accident study (reference 2) shows hard soil and grassy land account for 11 of the 18 cases reported. Results of this latter study (Table 1-2) illustrate the frequency of occurrence of types of accidents, impact attitude, cabin damage, head impacts with the structure or instruments and injuries or fatalities. The study described in reference 2 provided the framework for a series of crash tests, which are reported in reference 3. In this latter program FAA/NASA sponsored comparative tests of light aircraft impacting on soil and concrete have shown that the airplane crash loads and post-impact behavior can be significantly different between the two terrains. Figure 1-1 illustrates the results between a concrete and a soil impact surface for a high-wing single-engine airplane impacting approximately with the same velocity and pitch attitude. The impact onto concrete is survivable both in terms of acceleration loads experienced by the occupants, as well as the ability of the structure to maintain a habitable and protective shell, while the impact into the soil terrain results in high acceleration levels and loss of the structure's protective shell, i.e., a nonsurvivable event.

Military and commercial helicopters which travel off-shore frequently encounter water impacts which have been shown to produce a different set of loads when compared to accidents involving concrete surfaces. The difficulty in modeling water and soil impacts relates to the ability to accurately depict the force distribution on the fuselage as the vehicle penetrates the terrain. As part of the aforementioned reference 3 study, program KRASH was modified to model inputs on a flexible surface. An option was incorporated into the program which allows for the imput of a soil flexibility term. This provision allows for the soil (represented by a spring) to act in series with the fuselage's crushable structure. This approach is limited because it does not allow for shape and/or attitude dependencies, nor does it address the water penetration issue.

Another significant aspect of aircraft accidents is the type of injury that occupants can incur. Two of the more significant potential impact injuries are (1) spinal compression due to vertical forces and (2) head concussion due to longitudinal forces. KRASH, from its inception, has had a means of measuring spinal injury included in its coding. The spinal injury potential is monitored by the Dynamic Response Index (DRI) term in KRASH. Recently, seat dynamic test requirements have been implemented in the Federal Aviation Regulations (FARs) for normal fixed-wing and transport fixed-wing airplanes

TABLE 1-1.FREQUENCY DISTRIBUTION OF ROTORCRAFT ACCIDENTS
(REFERENCE 1)

TERRAIN TYPE	FREQUENCY (PERCENT) CIVIL	ARMY	NAVY
SOFT GROUND (SOFT, SANDY, PLOWED)	40	49	44
VEGETATION (TREES, LARGE SHRUBS)	16	30	8
UNEVEN GROUND (ROCKS, STUMPS, LOGS)	9	10	3
PREPARED SURFACE (PAVED, HARD DIRT, GRAVEL)	18	7	0
WATER	11	2	39
SNOW/FROZEN	6	2	3

Table 1-2. RESULTS OF SELECTED CAMI ACCIDENT DATA (REFERENCE 2)

Frequency of Occurrence		Damage, Failures, Injuries	
Phase of Operation		Cabin Damage	
Takeoff	4	Intact, None	4
Landing	4	Minor, Moderate	8
(a) Cruise	8	Substantial, Destroyed	6
Aerial Application	2		
		Structure Damage	
Type of Accident		Intact, None	0
Stall	3	Minor, Moderate	7
Ground/Water Impact	5	Substantial, Destroyed	11
Contact w/tree/object	5		
Landing Short	1	Impact with Control Panel/Knobs	
Side of Hill	2	Yes	15
Miscellaneous	2	No	1
		Unknown	2
Angle of Impact (degrees)			
0-10	4	Seat Failures	
11-20	5	Yes	9
21-30	1	No	3
31-45	3	Unknown	6
46-90	4		
Unknown	1		
		Injuries (Total)	
Roll/Yaw Attitude		Fatalities	15
Significant Roll/Yaw	3	Serious and/or Critical	15
Slight or no Roll/Yaw	9	Moderate	6
Overturn	2	Minor, None	4
Unknown	4		
		Lap Belt Failures (TOTAL)	
Terrain		Yes	6
Hard Soil	7	No	27
Grassy Land	4	Unknown	7
Water	1		
Mud/Swamp	2		
Trees	1		
Mountainous/hilly	2		
Unknown	1		

(a) Generally impact occurs with tree, object, or ground, due to bad weather or stall.

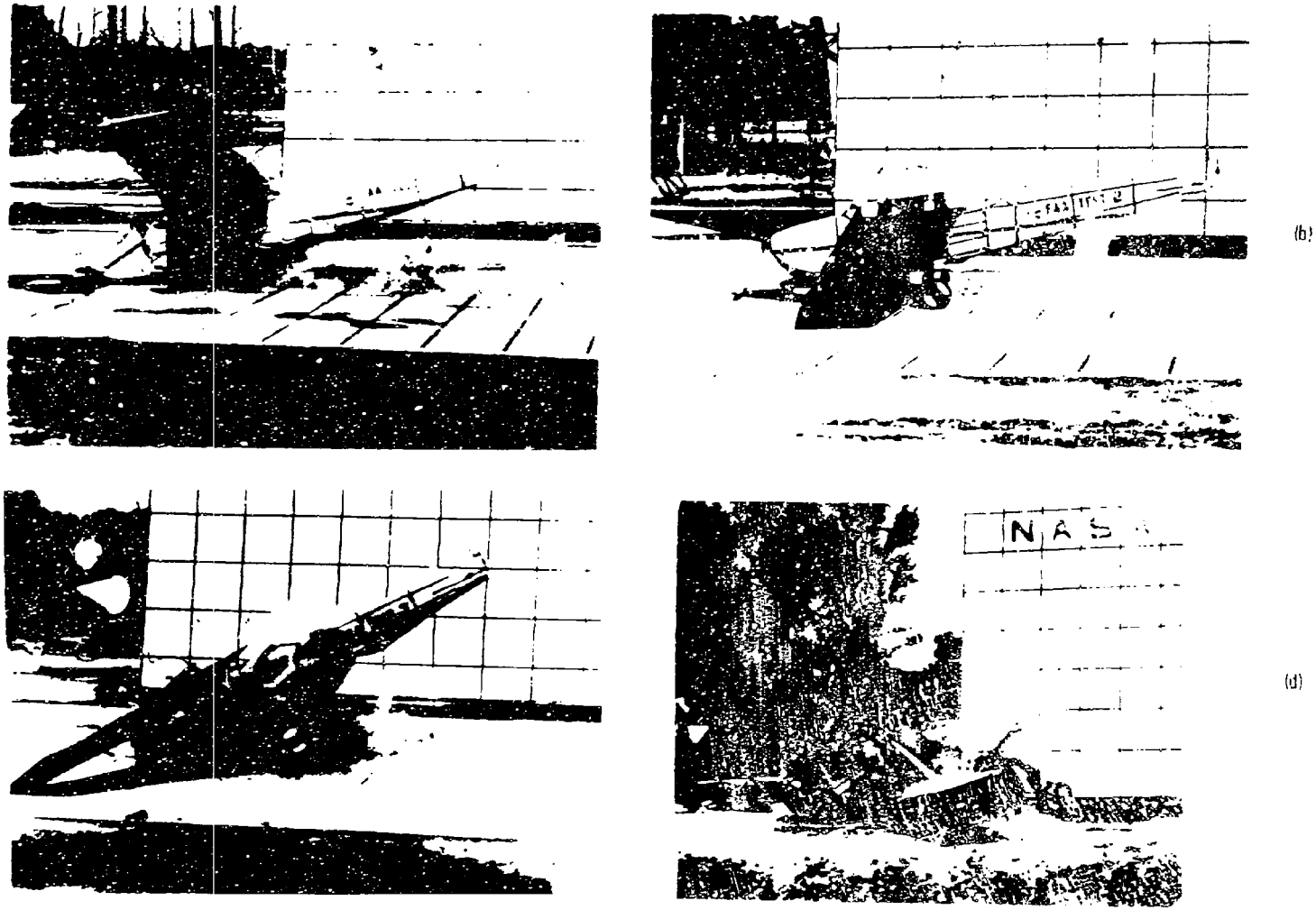

Figure 1 1. Post Impact Views of Full-Scale Crash Test Specimen

and have been prepared for rotary-wing aircraft. Included in these test criteria is a measurement of the Head Injury Criteria (HIC). This injury potential in an accident results from the impact of the occupants head with the aircraft structure (e.g., instrument panel, forward seat back). The current KRASH code includes the ability to define when and at what velocity a mass and the structure interact. However, the definition of the program code is incomplete in that the consequence of the impact, specifically the head injury potential, is not considered.

The study documented in this report is divided into two areas:

Structure and Terrain Interaction
Head and Structure Interaction

For the structure and terrain interaction, a literature survey was performed. An assessment of the state-of-the-art in methodology to treat water or soil impacts is included. For each type of impact, the respective approaches to incorporating additional coding into program KRASH are discussed. For the head and structure impact assessment, the Head Injury Criteria (HIC) and Severity Index (SI) calculations are coded into KRASH, and the incorporation theory is discussed.

SECTION 2
WATER AND SOIL IMPACT EVALUATION

2.1 LITERATURE SURVEY

2.1.1 Water Impact

Twenty-eight (28) reports are included in the "Water Impact" Literature Survey. Figure 2-1 shows these reports by number versus subject matter. The subject matter includes:

Data
- Accident
- Full-size tests
- Scale model tests

Theory/Methodology
Design relationships (expressions or hardware)
Correlation (test versus analysis)
Shapes
- Cones
- Spheres
- Disks
- Chines or wedges
- Rectangular lifting surface

Trend data (parameter variation)
Configurations
- Helicopter
- Transport airplane
- Apollo capsule
- Space Shuttle vehicle
- Space Shuttle Solid Rocket Booster (SRB)
- Missile
- Hydrofoil
- Prismatic float and flexible wing

Computer code
Summary of available techniques, phases, data

Appendix A contains a listing and an abstract for the 28 reports. All reports are referred to as A-1 through A-28.

Six reports (A-2, 10, 12, 13, 25, 27) provide material that is too general or not directly applicable to this study.

The remainder of the reports provide useful information, but are not all directly applicable for one or more reasons. For example, reports A-4, A-5, and A-6 are related to the Apollo capsule which at its base is spherical in shape. The water impact velocity range is in the region of concern (7.5 ft/sec - 30 ft/sec) and the measured pressures, forces, and accelerations provide a relationship between response, magnitude, shape, and velocity. However, there are no equations which can be programmed. Reports A-14 through A-22 are based on studies of the Space Shuttle Solid Rocket Booster (SRB). For the most part, the SRB studies were performed for a vertical velocity impact range at the high end or above the magnitude of concern in survivable airplane water impact studies. Four of these studies involved scale model

REPORT A-	1	2	3	4	5	6	7	8	9	10	11	12	13	14	15	16	17	18	19	20	21	22	23	24	25	26	27	28	29	30
ACCIDENT DATA													X																	
FULL-SIZE TESTS									X			X			X		X													
SCALED MODEL TESTS			X	X	X	X	X				X			X		X		X	X				X		X	X	X	X		
THEORY/METHODOLOGY	X						X	X	X	X		X		X		X		X			X		X	X	X	X	X			
DESIGN RELATIONSHIP															X	X										X		X		
CORRELATION				X			X		X					X									X	X	X					
SHAPES:																														
CONE	X											X																		
SPHERE	X											X																		
DISK												X																		
CHINE/WEDGE																							X				X			
(RECTANGULAR LIFTING SURFACE)																								X						
TREND DATA															X	X														
CONFIGURATION:																														
HELICOPTER							X																							
TRANSPORT A/P			X										X													X		X		
APOLLO				X	X	X																					X			
SPACE SHUTTLE (S.S.)								X			X																			
MISSILE										X		X																		
HYDROFOIL									X																					
MISCELLANEOUS																									(1)					
SRB (2)														X	X	X	X	X	X	X	X	X								
COMPUTER CODE										X										X	X	X								
SUMMARY OF DATA/ TECHNIQUES		X											X	X																
RATING LEVEL	B	C	B	B	B	B	B	B	B	C	A-	C	C	B	B	B	B	B	B	B	B	B	A	B	C	A-	C	A-		

(1) PRISMATIC FLOAT AND FLEX. WING
(2) SOLID ROCKET BOOSTER (SRB)

RATING A CONTAINS MATERIAL THAT COULD BE USED IN ANALYTICAL METHOD DEVELOPMENT
B CONTAINS MATERIAL OF INTEREST
C MATERIAL IS TOO GENERAL OR NOT DIRECTLY APPLICABLE

igure 2-1. Water Impact Survey; Report Numbers versus Subject Matter

tests, while two (A-15, A-17) involved full-scale segment representations. Report number A-14 describes both analysis and scale model tests of the SRB nozzle water impact environment. Report A-15 describes a series of water impact tests using full-scale segment representations of the SRB aft skirt structure. Report number A-16 describes methodology used to predict full-scale SRB water impact loads from scale model test data. Report number A-17 presents results of water impact tests using an aft skirt ring segment of the SRB. Report A-18 describes the results of model testing to expand the data base for design refinements. Report A-19 provides loads for the SRB (less nose cone and nozzle extension) from initial water contact through to final settling in the water. Reports A-20 through A-22 present computer program codes which, while not directly applicable, might be helpful in developing the needed coding.

Report A-1 describes pressure and acceleration trends as a function of velocity and shape and is based on "virtual mass" calculations. This report is helpful in understanding water impact phenomena and theories, but is not presently being considered for programming, primarily because it does not treat the horizontal velocity component. Report A-3 provides some data for selected water impacts of a transport category airplane. Of interest is the use of scale-strength (pressure) bottoms. The performance of the major assemblies (nose gear, main gear) in calm water and waves are discussed. Report A-7 is the only helicopter report included in the survey. This report deals with flotation capabilities and ditching operations. Report A-8 is a theoretical study of potential water-impact forces that the Challenger Orbiter may have experienced. The report presents some analytical relationships. However, a preliminary evaluation indicates that these expressions do not correlate well with available test results when applied to transport airplane scale and model tests data. Report A-9 describes a theoretical and experimental investigation of supercavitating hydrofoils operating near the free water surface. The report provides an array of lift and drag coefficient data for two hydrofoils, one with a flat surface and the other with a cambered lower surface. The data is applicable to a particular design (e.g., single hydrofoil supported by one strut, aspect ratio of 3) and operating condition (e.g., speed >80 knots, one chord depth, zero cavitation number). Report number A-24 provides data similar to number A-9 except that it is for submerged and planing rectangular lifting surfaces.

Reports A-11, A-26, and A-28 provide valuable design-related information. These reports contain summary results for transport-sized scale model airplane ditching test and present useful guidelines with regard to design characteristics, ditching procedures, anticipated structural failures, and optimum impact conditions. These reports also present some simplified analytical expressions which might be useful for design consideration. However, they do not provide information that can be incorporated into a computer code which would meet the objectives of this study.

Report A-23 is considered to provide the most useful expressions for initiating computer modeling. This report provides a theoretical basis for analyzing the impact of warped planing surfaces with combined horizontal and vertical impact velocities, with the horizontal velocity being dominant. Virtual mass theory is used; however, a technique is presented that allows the determination of virtual mass from planing lift data. This technique simplifies the computational procedure and eliminates the uncertainties in

determination of virtual mass. Report A-23 also extends the theoretical development to include the effects of water surface wave motion. The only significant effect missing in the theory of report A-23 is time-varying airplane pitch attitude. Also, the theory requires lift curve data for the impacting surfaces being investigated. However, representing a transport airplane lower fuselage shape as a wedge shaped planing surface appears to yield useful results.

The theoretical model from report A-23, expanded to include airplane pitch motions, has been investigated with a Continuous System Modeling (CSMP) computer program. The results indicate that the water impact load versus depth of water penetration takes on the form of a nonlinear hardening spring, as shown in figure 2-2. Manipulation of the equations in report A-23 yields the following form for the vertical impact force (perpendicular to the water):

$$F_z = \left[\frac{1.8\ \rho}{\tan^2 \beta}\right]\left[\frac{1 - \sin \tau}{\tan \tau}\right] \dot{y}^2\ z^2 \qquad (2\text{-}1)$$

$$F_s = -\tan \tau\ Fz \qquad (2\text{-}2)$$

with

$$\dot{y} = \dot{z} \cos \tau + \dot{s} \sin \tau \qquad (2\text{-}3)$$

where

τ = Airplane pitch attitude, degrees (positive move up)

$\dot{z}$ = Vertical sink rate at point of contact, in/sec (positive down)

$\dot{s}$ = Horizontal velocity of airplane, in/sec (positive forward)

$\dot{y}$ = Velocity of contact point normal to airplane fuselage, in/sec (positive down)

z = Depth of fuselage penetration, in (positive down)

ρ = Water density, 93.6E-6 pounds sec^2/in^4

β = Deadrise angle of planing surface used to represent fuselage, degrees

F_s = Horizontal force on fuselage, pounds

The slight hysteresis loop in figure 2-2 results from a decrease in $\dot{y}$ during unloading due to $\dot{z}$ in equation (2-3) switching from positive (downward motion) to negative (upward motion). The results shown in figure 2-2 are for a

deadrise angle of beta = 15 degrees, initial $\dot{z}$ = 36 in/sec, initial $\dot{s}$ = 2552 in/sec (126 knots), initial pitch attitude of τ = 12 degrees, and airplane weight of 380,000 pounds. Although airplane weight is not involved in equation (1), the weight will determine the maximum penetration resulting from a given F_z vs. z curve. The derivation of equation (2-1) is based on the assumption of chines-dry planing with a constant deadrise angle using equation (45) from report A-23 for planing lift coefficient:

$$C_{L_b} = 3.6 \frac{z^2}{b^2} \sin \tau \cos \tau \, (1-\sin \,) \cot^2 \beta \qquad (2\text{-}4)$$

where

b = maximum beam at chine, in.

C_{L_b} = planing lift coefficient, L / $1/2\rho V^2 b^2$

The water penetration and rebound shown in figure 2-2 occur in about 0.53 seconds. During this relatively brief interval, the forward velocity $\dot{s}$ has reduced only slightly from 126 knots to 124.8 knots, and the airplane Pitch attitude has decreased from 12 degrees to 10.9 degrees. The peak vertical acceleration is 0.29 g; this is a relatively moderate water impact since $\dot{z}$ is only 3 ft/sec. The energy absorbed by the hysteresis loop in figure 2-2 is relatively small, so that upon exiting the water, the upward velocity is 2.6 ft/sec. If 1g lift is present during the entire event, then the airplane will continue upward and will not re-contact the water.

Despite the limitations of the methodology described, it is felt that equation (2-1) represents a useful model of the loading encountered during water impact with a relatively large forward velocity component ($\dot{s} >> \dot{z}$). Equation (2-1) can be simplified by assuming τ and s are both constant during the impact event, yielding

$$F_z = A(\dot{z} \cos \tau_o + \dot{s}_o \sin \tau_o)^2 \, z^2 \qquad (2\text{-}5)$$

where

$$A = \frac{1.8 \, \rho}{\tan^2 \beta} \left(\frac{1 - \sin \tau_o}{\tan \tau_o} \right)$$

F_z is a function only of z and $\dot{z}$, with the latter dependence giving the hysteresis effect.

For incorporation into program KRASH, the remaining problem is how best to integrate equation (2-5) into the existing KRASH coding. The simplest method would probably be to take z and $\dot{z}$ as the values from the external spring that has the greatest water penetration. The total load F_z (and the corresponding drag load F_s, equation (2-2)) could then be applied to that spring, or

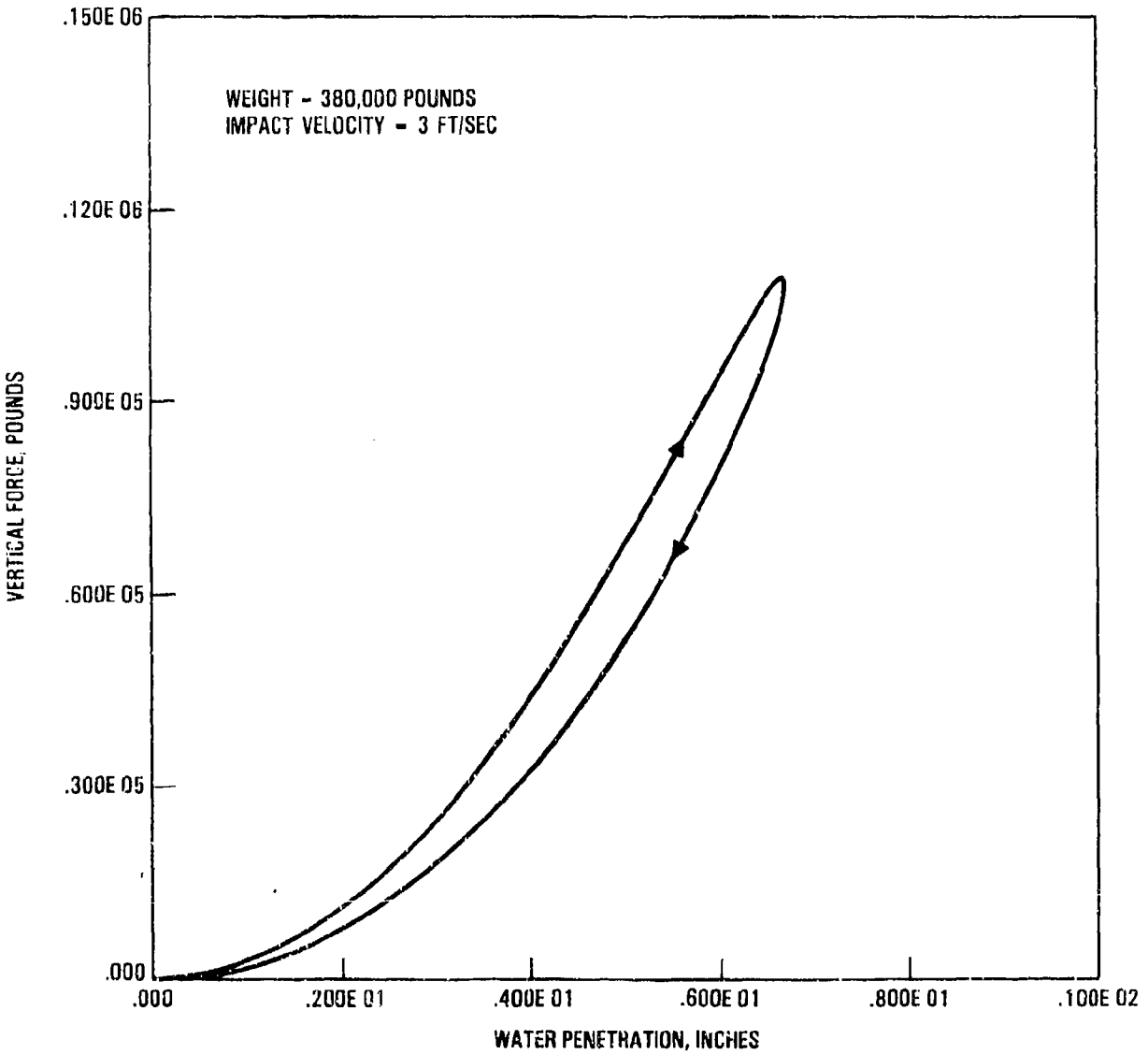

Figure 2-2. Water Impact Vertical Load Versus Depth of Penetration

distributed in some fashion among all springs that are in the water. Note that the structural flexibility represented by the KRASH external spring is in series with the water flexibility shown in figure 2-2.

Such a method should give useful results for the initial water impact, but subsequent impacts in other regions (such as the wing engines) could not be analyzed meaningfully. Such impacts might best be treated with a separate model that emphasizes the dominance of the drag load as opposed to the vertical load.

2.1.2 Soil Impact

A Literature Survey for soil impacts was performed as part of a general aviation modeling and test program and is described in reference 3. Reference 3 included 26 reports. This survey updates that study and expands the number of applicable reports to 40.

An abstract of each of the 40 reports is included in Appendix B. All reports are referred to as B-1 through B-44. Reference 3 is denoted as report B-27 in this Literature Survey. The literature in B-27 was reviewed with regard to aircraft structure and flexible ground interaction. A summary of the literature as stated in B-27 is as follows:

> "The test data that are available are generally obtained for the purpose of supporting analyses or for the development of procedures and criteria to evaluate aircraft performance and not for the purpose of helping predict dynamic responses where in large deformations occur. Even the full-scale crash tests that have previously been performed on flexible ground surfaces have not addressed themselves to the significance of the terrain properties on structure and, ultimately, occupant response. For example, little or no measurements of ground flexibility, moisture, finish, or distribution as a function of depth or space have been made in any of the full-scale crash tests reported herein. No measurements have been made to ascertain penetration by airframe or the relationship of penetration to airframe size of shape or to the impact velocities.
>
> While the penetration of ground by tires (sinkage) for the landing gear-ground interaction is available, these data do not relate easily to the impact velocity combinations and varied shapes that penetrate flexible ground during a crash condition.
>
> The research effort with regard to developing analytical models to describe landing gear and soil interaction and provide flotation criteria for aircraft operating from unpaved runways is substantial. A heavy reliance is placed on the use of the Mobility Number $(Q) = \frac{CI(bd)}{F_t} \left(\frac{\delta_t}{h_t}\right)^*$

where CI = Cone Index

bd = Tire Print Area

F_t = Tire Force

δ_t = Tire Deflection

h_t = Height of Tire

However, the analytical techniques developed for landing gear and soil interaction use are not directly applicable to structural crashworthiness investigations. Modifications are needed which account for airframe shape, crash attitude, shear flow distribution, structure flexibility, and dynamic load effects.

The analysis of flexible ground and structure interaction during relatively high dynamic impact conditions would benefit from an orderly and concerted effort to accumulate data from typical airframe and terrain interaction tests and supportive laboratory soil tests. As a minimum, spatial and depthwise material properties (CBR,** soil strength, moisture content), airframe response in the region of impact, airframe configuration (shape and size), post-impact terrain, penetration (size and depth) for a range of typical airplane impact velocities and attitudes, and soil configuration is needed. The data should be obtained for the purpose of developing curves which relate vertical force to sinkage as a function of CBR, soil shear strength to CBR, and horizontal force to frontal area as a function of shear strength."

---

*The above mobility number is for clay soil. Mobility numbers for other types of soil take other forms.

**CBR = California Bearing Ratio

Reports B-27, B-29, and B-30 discuss full-scale crash tests which involved impacts onto soil. Report B 28 describes an analysis and evaluation of the soil properties for the tests described in B-27, B-29, and B-30.

Report number B-27, in addition to providing the Literature Survey, describes test and analysis of four full-scale light fixed-wing airplane tests. One of the tests involved an impact onto soil. Report B-29 is a summary report of the test results for the four impacts discussed in B-27. The effect of the impact onto soil versus a similar impact onto concrete is dramatically different as can be observed in figure 2-3. The impact onto concrete results in moderate airplane axis vertical and longitudinal loads and the airplane sustains some lower forward fuselage damage but slides-out. In the soil

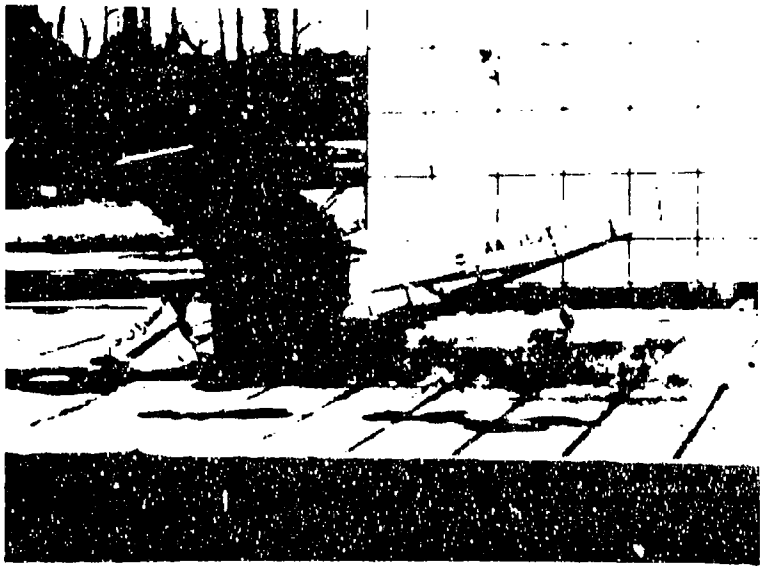

(a) CONCRETE

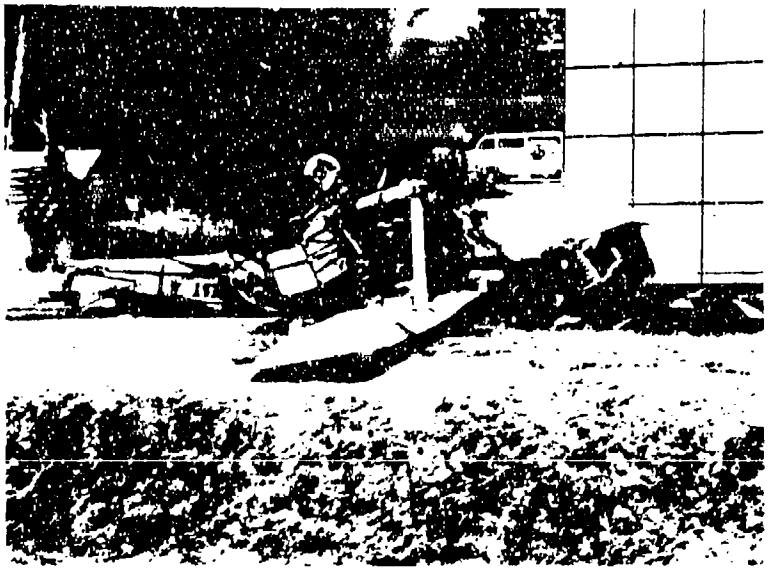

(b) SOIL

Figure 2-3. Post Impact Views of Full-Scale Crash Tested Airplanes

impact with approximately the same initial velocities and airplane attitude, the airplane longitudinal forces are extremely high causing a complete crush of the forward fuselage and resulting in flip-over of the high-wing airplane. The low-wing airplane impact into soil as reported in B-30 shows extremely high forces along the airplane longitudinal axis but, because of the lower c.g., does not flip over. Report B-28 describes the soil for both the low-wing and high-wing airplane tests with average values of:

CBR	3.5
Airfield Index	5.0
Moisture	14.5%

The report B-28 describes the post-impact inspection of the two tests as follows:

High-wing: crater 3.3 ft wide, 11.5 ft long
Low-wing: crater 3.3 ft wide, 5.0 ft long

The depth of the crater might have been 4 inches, but this was stated to be an inconclusive measurement. The report goes on to indicate that the crater was formed mostly by shearing and removal of the soils as the fuselage plowed through.

Report B-31 is the U.S. Army Crash Survival Design Guide - Volume III. This report is included in the survey since it provides a discussion on plowing and crash design for high longitudinal forces. The design guide also provides some empirical relationships.

Reports B-32 to B-37 provide discussions of test results involving airplane tires/landing gears impacting soil terrain. Report B-32 describes a dynamic tire/soil contact surface interaction model for aircraft ground operations. The model predicts contact pressure distribution, soil deformation pattern, and tire footprint area shape developed beneath the moving tire wheel. Soils ranged from a CBR of 2 to 6 and a CI of 80 to 240. Report B-33 addresses rolling resistance or drag of an improved pneumatic tire wheel rolling at high velocities in soft soil. Curves depicting drag/lift ratio versus wheel speed as a function of soil property and rut depth are presented and the study was performed for near-saturated clay. Report B-34 describes tests to investigate the interaction of soil surfaces with the landing gear of the F-4E aircraft. CBR values generally ranged from 4.0 to 8.0 although some values were as high as 80.0. CIs generally ranged from 40 to 190 and moisture content was $\leq$11.5% (generally 4 percent to 6 percent). Report B-35 describes the results of flight tests involving a C141 airplane flotation system operating on unsurfaced runways. The soil involved in the tests is termed "heavy clay." CBR values varied substantially (2 to 20) depending upon location and depth. Operational speeds were 20 to 40 knots taxi velocity, sink speeds of 2, 5, and 8 ft/sec., airplane gross weight of 190,000 lb. to 257,000 lb., and tire pressures of 185 psi to 220 psi. Report B-36 describes an investigation to determine aircraft tire behavior and operating problems in soil of different characteristics. Four clay test beds and sand test beds were involved. Forward speeds up to 95 knots were tested. Airfield Index (AI) numbers of 1.6 to 3.2 were obtained for the clay test beds. The AI value for the sand varied from 2 to 10 depending on depth. The highest value occurred at approximately 10 inches and the lowest near the surface. Rut depths of 2 to 4 inches were

experienced under loads of 4,000 lbs. The ratio of drag to normal forces was as high as .30 to .44 in soil versus .05 on concrete. The report shows trends as function of weight, velocity, soils, and tire pressure. Report B-37 discusses test with single aircraft tires and military truck in buckshot clay test beds whose strength range from CIs of 110 to 600. Tire loads varied from 25,000 lb. to 35,000 lb. and truck loads from 6,300 lb. to 41,700 lb. The relationship between AI versus CBR and AI versus CI are presented.

Reports B-38 and B-39 described theoretical approaches applicable to tire/soil modeling. Report B-38 is an earlier publication which suggests one approach based on "Princeton Impact" test data and a viscoelastic solution of a sphere on the half space. Report B-39 reviews the literature concerning aircraft-surface dynamic simulation techniques. The connection between airframe and landing gear is provided by a suspension device. This connection can be as simple as a linear spring and damper in parallel or more realistically involve nonlinear stiffness and velocity squared dampers. In addition, the damping coefficient may be a nonlinear function of the strut stroke. Some simulations have included active suspensions. Tires are generally modeled as point-contact followed with either linear or nonlinear stiffness and damping in parallel. More recent models better approximate the enveloping effect of the tire traversing short wavelength obstacles. A radial tire spring has been used in several models.

Generally the simulation is written for motion over rigid surfaces. Some model surface elevation while others are specifically designed for discrete obstacles (e.g., double (1-cos) bump). Yielding surfaces (soil) are represented by some combination of linear or nonlinear springs and dampers. The simulations of most interest in study are those which contain tire/soil interaction. The tire behavior is not as important as the soil representation.

Report B-10 developed modulus of deformation relationships for three shapes: spheres, plates, shells. The relationships are as follows:

$$E_{d_s} = 582.R + 35.08R^2$$

$$E_{d_r} = 4787.6R + 230.24R^2$$

$$E_{d_c} = 1049 \text{ lb/in.}$$

where R = radius, inches

The information is categorized according to specific content in table 2-1 and by soil/interaction tests parameter data in table 2-2 for all applicable reports.

The Literature Survey updated to include 40 reports indicates that the following three alternate approaches can be considered for further development with program KRASH:

- Mobility numbers
- Soil modeling
- Pressure-depth relationships

TABLE 2-1. LITERATURE MATRIX CATEGORIZATION (SHEET 1 OF 3)

Specific Contents and Areas of Applicability	REFERENCE NO. E-	1	2	3	4	5	6	7	8	9	10	11	12	13	14
	ANALYSIS														
	Analytical Model														
	Surface		o	o	o	o		o	o		o	o			
	Tire/Wheel/Gear				o	o			o						
	Interaction		o	o	o	o									
	Data Correlation			o		o					o	o			
	Parametric Study														
	LANDING SURFACE CHAR.														
	Material Prop.	o	o	o	o	o	o				o	o		o	o
	Roughness Prop.		o	o											
	Performance Char.	o	o	o				o	o	o	o	o		o	o
	LANDING SURFACE/ GEAR INTERACTION TESTS														
	Test Procedures	o	o	o		o	o	o			o			o	o
	Data Analysis	o	o	o		o		o			o			o	o
	CRASH TESTS														
	Test Procedures														
	Data Analysis														
	Empirical Criteria														
	DESIGN														
	Procedures			o	o				o	o	o	o	o	o	
	Criteria				o			o	o	o	o	o	o	o	
	Design Tools														
	Nomographs								o	o	o	o	o	o	
	Computer Prog.			o	o	o				o	o	o			

TABLE 2-1. LITERATURE MATRIX CATEGORIZATION (SHEET 2 OF 3)

Specific Contents and Areas of Applicability	REFERENCE NO. B-	15	16	17	18	19	20	21	22	23	24	25	26
	ANALYSIS												
	Analytical Model												
	Surface					o		o				o	
	Tire/Wheel/Gear					o		o					
	Interaction	o	o			o							
	Data Correlation	o	o					o				o	
	Parametric Study	o											
	LANDING SURFACE CHAR.												
	Material Prop.	o		o	o			o				o	o
	Roughness Prop.	o				o		o					
	Performance Char.	o	o	o	o			o					
	LANDING SURFACE/ GEAR INTERACTION TESTS												
	Test Procedures	o		o	o			o					
	Data Analysis	o		o	o			o					
	CRASH TESTS												
	Test Procedures						o		o	o	o		
	Data Analysis						o		o	o	o		
	Empirical Criteria												
	DESIGN												
	Procedures	o	o					o					
	Criteria							o					
	Design Tools												
	Nomographs												
	Computer Prog.	o	o			o		o					

TABLE 2-1. LITERATURE MATRIX CATEGORIZATION (SHEET 3 OF 3)

Specific Contents and Areas of Applicability	REFERENCE NO. B-	27	28	29	30	31	32	33	34	35	36	37	38	39	40
	ANALYSIS														
	Analytical Model														
	Surface						o						o	o	
	Tire/Wheel/Gear						o	o						o	
	Interaction						o							o	
	Data Correlation														
	Parametric Study														
	LANDING SURFACE CHAR.														
	Material Prop.		o				o		o		o	o	o		o
	Roughness Prop.														
	Performance Char.								o	o	o				
	Literature Survey	o													
	LANDING SURFACE/ GEAR INTERACTION TESTS														
	Test Procedures											o			
	Data Analysis											o			
	CRASH TESTS														
	Test Procedures	o		o	o										
	Data Analysis	o		o	o										
	Empirical Criteria														
	DESIGN														
	Procedures					o								o	
	Criteria					o									
	Design Tools														
	Nomographs					o									o
	Computer Program	o												o	

TABLE 2-2. SOIL/INTERACTION TES. PARAMETER INDEX (SHEET 1 OF 5)

REFERENCE NO. B-	1	2	3	4	5	6	7	8
LANDING SUR./SOIL								
Type	Clay	Clay	-	-	Clay/Sand	Clay/Sand	Sand	-
% Water Content	30.1-34.5	-	-	-	-	8	1	-
Density (lb/ft^3)	88.5-92.3	-	-	-	-	-	98-103	-
CBR (CI) [CPR]	-	-	-	-	1.5-4.4	(15-47)	(7-90)	-
Others	-	Hardness	-	-	-			
TIRE/WHEEL								
Size (a)	-	29x11-10,8PR 7.5x10,8PR	-	-	29x10-11,8PR	11x20,12PR	*	-
Pressure (lb/in^2)	-	-	-	-	30-70	15-80	2-48	-
Number Per Gear	-	1	-	-		1	1	-
VEHICLE								
Type	-	Airplane	-	-	Cart	Cart	Cart	-
Load (lb)	-	9755-10547	-	-	2600-5300	3000	100-7760	-
Sink Speed (ft/sec)	-	6.6-34.7	-	-	0	0	-	-
Long. Speed (ft/sec)	-	90.2-145.2	-	-	0-169	1	-	-
Pitch Angle	-	(-6.5)-7.0	-	-	0	0	0	-
Yaw Angle	-	0.1-4.0	-	-	0	0	0	-
REFERENCED DATA (b)	5	-	5,17	5,17	-	-	-	6,13,15
							* 4x7,2PR 4x20,2PR 6x16,2PR 9x14,2PR 16x15-6,2PR 11x20,12PR 1.75x26,2PR 9x14,2PR 4.5x18,4PR	

TABLE 2-2. SOIL/INTERACTION TEST PARAMETER INDEX (SHEET 2 OF 5)

REFERENCE NO. B-	9	10	11	11	12	13	14	15
LANDING SUR./SOIL								
Type	-	Clay/Sand	Clay/Sand	Clay/Sand	-	Clay	Clay/Sand	Clay/Sand
% Water Content	-	2.5-42.2	1.5-29.3	1-42	-	16.2-24.8	6-35.4	0.8-29.6
Density (lb/ft^3)	-	75.1-99.5	75.5-97.4	75-102	-	93.9-101.8	83.6-104	77.2-120.8
CBR (CI) [CPR]	-	0.7-1.4	[8-35.7]	(20-45)	-	7-17	1-2.3	0.8-64
Others	-	-	-	-	-	-	-	-
TIRE/WHEEL								
Size (a)	-	7.00x6,6PR 8.50x10,8PR	-	7.00x6,6PR	-	*	29x11-10,8PR	46x16,26PR 32x11.5-15,12PR
Pressure (lb/in^2)	-	-	-	2.2-12.5	-	-	30-70	30
Number Per Gear	-	1	-	2	-	1,2,3,12	1,2	8
VEHICLE								
Type	-	Cart	Flat Plate	Cart	-	Cart	Cart	Airplane
Load (lb)	-	300-2000	-	800-1400	-	1000-273,000	2600-5200	156,500
Sink Speed (ft/sec)	-	0	-	0	-	0	0	0
Long. Speed (ft/sec)	-	20	-	10	-	0.5-25.3	0-147	<10
Pitch Angle	-	0	-	0	-	0	0	-
Yaw Angle	-	0	-	0	-	0	0-6	-
REFERENCED DATA (b)	-	5,6,13,8	13,6,15	13,6,15	-	- * 9.00x14,8PR 34x9.9,14PR 20.00x20,22PR 25.00x28,30PR 56x16,24PR 17.00x16,12PR 30x11.5,24PR 56x16,32PR 56x16,38PR	-	-

(a) Tire Size: Diameter x Width, PR = ply rating
(b) Report Number in the Literature Survey

TABLE 2-2. SOIL/INTERACTION TEST PARAMETER INDEX (SHEET 3 OF 5)

REFERENCE NO. B-	15	16	17	18	19	20	21	22	23	24	25	26
LANDING SUR./SOIL												
Type	Sand	-	Clay	Sand	-	-	Soil	-	-		-	Sand
% Water Content	-	-	31.7-33.4	.2-.5	-	-	30,20	-	-		-	46-56
Density (lb/ft^3)	-	-	84.6-86.1	90.3-104.6	-	-	91.2,107.9	-	-		-	-
CBR (CI) [CPR]	2.5-5.5		1.3-2.8	(3.75-54)	-	-	2.10	-	-		-	-
Others	-	-	-	-	-	-	-	-	-		-	-
TIRE/WHEEL												
Size (a)	46x16,26PR 32x11.5-15,12PR	-	-	*	-	-	-	-	-		-	-
Pressure (lb/in^2)	30,36	-	70	-	-	-	50-100	-	-		-	-
Number Per Gear	4,8	-	1,2	1	-	-	1	-	-		-	-
VEHICLE												
Type	Airplane	-	Cart	Cart	-	-	Cart	-	-		-	-
Load (lb)	138,000-180,000	-	-	465-4500	-	-	2000-3000	-	-		-	-
Sink Speed (ft/sec)	2-4	-	-	0	-	-	0	-	-		-	-
Long. Speed (ft/sec)	RTO	-	12-147	.5-18	-	-	0-66	-	-		-	-
Pitch Angle	-	-	0	0	-	-	0	-	-		-	-
Yaw Angle	-	-	0	0	-	-	0	-	-		-	-
REFERENCED DATA (b)		15	5,26									
				* 6.00x16,4PR 4.15X18,4PR 9.00X14,2PR 11.00X20,12PR 9.00X14,8PR 6.00X16,2PR								

(a) Tire Size: Diameter x Width, PR = ply rating
(b) Report Number in the Literature Survey

TABLE 2-2. SOIL/INTERACTION TEST PARAMETER INDEX (SHEET 4 OF 5)

REFERENCE NO. B-	27	28	29	30	31	32	33	34
LANDING SUR./SOIL								
Type	-	Soft Soil	-	-	-	Soft Soil	Clay/Sand	-
% Water Content	-	14.5 avg.	-	-	-			<11.5
Density (lb/ft^3)		96 avg.	-	-	-	2-6 (80-240)	- 4-8 (40-90)	
CBR (CI) [CPR] <AI>	-	3.5 <5> avg.	-	-	-	-	-	-
Others	-	-	-	-	-	-	-	-
TIRE/WHEEL								
Size (a)	-	-	-	-	-	11x20,12PR	*	-
Pressure (lb/in^2)	-	-	-	-	-	15-60	2-48	-
Number Per Gear	-	-	-	-	-	1	1	-
VEHICLE								
Type	Airplane	-	-	-	-	Cart	Cart	Cart/Airplane
Load (lb)	2400	-	-	-	-	3000	100-7760	17000/54000
Sink Speed (ft/sec)	43.4	-	-	-	-	0	-	-
Long. Speed (ft/sec)	69.6	-	-	-	-	1	-	-
Pitch Angle (deg)	-34.8	-	-	-	-	0	0	-
Yaw Angle (deg)	0	-	-	-	-	0	0	-
Roll Angle (deg)	0	-	-	-	-	-	-	-
REFERENCED DATA (b)	28	-	27,28	28	-	-	-	-

TABLE 2-2. SOIL/INTERACTION TEST PARAMETER INDEX (SHEET 5 OF 5)

REFERENCE NO. B-	35	36	37	38	39	40
LANDING SUR./SOIL						
Type	Clay/Sand	Clay/Sand	Clay	Clay/Sand	-	Sand
% Water Content	-	-	20-30	-	-	6-20
Density (lb/ft^3)	-	-	-	-	-	-
CBR (CI) [CPR] <AI>	2-20	<1.5-2.5>clay	(100-600)	-	-	-
Others	-	<2-10>sand	<2-12>	-	-	-
TIRE/WHEEL						
Size (a)		29.0x11-10,8pr	20-20,20 PR 49-17,26 PR	-	-	-
Pressure (lb/in^2)	-	70	-	-	-	-
Number Per Gear	-	-	1	-	-	-
VEHICLE						
Type	C-141	Cart	Cart/Truck	-	-	*
Load (lb)	190,000- 257,000	-	35000/41708	-	-	-
Sink Speed (ft/sec)	2-8		0	-	-	30
Long. Speed (ft/sec)	20-40	95	0.5-25.3	-	-	-
Pitch Angle (deg)	-	-	-	-	-	-
Yaw Angle (deg)	-	-	-	-	-	-
REFERENCED DATA (b)	-	-	-	-	-	- *sphere plate shell

(a) Tire Size: diameter x Width, PR = ply rating
(b) Report Number in the Literature Survey

The mobility number concept derives from the development of flotation criteria for aircraft operating on unpaved runways. A mobility number is established for a particular soil and known rut measurements for a specific tire size and force. Report B-37 provides nomographs and a description of this concept. The drawbacks for this approach are: (1) it is based on tire data; (2) it is limited to a few available test points; and (3) need to translate into viable terms for applicability to airframe structure.

The soil modeling approach involved programming characteristics of yielding surfaces which are represented by nonlinear springs and dampers. Report number B-2 provides some soil damping characteristic data for a range of soil hardness characteristics. This data appears incomplete and inconsistent.

Two basic approaches to incorporating soil interaction into KRASH are available:

1. Empirical definition of soil pressure versus depth.
2. Theoretical definition of soil as a viscoelastic medium.

The first approach involves the following steps:

1. Establish standard curves or tabulated data of soil type. Included in this tabular data are indices such as CI, CBR, AI, and pressure-depth relationships. Figures 2-4 through 2-9 indicate how some of the data can be related.

2. As input to the program, denote at each location of interest:

   - Soil type or number (e.g., CBR=5, 10, 15, 20)
   - Shape term or factor (flat plate, sphere, cone)
   - Pressure versus depth as function of shape

3. Develop a new "panel" designation which is described by corner mass points and pressure allowables.

4. Calculate forces developed at specified location due to wetted area resulting from penetration depth, and as function of attitude. The force which acts on plates or panels (new KRASH requirement) is distributed to designated node points and/or to specified masses.

The main difficulty with the empirical soil pressure versus depth approach is that the correct pressures are dependent not only on soil type and impacting shape but also the magnitude and direction of the impact velocity vector. It would be very difficult to establish the data necessary to cover all combinations of soil type, impacting surface shape and impact velocity and direction.

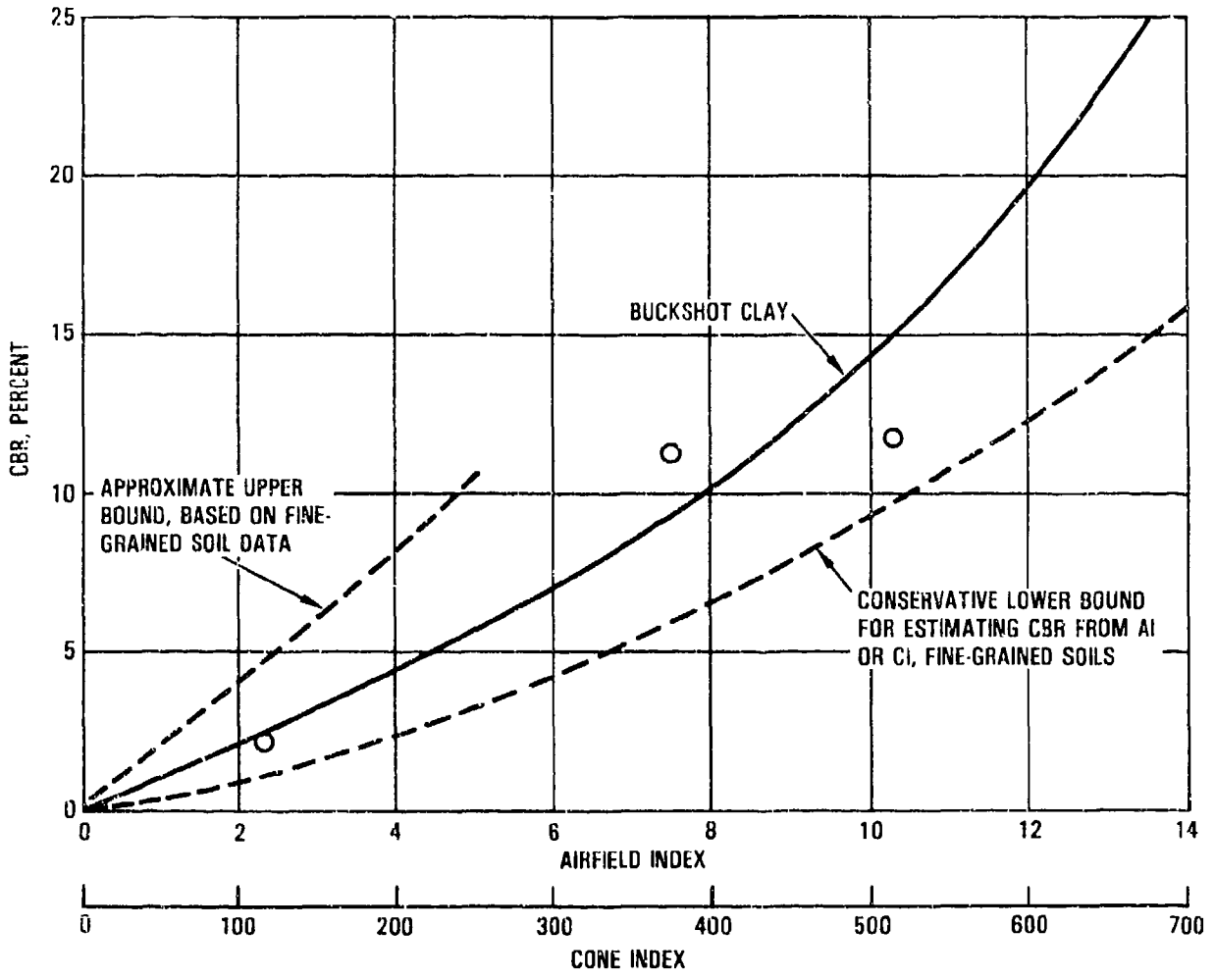

Figure 2-4. Relations of CBR to Cone Index and to Airfield Index for Homogeneous (Laboratory Test Pit) Buckshot Clay

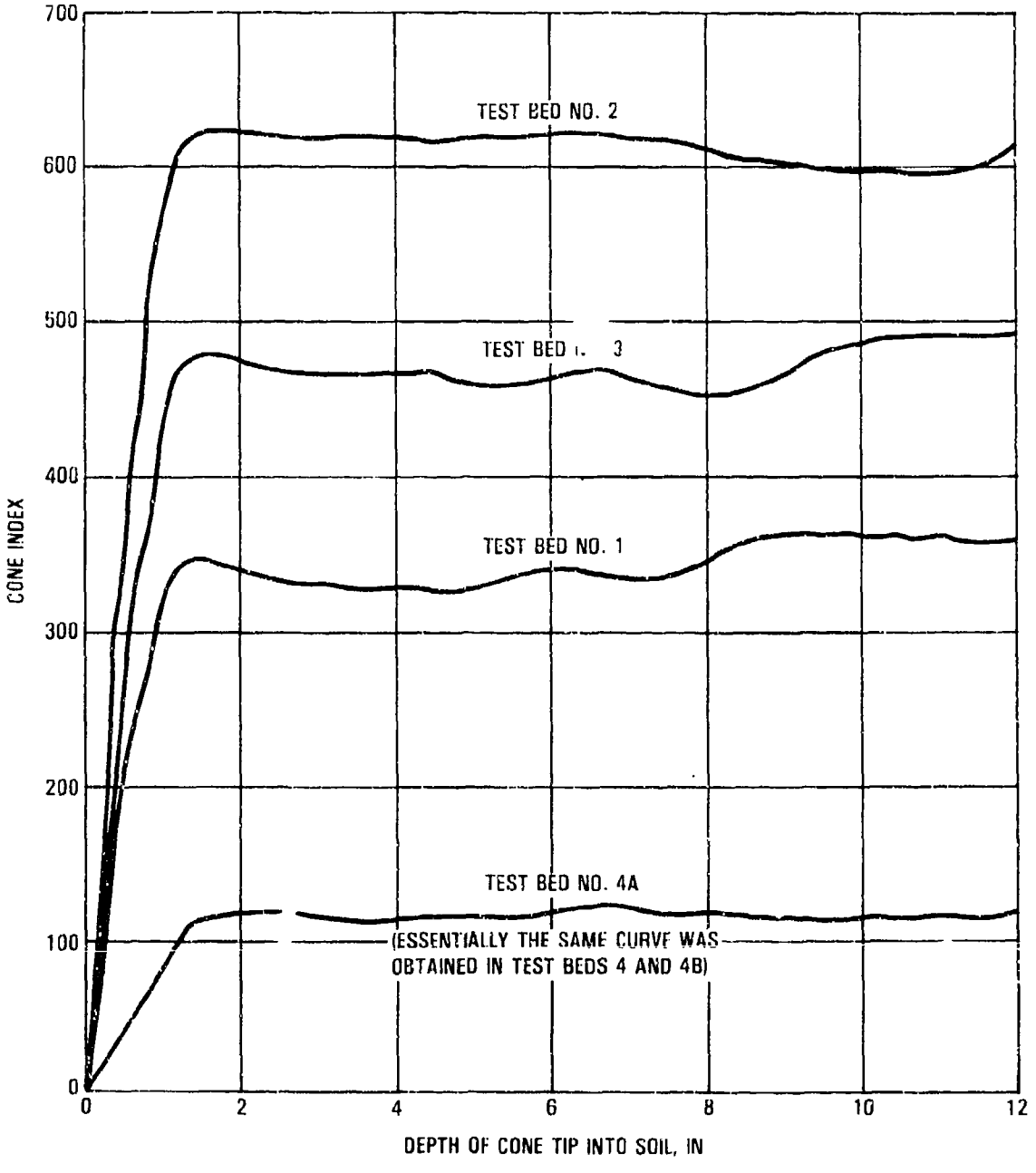

Figure 2-5. Representative Cone Index Versus Depth Curves for the Four Soil Strength Levels Tested

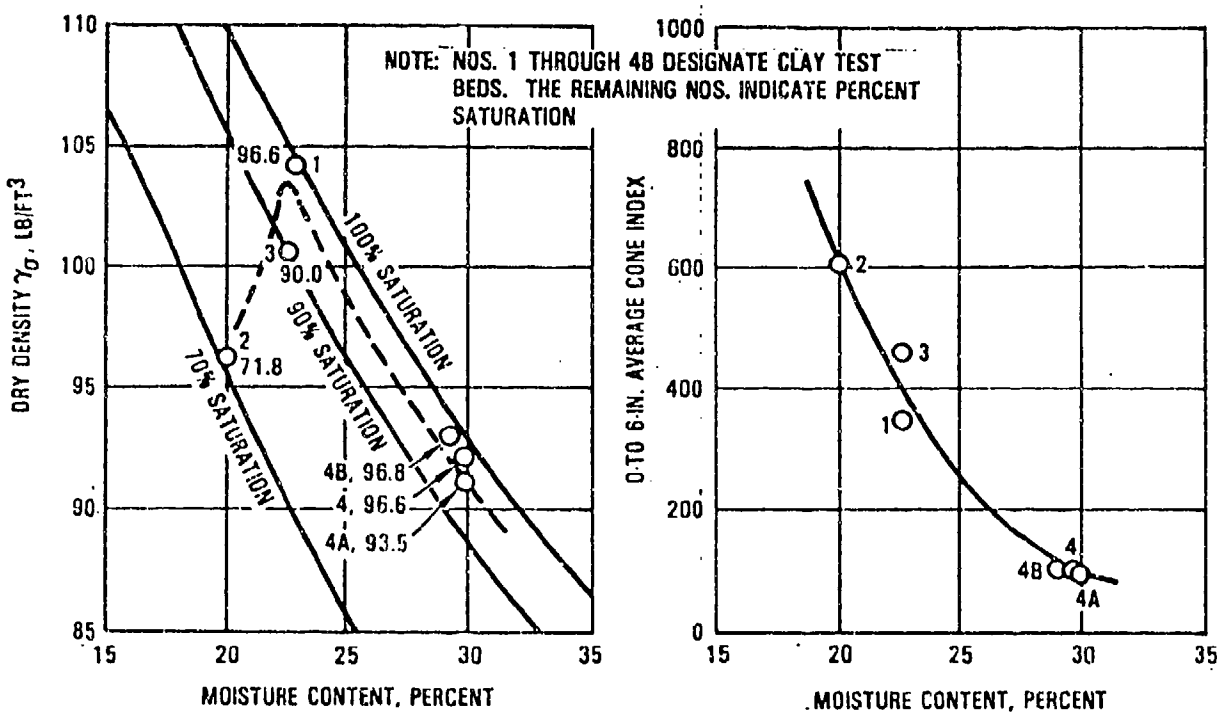

Figure 2-6. Relationship of Dry Density and Cone Index to Moisture Content

The approach involving modeling the soil as a viscoelastic medium also holds the promise of yielding a workable program. Report B-32 describes the development of a viscoelastic soil model that interacts with a flexible tire model. The resulting system is capable of predicting the tire/soil contact pressure distribution and the resulting tire/soil deformations and vertical drag loads. It would appear that similar techniques could be used to model the interface of airplane structure with soil. On the negative side, the solution in B-32 is only for a steady state condition (tire rolling at constant velocity); a dynamic impact complicates what is already a complex problem. Semi-empirical methods similar to those employed by Crenshaw (report B-4) for the tire/soil dynamics problem are probably the most practical methods of incorporating a viscoelastic soil model into KRASH.

Crash impacts with soil also tend to involve plowing, raising the possibility of using equivalent mass techniques and conservation of momentum. Finally, any method used must be integrated into the current KRASH model with external springs representing the lower fuselage flexibility.

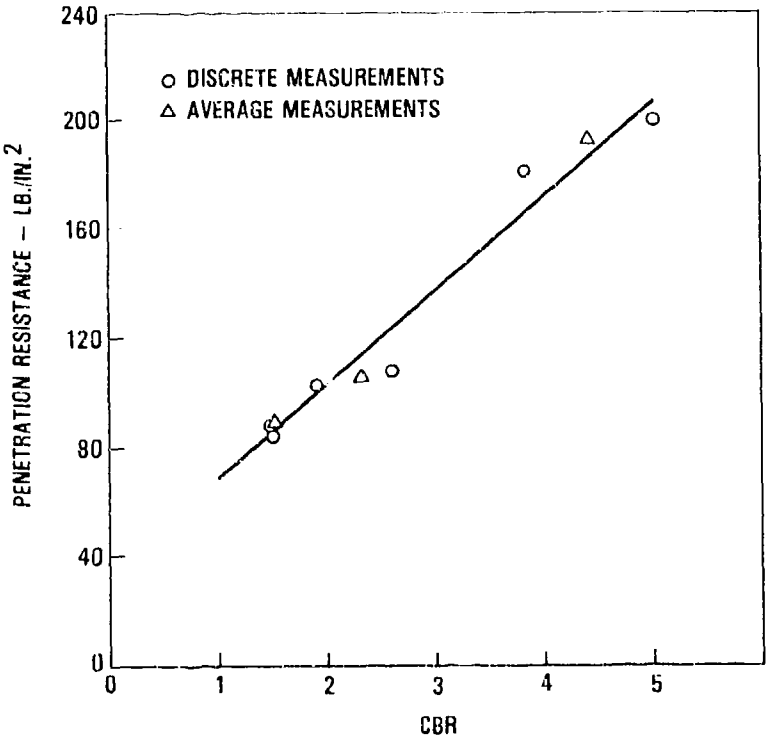

Figure 2-7. Penetration Resistance Versus CBR in Buckshot Clay

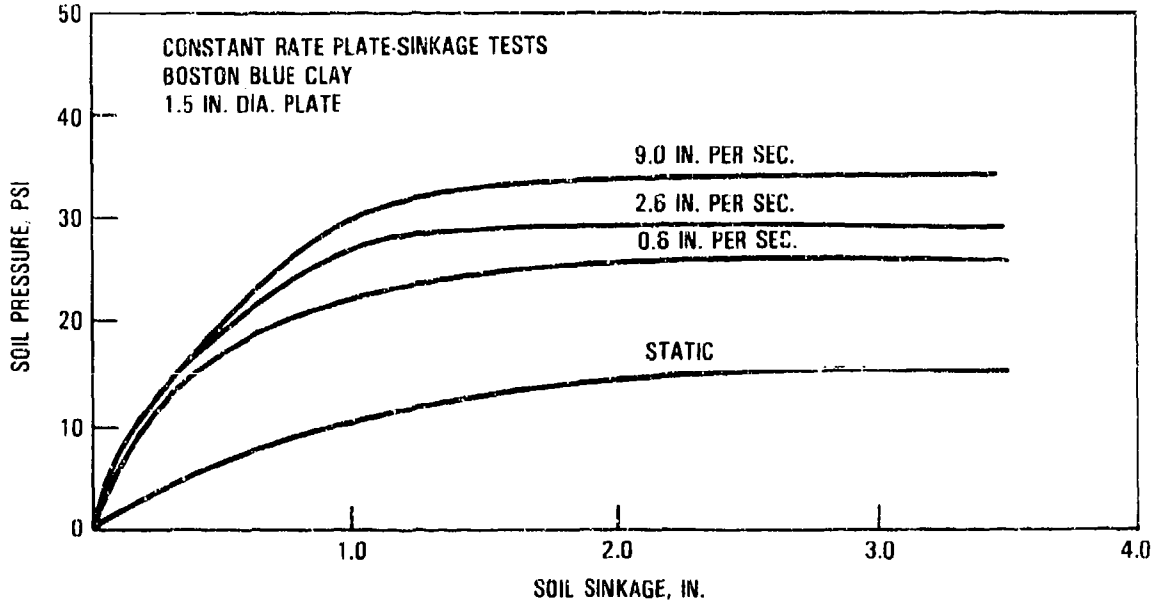

Figure 2-8. Soil Pressure Versus Soil Sinkage as Function of Loading Rate

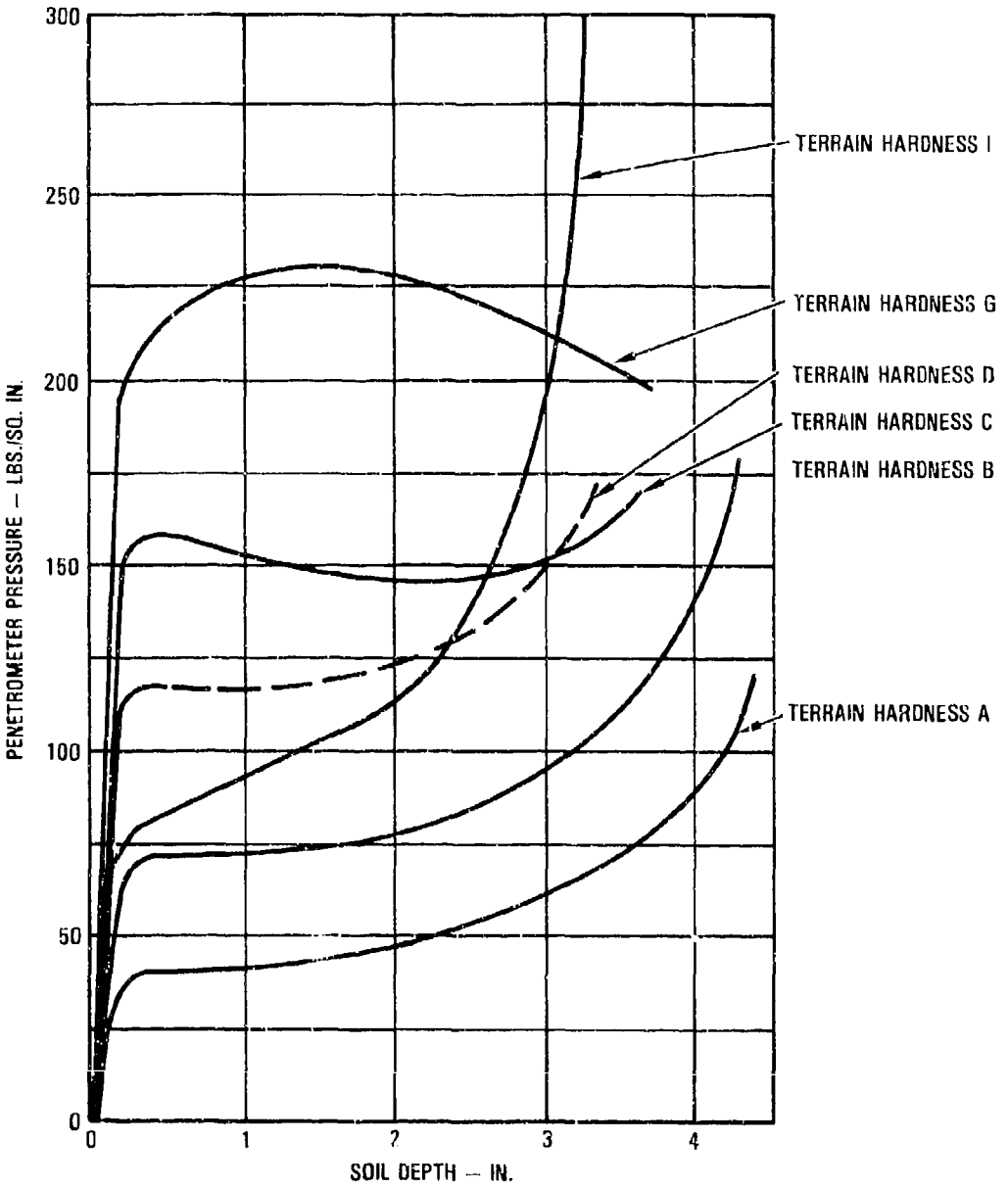

Figure 2-9. Penetrometer Pressure Versus Soil Depth as a Function of Terrain Hardness

SECTION 3
HEAD IMPACT CALCULATIONS

3.1 GENERAL DISCUSSION

Program KRASH has been revised to include the capability to analyze the dynamic response of an occupant's head impacting a surface with nonlinear load-deflection characteristics. This problem is treated in two parts. During the normal KRASH time-history, any mass or node point identified as a "head" triggers additional calculations that lead to a time-history output of the velocity and position of the head, both relative to a user-defined mass or node point. At a user-specified input distance, the velocity of the head is saved for a separate dynamic analysis of the head impact. At the conclusion of the normal KRASH analysis, a subroutine is called which performs a separate, independent time-history analysis of a head impacting a surface with nonlinear load-deflection characteristics.

Two head injury severity indices are calculated;

Head Injury Criterion (HIC)
Severity Index (SI)

3.2 HEAD VELOCITY

Figure 3-1 illustrates a typical KRASH model of a seat, occupant and head. The head velocity option calculates a time-history of a user-specified head point velocity, relative to a specified reference point. In Figure 3-1, the head point is shown as i_H, M_H (a node point), and the reference point is chosen as i_R, M_R on the floor. The relative head velocity is given in ground axes by

$$\begin{Bmatrix} \dot{x}_H \\ \dot{y}_H \\ \dot{z}_H \end{Bmatrix} = \begin{Bmatrix} \dot{xnp} \\ \dot{ynp} \\ \dot{znp} \end{Bmatrix}_{i_H, M_H} - \begin{Bmatrix} \dot{xnp} \\ \dot{ynp} \\ \dot{znp} \end{Bmatrix}_{i_R, M_R} \qquad (3\text{-}1)$$

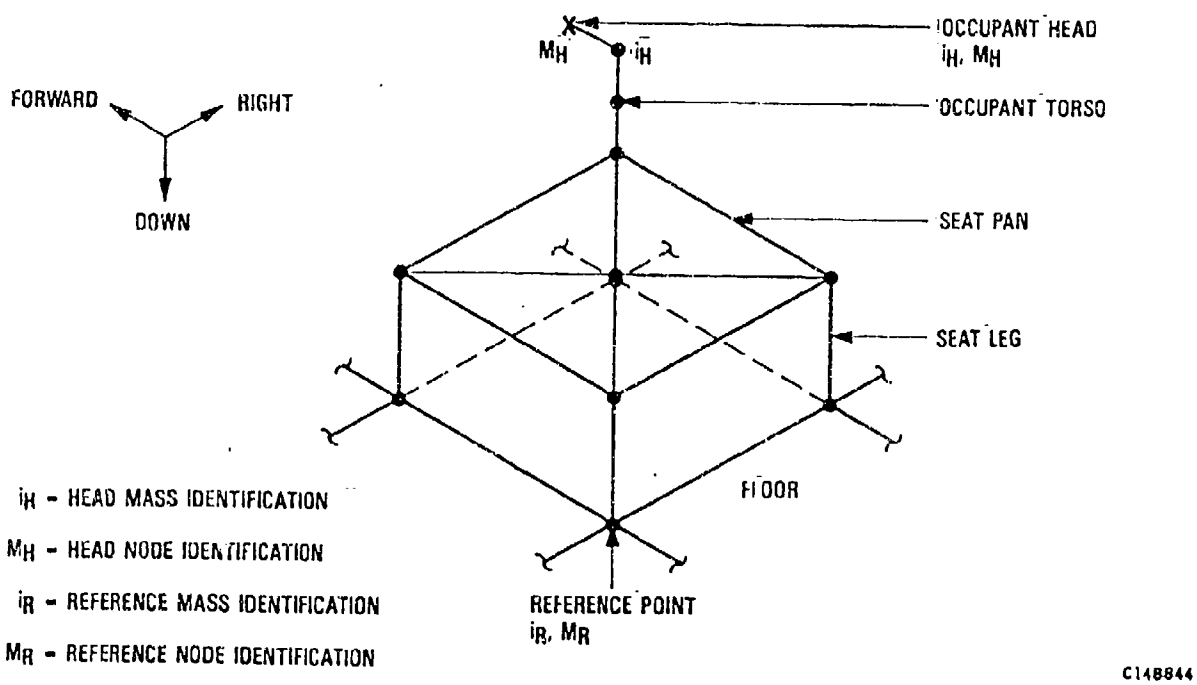

Figure 3-1. Typical Seat-Occupant-Head Model

The node point vectors on the right hand side of equation (3-1) are calculated in reference 6, Section 1.3.5.3.1. The relative head displacement, in ground axes, is calculated as

$$\begin{Bmatrix} dx_H \\ dy_H \\ dz_H \end{Bmatrix} = \begin{Bmatrix} xnp \\ ynp \\ znp \end{Bmatrix}_{i_H, M_H} - \begin{Bmatrix} xnp \\ ynp \\ znp \end{Bmatrix}_{i_R, M_R} \tag{3-2}$$

where the right hand vectors are given in reference 6, Section 1.3.5.3.1. The velocities in equation (3-1) are transformed to mass i_H axes, a system fixed in the head mass.

$$\begin{Bmatrix} U_H \\ u_H \\ w_H \end{Bmatrix} = \left[A_{i_H}\right]^T \begin{Bmatrix} \dot{x}_H \\ \dot{y}_H \\ \dot{z}_H \end{Bmatrix} \tag{3-3}$$

where the $[A_i]$ transformation matrix is evaluated for $i = i_H$. The components of equation (3-3) are used to calculate the magnitude of the resultant head velocity vector

$$V_H = \sqrt{u_H^2 + v_H^2 + w_H^2} \tag{3-4}$$

The relative displacements in equation (3-2) are transformed into an axis system fixed in the reference mass i_R.

$$\begin{Bmatrix} dx'_H \\ dy'_H \\ dz'_H \end{Bmatrix} = \left[A_{i_R}\right]^T \begin{Bmatrix} dx_H \\ dy_H \\ dz_H \end{Bmatrix} \tag{3-5}$$

For each user-defined head mass, the program output consists of a time-history table of the head velocity components (u_H, v_H, w_H), the resultant velocity V_H and the relative displacement of the x direction dx'_H. While the above equations show the general case wherein both the head point and reference points are node points, each can also be simply a mass point. Up to 20 separate head point/reference point combinations can be analyzed.

If the user wishes to calculate head impact loads based on the head velocity from equation (3-4), then a displacement dx_{impact} is input for each head point. The program compares dx'_H from equation (3-5) to the input displacement dx_{impact}. When the displacement equals dx_{impact}, then the head impact velocity is set to the current value of the time-varying head velocity V_H.

$$V_{H_{IMPACT}} = V_H \text{ when } dx'_H = dx_{IMPACT} \tag{3-6}$$

The actual head impact loads are not modeled in the main portion of KRASH. Therefore, the head impact loads do not act on the head mass, and the head mass continues to move as though no impact had occurred.

3.3 HEAD IMPACT LOAD

The load generated by a head impacting a surface is calculated in a subroutine in KRASH after the completion of the normal time history analysis. The impact velocity for the head load analysis can either be input directly by the user, or can be taken at $V_{H\text{-}IMPACT}$ from the head velocity analysis in the main time-history section of KRASH.

The head load subroutine analyzes a simple single degree-of-freedom model of a mass impacting a surface with a given impact velocity. Figure 3-2 illustrates the head impact model. The head acceleration is given by

$$\ddot{x} = -F_H/M_H \tag{3-7}$$

The head force F_H is a function of displacement x and velocity $\dot{x}$. The impact surface load-deflection models provided are illustrated in figure 3-3.

The head forces for each model are given by

$$F_{H_1} = a_1 e^{b_1 x} + c_1 \tag{3-8}$$

$$F_{H_2} = a_2 \ln (b_2 x + c_2) \tag{3-9}$$

$$F_{H_3} = k_H x + C_H \dot{x} \tag{3-10}$$

The total head force is the sum of the 3 different models.

$$F_H = F_{H_1} + F_{H_2} + F_{H_3} \tag{3-11}$$

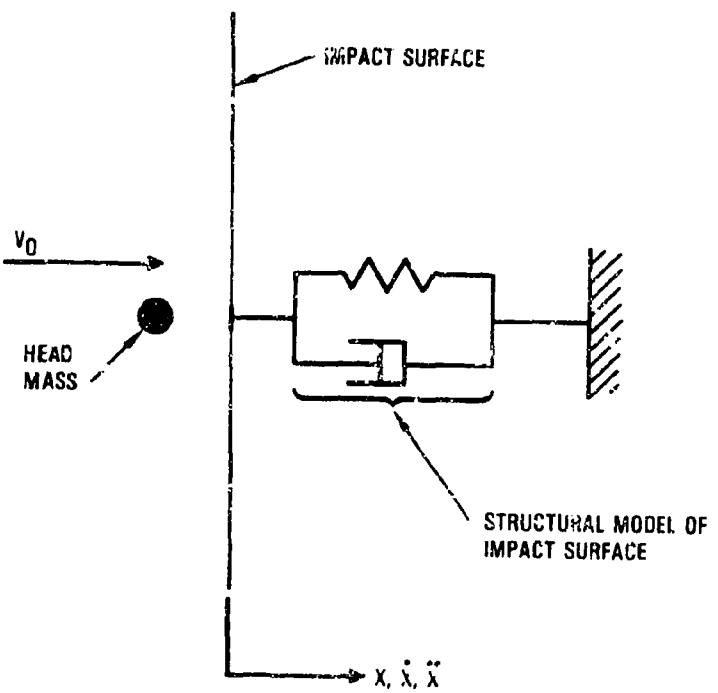

Figure 3-2. Head Impact Model

• EXPONENTIAL MODEL

$$F_{H_1} = a_1 e^{b_1 x} + c_1$$

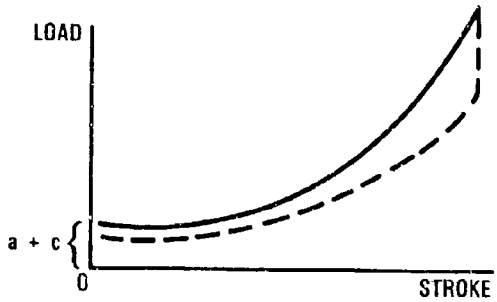

• LOGARITHMIC MODEL

$$F_{H_2} = a_2 \ell n\,(b_2 x + c_2)$$

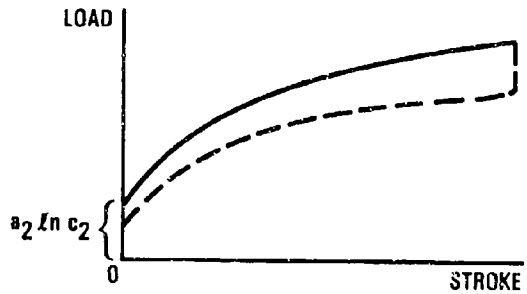

• LINEAR SPRING-DAMPER MODEL

$$F_{H_3} = k_H x + C_H \dot{x}$$

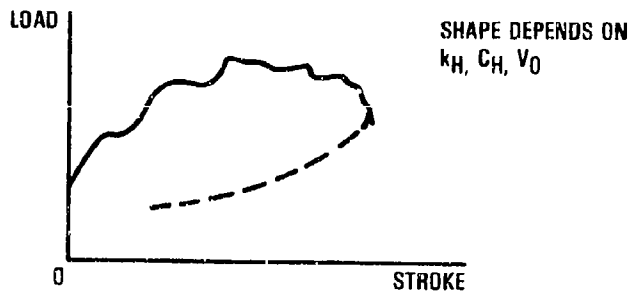

Figure 3-3. Impact Surface Structural Models

The head load during unloading ($\dot{x} < o$) is shown by the dashed lines in figure 3-3. If the damping coefficient C_H is zero, the unloading force is just an input constant times the loading force, at the current deflection.

$$F_{H_u} = C_H F_H \tag{3-12}$$

If the damping coefficient C_H is nonzero, equation (3-12) is not used, and the shape of the unloading curve is governed by the effect of C_H on F_{H3}. The total head force is also restrained to be positive; if equation (3-11) yields a negative value for any reason (usually due to a large $C_H\dot{x}$ during unloading), the total force is set to zero.

3.4 HIC AND SI CALCULATIONS

Once the time history calculations are complete, the HIC and SI can be calculated. These are given by (references 4, 5):

$$SI = \int_{t_o}^{t_f} a^{2.5}(t)dt \tag{3-13}$$

and

$$HIC = \left\{ (t_2 - t_1) \left[\frac{1}{(t_2 - t_1)} \int_{t_1}^{t_2} a(t)dt \right]^{2.5} \right\}_{max} \tag{3-14}$$

where a(t) is the time history of head acceleration in g's. For the SI calculation, t_o and t_f are the start and end times of the head acceleration time history. For the HIC calculation, equation (3-14) is evaluated with a number of t_1, t_2 combinations within the head acceleration time-history, and the largest value is taken as the HIC. Normally, the time interval $(t_2 - t_1)$ is no larger than 0.050 seconds. KRASH does not limit the time span used to calculate HIC, but the time span is printed out.

Figure 3-4 illustrates a typical head acceleration time history. Points A and B are the integration limits t_1, t_2 in equation (3-14) that result in the largest value of HIC. The contribution of $\Delta t = t_2 - t_1$ to HIC in equation (3-14) is $(\Delta t)^{-1.5}$, so larger t's reduce the HIC value. Counteracting that trend is the fact that the integral in equation (3-14) increases with increasing Δt. Therefore, the peak value occurs at an intermediate Δt, such as A-B (Δt = 0.013 sec) in figure 3-4. Tolerable levels for both HIC and SI are around 1000, although localized loading can reduce the value to around 400.

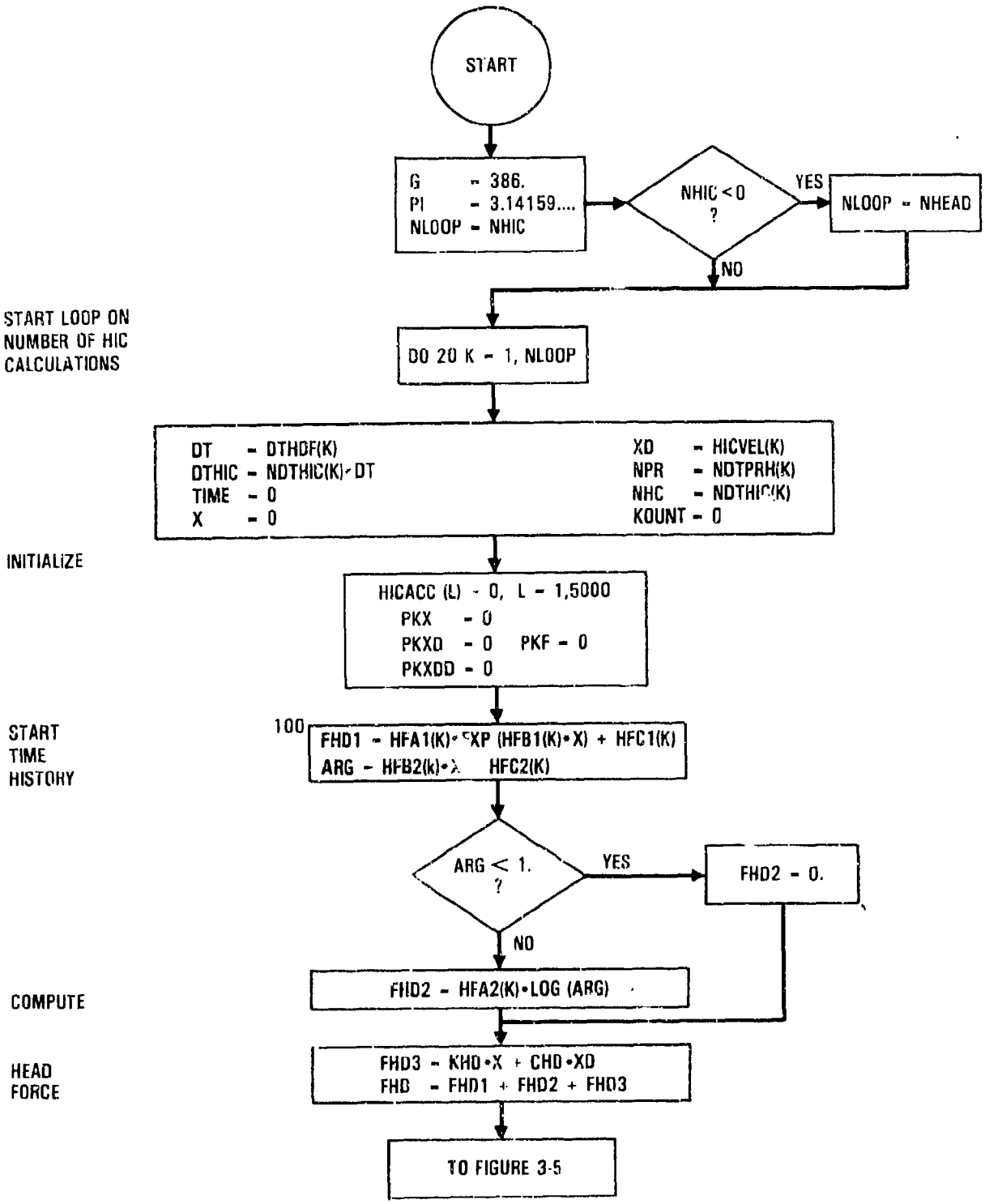

Figure 3-4. Flow Diagram for Head Impact Load Calculation

SECTION 4
SUMMARY OF RESULTS

Twenty-eight (28) reports are included in a "Water Impact" literature survey. The reports are categorized according to subject matter. For each report an abstract is presented in appendix A. Several reports, namely references A-11, -26 and -28 provide valuable design related information. These reports present some simplified analytical expressions which may be useful for design considerations. However, these reports do not provide information that can be readily incorporated into the KRASH computer code, report A-23 is considered the most useful for this purpose. Representing a transport airplane lower fuselage shape as a wedge shaped planing surface appears to yield useful results. Modeling of the report A-23 theoretical expressions expanded to include airplane pitch motions indicates that the water impact load versus depth of water penetration takes the form of a nonlinear hardening spring. A relationship is developed in between the vertical force and depth of fuselage penetration and sink rate which could be coded into KRASH. While such an approach would give useful results for the initial water impact, the subsequent impacts (e.g., wing engine) would have to be treated in a separate model.

The literature survey for soil impacts expands a previous study of 26 reports into 40 applicable reports. An abstract of each of the 40 reports is included in appendix B. The current literature survey results indicate that two basic approaches for incorporating soil interaction into the KRASH code are:

1. Empirical definition of soil pressure versus depth
2. Theoretical definition of soil as a viscoelastic medium

The empirical soil pressure versus depth approach involves several steps. The difficulty is obtaining data to cover all combinations of soil type, impacting surface shape, impact velocity, and direction. The modeling of soil as a viscoelastic medium also holds promise. This approach would require using similar approaches used to model soil and flexible tire interaction. The difficulty is expanding steady state solution to dynamic impact conditions.

This report describes the calculation of loads resulting from a head impact as a new feature in program KRASH. The program is revised to provide a new head load subroutine to analyze a simple single degree-of-freedom model of a mass impacting a surface with a given impact velocity. Both the Head Injury Criteria (HIC) and Severity Index (SI) are calculated. This report describes the procedure and flow diagram associated with this new KRASH feature.

SECTION 5
CONCLUSIONS

1. Twenty-eight (28) reports related to water impact were reviewed and evaluateded.

2. Forty (40) reports related to soil impact were reviewed and evaluated.

3. Potential approaches as well as limitations to incorporate water and soil impact equations into the KRASH coding are described.

4. The program KRASH code has been revised to provide Head Injury Ctieria (HIC) and Severity Index (SI) calculations.

SECTION 6
REFERENCES

1. Cronkhite, J. D., "Design of Airframe Structures for Crash Impact," Presented at AHS Crashworthy Design of Rotocraft meeting, Atlanta, Georgia, April 1986.

2. Wittlin, G. and Gamon, M. A., "A Method of Analysis for General Aviation Airplane Structural Crashworthiness," FAA-RD-76-123, September 1976.

3. Wittlin, G. and Gamon, M. A., "Full-Scale Crash Test Experimental Verification of Method of Analysis for General Aviation Airplane Structural Crashworthiness," FAA-RD-77-188, February 1978.

4. Laananen, D. H., "Aircraft Crash Survival Design Guide, Volume II - Aircraft Crash Environment and Human Tolerance," USARTL-TR-79-22B, January 1980.

5. Dynamic Evaluation of Transport Airplane Seats Advisory Circular, May 1985.

APPENDIX A
WATER IMPACT LITERATURE SURVEY

WATER IMPACT LITERATURE SURVEY REPORTS

1. Collopy, F. H., "Determination o the Water Impact Shock Environment," Shock & Vibration Bulletin 35, Part 7, April 1966.

2. Szebehely, V. G., "Hydrodynamic Impact," Applied Mechanics Reviews, Vol. 12, No. 5, May 1959.

3. Thompson, W. C., "Rough-Water Ditching Investigation of a Model of a Jet Transport with the Landing Gear Extended and with Various Ditching Aids," NASA TN D-101, October 1959.

4. Stubbs, S. M., and Hathaway, M. E., "Effects of Bottom Structure Flexibility on Water Landing Loads of Apollo Spacecraft Models," NASA TN D-5108, March 1969.

5. Stubbs, S. M., "Dynamic Model Investigation of Water Pressures and Accelerations Encountered During Landings of the Apollo Spacecraft," NASA-TN-D3980, September 1967.

6. Stubbs, S. M., "Water Pressures and Accelerations During Landing of a Dynamic Model of the Apollo Spacecraft with a Deployed - Heat-Shield Impact - Attenuation System," NASA-TN D-4275, March 1968.

7. Alcedo, A. M., "Design and Testing of Float Landing Gear Systems for Helicopters," Journal of AHS, 1979.

8. Verzbicki, T., and Yue, D. K., "Impact Damage of the Challenger Crew Compartment," SAE, October 1986.

9. Johnson, V. E., Jr., "Theoretical and Experimental Investigation of Supercavitating Hydrofoils Operating Near the Free Water Surface," NASA TR-R-93, 1961.

10. Van Denk, S., and Smith, C. W., "Water Entry Impact Shock on Flat Faced Cylindrical Missiles," NSWC-TR82-438, September 1982.

11. Thomas, W. L., "Ditching Investigation of a 1/20th Scale Model of the Space Shuttle Orbiter," NASA CR 2593, October 1975.

12. May, A., "Water Entry and Cavity-Running Behavior of Missiles," AD-A020 429, SEHAE, TR-75-2, 1975.

13. Johnson, R. A., "Study of Transport Airplane Unplanned Water Contact," DOT/FAA/CT-84/3, February 1984.

14. Rawls, E. A., and Kross, D. A., "A Study of the Space Shuttle Solid Rocket Booster Nozzle Water Impact Recovery Loads," Shock & Vibration Bulletin 46, August 1976.

15. Kross, D. A., Murphy, N. C., and Rawls, E. A., "Water Impact Laboratory and Flight Test Results for the Space Shuttle Solid Rocket Booster Aft Skirt," Shock & Vibration Bulletin 54' June 1984.

16. "Methods for Data Production and Loads Analysis of Space Shuttle Solid Rocket Booster Model Water Impact Tests," TN-FT-76-4, September 1976.

17. "Water Impact Test of an Aft Skirt End Ring Segment of the Space Shuttle Solid Rocket Booster (SRB)," TN-SM-83-1, March 1983.

18. "Space Shuttle Solid Rocket Booster Water Impact Cavity Collapse Loads," DP-AH-74-2, May 1974.

19. "Preliminary Water Impact Loads for the Space Shuttle Rocket Booster (SRB)'" E022-75-50' April 1975.

20. "SRB Water Impact Slapdown Loads Computer Program CN D100/SDL/ADS," TN-FT-76-5, September 1976.

21. "Computer Program for Calculation of Space Shuttle Solid Rocket Booster Nose Cone Frustrum Water Impact Loads," TN-FT-76-9, September 1976.

22. "Event Retrieval Program C/0100/Design," TN-FT-76-6, September 1976.

23. "Impact Loads on Warped Planing Surfaces Landing on Smooth and Rough Water," SIT-DL-71-1514, March 1971.

24. "A Method for Calculation of Hydrodynamic Lift for Submerged and Planing Rectangular Lifting Surfaces," NASA-TR-R-14, 1959.

25. "Comparison of Hydrodynamic - Impact Acceleration and Response for Systems with Single and with Multiple Elastic Modes," NACA-TN-4194, February 1958.

26. "Investigations of the Behavior of Aircraft When Making a Forced Landing on Water (Ditching)," R&M No. 2917, March 1957.

27. "Forces on a Flexible Shell During Impact," NASA TM X-1781, May 1969.

28. "Ditching Investigations of Dynamic Models and Effects of Design Parameters on Ditching Characteristics," NACA-TR-1347, 1958.

ABSTRACTS

1. Collopy, F. H., "Determination of the Water Impact Shock Environment," Shock and Vibration Bulletin 35, Part 7, April 1966.

Describes the various phases of the water entry phenomenon and the theoretical approach which can be utilized in deriving equations which properly describe the resulting motions.

2. Szebehely, V. G., "Hydrodynamic Impact," Applied Mechanics Review, Vol. 12, No. 5, May 1959.

The aim of this paper is to acquaint the reader with the background of and accomplishments in the field of water entry. The survey reviews the essential tools which are at the disposal of the designer, emphasizing the principles on which present day techniques are based and their applications. Attention is directed to papers of general interest, study of which might prove to be alleviatory regarding the reading of the well over two hundred publications in this field, many rediscovering a few basic principles.

Upon defining the technical subject and listing fields of applications, current theories and applicable physical principles are described. This summarizing part of the paper is followed by general comments regarding experimentations and design applications. A short literature survey is attached, which is divided into two major parts. First, papers of general interest are mentioned. This is followed by a review of the most significant publications related to seaplane landing, torpedo entry and ship slamming. A discussion of experimental papers concludes the literature survey. The last part of this review describes the present state of the art, points out fruitful areas of further work, and gives applications to missile and space technology.

3. Thompson, W. C., "Rough-Water Ditching Investigation of a Model of a Jet Transport with the Landing Gear Extended and with Various Ditching Aids," NASA TN D-101, October 1959.

The rough-water ditching characteristics of a jet transport airplane with the landing gear extended and with various ditching aids were investigated at the Langley tank catapult. A dynamic model with certain portions of the model approximately scale strength was used to determine the probable ditching behavior and to some extent the resultant damage. The ditching aids included two sets of twin hydro-skis, two sets of twin hydrofoils, and a single hydrofoil. The rough-water tests were made in waves 4 feet high by 200 feet long and 4 feet high by 120 feet long (full scale). Data were obtained from visual observations, acceleration records, and motion pictures.

A rough-water ditching with the landing gear retracted will likely result in most of the fuselage bottom being torn away and the airplane sinking within a very short time. Ditching with the landing gear extended will likely result in a dive if the main gear does not fail or in a deep run with appreciable damage throughout the fuselage bottom if the main gear fails. Hydro-skis or hydrofoils may be used to improve the ditching performance and minimize the amount of damage to the fuselage bottom.

4. Stubbs, S. M., and Hathaway, M. E., "Effects of Bottom Structure Flexibility on Water Landing Loads of Apollo Spacecraft Models," NASA TN D-5108, March 1969.

A landing investigation has been made to determine the effects of heat-shield flexibility on pressures and accelerations for water landings of Apollo spacecraft models. An additional purpose was to obtain accurate acceleration

data on the landing impact of a spherical body in water for use in refinements of rigid-body analytical calculations. Two solid models and one flexible-bottom model were tested to determine impact pressures and accelerations. The flexible bottom was scaled in stiffness from an early Apollo heatshield structural design. The test conditions were limited to symmetrical landing attitudes (0°) without horizontal velocity in order to obtain pressure profiles and loads on the bottom surfaces of the models from a limited number of data channels. Two vertical velocities were used to determine the effect of velocity on the forces applied to the flexible bottom.

Good agreement was obtained between computed and experimental acceleration results for the solid models. Results from this investigation indicate that a virtual water mass factor of 0.9 should be used in computing impact forces for rigid spherical surfaces shaped like the Apollo aft heat shield. Pressure profiles were obtained from which forces and accelerations could be derived. The pressures, forces, and accelerations on the solid models vary approximately as the square of the velocity. The data from the solid models can be accurately converted to vehicles of other scales without major problems.

Maximum forces on the bottom surface of the particular flexible-bottom model used in this investigation were approximately 6700 lb (30 kN) compared with maximum forces of 3800 lb (17 kN) for the solid model for a landing velocity of 15 ft/sec (4.6 m/sec)- Pressures, forces, and accelerations do not vary as the square of the velocity for flexible-bottom vehicles. The applied water forces on the bottom were changed substantially by the motions of the flexible structure; this indicates a significant interaction between the structural oscillations and water pressures.

5. Stubbs, S. M., "Dynamic Model Investigation of Water Pressures and Accelerations Encountered During Landings of the Apollo Spacecraft," NASA-TN-D3980, September 1967.

An experimental investigation was made to determine impact water pressures, accelerations, and landing dynamics of a 1/4-scale dynamic model of the command module of the Apollo spacecraft. A scaled-stiffness aft heat shield was used on the model to simulate the structural deflections of the full-scale heat shield. Tests were made on water to obtain impact pressure data at a simulated parachute letdown (vertical) velocity component of approximately 30 ft/sec (9.1 m/sec) full scale. Additional tests were made on water, sand, and hard clay-gravel landing surfaces at simulated vertical velocity components of 23 ft/sec (7.0 m/sec) full scale. Horizontal velocity components investigated ranged from 0 to 50 ft/sec (15 m/sec) full scale and the pitch attitudes ranged from -40° to 29°. Roll attitudes were 0°, 90°, and 180°, and the yaw attitude was 0°.

Results indicated that maximum mean water pressures on sample panel areas of the vehicle aft heat shield (areas of approximately 2 ft^2 (0.2 m^2)) were about 214 psi (1475 kN/m^2) full scale. The mean pressure at the time of maximum acceleration was approximately 60 psi (414 kN/m^2) over a heat-shield area of about 20 ft^2 (1.9 m^2) full scale. Maximum normal, longitudinal, and angular accelerations for the 30 ft/sec (9.1 m/sec) vertical velocity on water were 38g, 7.5g, and 180 rad/sec^2, respectively ($1g = 9.8\ m/sec^2$). Normal

accelerations for water landings showed pronounced oscillations due to heat-shield vibration, and the 38g maximum acceleration is higher than that expected from a rigid vehicle. The vehicle occasionally turned over for landings in water at a 0° roll attitude. The roll axis is an axis parallel to the axis of geometric symmetry. The 180° roll attitude gave much improved stability with no turnover. The vehicle was found to float stably in an upright as well as in a near inverted attitude. Waves 2 feet (0.6 m) high and 36 feet (11 m) long (full scale) failed to upset the vehicle from either flotation position.

Additional landings investigated on water, sand, and hard clay-gravel composite surfaces resulted in maximum normal accelerations of 30g, 49g, and 42.5g, respectively. Heat-shield failure occurred for all tests but one made on sand and for all tests made on the hard clay-gravel landing surfaces.

6. Stubbs, S. M., "Water Pressures and Accelerations During Landing of a Dynamic Model of the Apollo Spacecraft with a Deployed - Heat-Shield Impact - Attenuation System," NASA-TN D-4275, March 1968.

An experimental investigation was made to determine impact water pressures, accelerations, and landing dynamics of a 1/4-scale model of the command module of the Apollo spacecraft with a deployed heat shield for impact attenuation. The landing system consisted of four vertically oriented hydraulic struts and six horizontally mounted strain straps. A scaled-stiffness aft heat shield was used on the model to simulate the structural deflections of the full-scale heat shield. Landings were made at simulated vertical parachute-letdown velocities of approximately 30 ft/sec (9.1 m/sec) full scale. Horizontal velocities from 0 to 50 ft/sec (15 m/sec), full scale, were tested, and the pitch attitudes ranged from -33° to 11°. Roll attitudes were 0° and 180°, and yaw attitude was 0°.

The model investigation indicated that the maximum mean water pressure on sample panels of the spacecraft heat shield with an area of about 1.6 feet^2 (0.15 m^2), full scale, was approximately 165 psi (1140 kN/m^2). The maximum mean pressures on panels with areas of 1.9 feet^2 (0.18 m^2) and 10.9 feet^2 (1.01 m^2) were about 110 psi (760 kN/m^2). Pressures for 0° and 180° roll were similar. The maximum mean pressure at the time of maximum acceleration was approximately 18 psi (120 kN/m^2) for the deployed-heat-shield system compared with 50 psi (340 kN/m^2) for a passive landing system.

Maximum normal and longitudinal accelerations for the 0° roll condition were 25g and 6g, respectively (1g = 9.8 m/sec^2). Maximum positive and negative angular accelerations were about 95 and -55 rad/sec^2. The vehicle with the deployed heat shield was stable for all conditions investigated.

7. Alcedo, A. M., "Design and Testing of Float Landing Gear Systems for Helicopters," Journal of AHS, 1979.

Since the use of helicopters over water has become wide-spread, the U.S. Federal Aviation Agency and the British Civil Aviation Authority have developed new regulations for flotation capabilities and ditching operations. These requirements and the design and testing of flotation landing gear

systems are discussed. Differences in flotation systems pertaining to cost, weight, efficiency, and capability are presented, including differences in their supporting systems; such as, float, inflation, and actuation system designs. Model tests used to verify the capability of the designs are also discussed. Flotation and ditching model tests, methods, and scaling laws are described.

8. Werzbicki, T., and Yue, D. K., "Impact Damage of the Challenger Crew Compartment," SAE, October 1986.

A free-fall water impact of the nose section of the Challenger orbiter including the crew compartment is investigated. Assuming the structure to be perfectly rigid, forces and accelerations acting on the capsule on entering the water are determined and compared with survivability limits of occupants. The peak decelerations corresponding to terminal velocities of 140 mph (62.6 m/s) and 180 mph (80.5 m/s) respectively were found to be 100g and 150g with a duration of approximately 25 ms. On the NASA human endurance diagrams, the calculated parameters fell within the area of severe injuries.

The local pressures were also calculated and found to be of an exponentially decaying character with a maximum value in the range of 4-6 MPa (600-900 psi). A simplified rupture analysis of the outer shell acted upon by the transient pressure pulse was performed and it was found that tearing and fracture of the fuselage will certainly occur almost instantly on contacting water. The fate of the crew compartment which is located inside the outer shell will then depend, to a large extent, on the pitch attitude, with the nose-down configuration leaving the largest safety margin.

It was concluded that abrupt decelerations and loss of integrity of the cockpit upon water impact have produced severe injuries. Whether or not those injuries were fatal can only be determined by performing a more detailed study of the crash event including collapse and shattering of the outer shell, crushing of the supporting structure and secondary impact of the inner shell.

The present findings also shed some light on the problem of survivability of the primary explosion. The air blast and subsequent aerodynamic forces broke the space shuttle into several pieces but reportedly caused little damage to the shell. Assuming that this was the case, the critical value of the local pressure that would initiate tearing fracture was calculated to be 170 psi. The corresponding maximum acceleration of the nose section of the orbiter is then 210g. The minimum acceleration which is associated with breaking off the crew compartment from the rest of the orbiter has not been calculated.

9. Johnson, V. E., Jr., "Theoretical and Experimental Investigation of Supercavitating Hydrofoils Operating Near the Free Water Surface," NASA TR-R-93, 1961.

The linearized theory for infinite depth is applied to the design of two new low-drag supercavitating hydrofoils. The linearized solution for the characteristics of supercavitating hydrofoils operating at zero cavitation number at finite depth is also accomplished. The effects of camber determined from the linear theory are combined with the exact nonlinear flat-plate solution to produce nonlinear expressions for the characteristics of arbitrary sections.

The resulting theoretical expressions are corrected for aspect ratio by conventional aeronautical methods.

An experimental investigation was made in Langley tank No. 2 of two aspect-ratio-1 hydrofoils, one with a flat surface and one with a cambered lower surface. A zero cavitation number was obtained in the tank by operating the hydrofoils near the free water surface so that their upper surfaces were completely ventilated. Some data were also obtained on these sections at finite cavitation numbers. For the condition of zero cavitation number the theoretical expressions developed are compared with the results of the present experimental investigation and with experimental results from other sources. Agreement between theory and experiment is found to be good for the lift coefficient, drag coefficient, center of pressure, and location of the upper cavity streamline provided the magnitude of camber is not excessive.

The theory is used to compare the maximum lift-drag ratios obtainable from various cambered sections of approximately equal strength. The analysis reveals that the maximum lift-drag ratio is not greatly dependent on the type of camber and that for operation at depths greater than about 1 chord, a lift-drag ratio of about 10 is close to the maximum value that can be attained on a single hydrofoil supported by one strut and operating at speeds in excess of 80 knots at zero cavitation number.

10. Van Denk, S., and Smith, C. V., "Water Entry Impact Shock on Flat Faced Cylindrical Missiles," NSWC-TR82-438, September 1982.

Impact shock dynamics, including shock force and impulse as functions of time are described for a flat faced cylindrical missile striking a smooth water surface with the missile's axis either normal or oblique to the water's surface. Shock dynamics calculations were facilitated by the development of a computer program, IMPACT, the use of which is described and a code listing given.

Cavity size and shape are presented. Stability characteristics during the early running phase are also discussed. In general, the report is intended to provide the necessary data for the design of water-entry ordnance.

11. Thomas, W. L., "Ditching Investigation of a 1/20th Scale Model of the Space Shuttle Orbiter," NASA CR 2593, October 1975.

An investigation was made to determine the ditching characteristics of the space shuttle orbiter. Tests were made with a 1/20-scale model in order to determine behavior patterns and accelerations imparted to the ditching vehicle. Ditchings were made with different configurations of weight and gear position. Also, the effects of different water surface conditions were investigated.

The test results indicated that the favorable conditions for ditching usually involve a landing attitude of 12°. Smooth ditchings were always associated with the landing-gear retracted and never with the landing-gear extended. Higher landing mass, generally, resulted in higher acceleration values in both the longitudinal and normal directions. Surface waves tend to increase the pitch accelerations but at the same time tend to reduce the accelerations in the longitudinal and normal directions.

12. May, A., "Water Entry and Cavity-Running Behavior of Missiles," AD-A020 429, SEHAE, TR-75-Z, 1975.

This report contains a comprehensive compilation of test data and analytical techniques for predicting the behavior of vehicles during water entry and during the cavity-running phase. It contains data to predict the water impact forces on nose shapes such as disks, cones, ogives, spheres, cusps, disk ogives, etc., during vertical and oblique water entry. Cavity development phenomena are discussed and approximate ways of predicting cavity size and shape are presented. Stability characteristics during the early running phase are discussed. In general, the report is intended to provide the necessary data for the design of water-entry ordnance.

13. Johnson, R. A., "Study of Transport Airplane Unplanned Water Contact," DOT/FAA/CT-84/3, February 1984.

This study provides for an identification of accident scenario(s) and associated occupant risks and survival equipment needs, relating to the inadvertent or unplanned water contact of transport category airplanes. This Identification was obtained, in part, from the results of contractual studies of transport accident data. The subject study concludes that while the unplanned water contact of a transport airplane occurs less frequent than corresponding ground contract, the impact loads are often higher, leading to greater fuselage damage. Also, the unplanned water contact occurs more frequent than a planned water landing (ditching) and usually involves adverse flooding conditions. These conditions, in turn, affect the ability of occupants to retrieve, deploy and/or don on-board flotation equipment.

14. Rawls, E. A., and Kross, D. A., "A Study of the Space Shuttle Solid Rocket Booster Nozzle Water Impact Recovery Loads," Shock & Vibration Bulletin 46, August 1976.

Solid Rocket Booster (SRB) nozzle water impact environments are predicted by simplified analytical techniques in combination with scale model testing. The analytical approach, which provides preliminary design data, is based on an equivalent wedge approximation for the significant design events of maximum positive and negative applied loadings. The experimental program is performed to verify the analysis and to obtain more detailed design data.

Scale model water impact tests are conducted at the Naval Surface Weapons Center's Hydroballistics Facility using an 8.56 percent model and atmospheric pressure scaling. The vertical and horizontal initial impact velocities, as well as initial impact angle, are varied to obtain parametric loads information. Overall vehicle accelerations, local pressures, and nozzle/bulkhead interface loads are measured. Test results are compared to the analytically derived values.

15. Kross, D. A., Murphy, N. C., and Rawls, E. A., "Water Impact Laboratory and Flight Test Results for the Space Shuttle Solid Rocket Booster Aft Skirt," Shock & Vibration Bulletin 54, June 1984.

A series of water impact tests has been conducted using full-scale segment representations of the Space Shuttle Solid Rocket Booster (SRB) aft skirt structure. The baseline reinforced structural design was tested as well as various alternative design concepts. A major portion of the test program consisted of evaluating foam as a load attenuation material. Applied pressures and response strains were measured for impact velocities from 40 feet per second (ft/s) to 110 ft/s. The structural configurations, test articles, test results, and flight results are described.

16. "Methods for Data Production and Loads Analysis of Space Shuttle Solid Rocket Booster Model Vater Impact Tests," TN-FT-76-4, September 1976.

This report presents the methodology used to predict full-scale Space Shuttle Solid Rocket Booster (SRB) water impact loads from scale model test data. Tests conducted included 12.5 inch and 120 inch diameter models of the SRB. Geometry and mass characteristics of the models were varied in each test series to reflect the current SRB baseline configuration. Nose first and tail first water entry modes were investigated with full-scale initial impact vertical velocities of 40 to 120 ft/sec, horizontal velocities of 0 to 60 ft/sec., and off-vertical angles of 0 to $\pm$30 degrees. The test program included a series of tests with scaled atmospheric pressure.

Scaling relationships were established analytically and later verified by test. Full-scale equivalent loads were subsequently estimated by applying these scaling relationships to the model test data for the current SRB baseline configuration. Load distributions on the cylindrical body, aft bulkhead, nozzle and skirt were predicted for the significant dynamic events of initial impact, cavity collapse, maximum penetration, rebound and slap-down.

Loads developed during water impact were found to have a significant influence on the structural design of the SRB. Initial impact loads are critical to the design of the nozzle, aft skirt, aft bulkhead, lower cylindrical body and auxiliary components mounted in the nozzle-skirt annulus region. Loads developed during cavity collapse also define design requirements for the aft skirt and lower cylindrical body. Hydrostatic loads developed during maximum penetration are significant to the design of the lower cylindrical body, while slapdown loads influence the design of upper cylindrical body and forward skirt.

17. "Water Impact Test of an Aft Skirt End Ring Segment of the Space Shuttle Solid Rocket Booster (SRB)," TM-SM-83-1, March 1983.

This report presents results of water impact tests using an aft skirt end ring segment of the Space Shuttle Solid Rocket Booster (SRB).

The tests were conducted in January 1983 by Chrysler Corporation, for NASA/MSFC at the Hydroballistics Facility of the Naval Surface Weapons Center, White Oaks, Maryland.

18. "Space Shuttle Solid Rocket Booster Water Impact Cavity Collapse Loads," DP-AH-74-2, May 1974.

The loads developed for the Baseline 4-11-73 Configuration, with and without nozzle extension, and were defined for the significant dynamic events of

(i) Initial Impact
(ii) Cavity Formation and Collapse
(iii) Maximum Penetration
(iv) Rebound and Slapdown

Preliminary structural analyses based on previous loads indicated that the considerable loads developed on the cylindrical body of the vehicle during cavity collapse constituted design conditions for which the loads should be more precisely defined. Therefore, additional model testing was conducted to expand the data base for this refinement. The more precisely defined loads which resulted are presented here. They supersede the cavity collapse loads presented earlier for the configuration without nozzle extension.

The cavity collapse loads presented here correspond to initial impact conditions within the range of vertical velocity (V_V) of 80 to 120 ft/sec, horizontal velocity (V_H) of 0 to 45 ft/sec and impact pitch angle of 0 to $\pm 10^{\circ}$.

19. "Preliminary Water Impact Loads for the Space Shuttle Rocket Booster (SRB)," ED22-75-50, April 1975.

Water impact loads have been estimated for the Space Shuttle Solid Rocket Booster (SRB) 11/1/74 baseline configuration. Design data for the significant loading events of initial impact, cavity collapse, maximum penetration, and slapdown are presented.

20. "SRB Water Impact Slapdown Loads Computer Program CN D100/SDL/ADS," TN-FT-76-5, September 1976.

A fortran computer program was developed to calculate Space Shuttle Solid Rocket Booster (SRB) water impact slapdown lateral loads, shears and bending moments. The SRB was modeled as a rigid free/free beam. Inputs include physical properties, pressures, and accelerations. Outputs are tabular longitudinal distributions listing and a data file. This file is formatted so that it can interface directly with existing plotting software. Plots that graphically illustrate calculated and input distribution can be readily obtained.

21. "Computer Program for Calculation of Space Shuttle Solid Rocket Booster Nose Cone Frustrum Water Impact Loads," TN-FT-76-9, September 1976.

The Space Shuttle Solid Rocket Booster (SRB) Nose Cone Frustum is to be recovered at sea for reuse in subsequent flights. It will use the drogue chute of the SRB main parachute system for deceleration and is expected to impact the water within the range of V_V = 40 to 60 FPS, V_H = 0 to 45 FPS, and $\theta_i = \pm 20^{\circ}$. As model test data were not available for direct assessment of nose cone water impact loads, a computer program using empirical methods was developed to predict these loads. This document describes the analytical methods and resulting computer program employed in defining the SRB Nose Cone Frustum water impact loads.

22. "Event Retrieval Program C/0100 Design," TN-FT-76-6, September 1976.

This program C0100/DESIGN, will obtain dependent variable data as a function of three independent variables. The dependent data has been generated at Solid Rocket Booster (SRB) events. User inputs the SRB event, the independent values, and C0100/DESIGN will output all dependent variables associated with the event.

23. "Impact Loads on Warped Planing Surfaces Landing on Smooth and Rough Water," SIT-DL-71-1514, March 1971.

The impact of planing surfaces on waves is analyzed according to an extension of the theory for smooth-water impacts in a way that takes account of the influence of wave kinematics. Impacts of the type incurred by seaplanes, in which the weight of the craft is sustained by wing lift, are studied. Data for planing, which is a special case of impact, are used to obtain the needed relationship between virtual mass and hull geometry.

Impact tests with two models having different amounts of warp, or longitudinal variation of deadrise are compared with theoretical calculations. It is felt that the chines-dry planing characteristics used in the calculations, which were obtained by extrapolation of chines-wet data, were overestimated; more so for the high-warp model than for the low-warp model. Certain observations are made concerning the influence of trim, deadrise, beam loading, glide path, warp rate and waves on the initial stages of the impact, when the vertical velocity is practically uniform, on the basis of the derived differential equation of motion. Complete calculations for impact in waves have not yet been carried out.

Additional experiments to determine the effect of warp rate on chines-dry planing characteristics would be very useful.

24. "A Method for Calculation of Hydrodynamic Lift for Submerged and Planing Rectangular Lifting Surfaces," NASA-TR R-14, 1959.

A method is presented for the calculation of lift coefficients for rectangular lifting surfaces of aspect ratios from 0.125 to 10 operating at finite depths beneath the water surface, including the zero depth or the planing condition. The theoretical expression for the lift coefficient is made up of a linear term derived from lifting-line theory and a nonlinear term from consideration of the effects of crossflow. The crossflow drag coefficient is assumed to vary linearly from a maximum at an aspect ratio of 0 to zero at an aspect ratio of 10. Theoretical values are compared with experimental values obtained at various depths of submersion with lifting surfaces having aspect ratios of 0.125, 0.25, 1.00, 4, 6, and 10.

The method of calculation is also applicable to hydrofoils having dihedral where the dihedral hydrofoil is replaced by a zero dihedral hydrofoil operating at a depth of submersion equal to the depth of submersion of the center-of-load location on the semispan of the dihedral hydrofoil.

Lift coefficients computed by this method are in good agreement with existing experimental data for aspect ratios from 0.125 to 10 and dihedral angles up to 30°.

25. "Comparison of Hydrodynamic - Impact Acceleration and Response for Systems with Single and with Multiple Elastic Modes," NACA-TN-4194, February 1958.

Hydrodynamic-impact tests were made with a multimode elastic model consisting of a rigid prismatic float and a flexible wing, and the results were compared with similar experimental results for a single-mode system and with theoretical solutions. The model had a ratio of sprung mass to hull mass of 0.48 and a first-mode natural frequency of 4.38 cycles per second. The tests were conducted in smooth water at fixed trims of 3° and 9° with flight-path angles of 14° and 6°, respectively, and over a range of velocity.

The analysis of the data and comparisons with other experimental and theoretical results indicated that the applied accelerations were in agreement with those obtained by the method of NACA Report 1074 and that the higher modes present in the multimode system had no significant effect on the applied accelerations.

26. Smith, A. G., Warren, C. H. E., and Wright, D. F., "Investigations of the Behavior of Aircraft when making a Forced Landing on Water (Ditching)," R&M Report No. 2917, March 1957.

This investigation reviews the work done up to 1948 on the behavior of aircraft when making a forced landing on water. It is confined in detail to the tests made on hydrodynamic and structural performance in the Free Launching Tank at the Royal Aircraft Establishment and the Controlled Launching Tank at the Marine Aircraft Experimental Establishment, and includes an analysis of the air-sea rescue questionnaires sent in by air crews who have experienced actual ditchings. Reference is also made to parallel work in the U.S.A. and Germany. The work done is primarily concerned with the contributions made to the Air-Sea Rescue Organization in the 1939-45 war period and the determination of the ditching characteristics and requirements for post-war civil and military aircraft.

The work is analyzed in terms of the techniques of testing used and the results obtained for:

a. The best approach and touchdown techniques

b. The hydrodynamic design and structural strength requirements to permit the aircraft to float for sufficient time to allow the occupants to escape to their dinghies.

It is now possible to understand broadly what features give good ditching characteristics and also the best procedure to be adopted by the crew and/or passengers to increase their chances of survival. More quantitative test techniques with better equipment are being developed to improve this understanding and to enable rational design ditching requirements to be formed. Work is required particularly on the effect of waves, the impact forces and pressure distribution on rationalized fuselage shapes and the optimum structural design to absorb the energy of impact by local failure without producing too severe a leakage.

It is clear that design for ditching must be restricted to the cases of a good approach and good behavior on the water, and that the best and simplest ditching positions must be available for aircraft occupants, e.g., aft-facing seats, otherwise the expenditure in weight may be prohibitive. The results given in this investigation show that these prerequisites can be quite simply achieved.

27. "Forces on a Flexible Shell During Water Impact," NASA TM X-1781, May 1969.

An experimental investigation was conducted to observe the structural loads produced during water impact of a 1/4-scale model of the Apollo command module. The heat shield of the model was scaled elastically from an early Apollo heat-shield design that had a symmetric thickness.

The model was tested at full-scale vertical velocities that ranged from 16 to 25 psi and at zero horizontal velocity. Pitch angles were varied from 0° to 20° with primary emphasis at 0°.

Test results were indicative that the flexible heat-shield model experienced impact loads on the structure which were up to twice as great as experienced by a rigid shell of the same geometry and weight under the same impact conditions. Maximum impact loads occurred at a pitch angle of 0° and decreased to near rigid-shell loads at pitch angles of approximately 15°.

This report contains an analysis of the higher impact loads on the flexible heat shield and the center of gravity of the model.

28. "Ditching Investigations of Dynamic Models and Effects of Design Parameters on Ditching Characteristics," NACA-TR-1347, 1958.

Data from ditching investigations conducted at the Langley Aeronautical Laboratory with dynamic scale models of various airplanes are presented in the form of tables. The effects of design parameters on the ditching characteristics of airplanes, based on scale-model investigations and on reports of full-scale ditchings are discussed. Various ditching aids are also discussed as a means of improving ditching behavior.

APPENDIX B
SOIL IMPACT LITERATURE SURVEY

LIST OF ILLUSTRATIONS

SOIL IMPACT LITERATURE SURVEY REPORTS

1. Cheng, Robert Y. K., "Effect of Shearing Strain-Rate on the Ultimate Shearing Resistance of Clay," NASA CR-2634, February 1976

2. Cook, C. E. and Gargiulo, J. D., "An Investigation of Landing Gear-Soft Soil Interaction Utilizing the OV-10A Aircraft," North American Aviation/Columbus, North American Rockwell, NR 70H-570, January 1971.

3. Crenshaw, B. M., "Aircraft Landing Gear Dynamic Loads Induced by Soil Landing Fields, Vol. I: Prediction Model and Wheel Loads," Flight Dynamics Laboratory, Wright-Patterson Air Force Base, AFFDL-TR-70-169, Vol. I, June 1972.

4. Crenshaw B. M., "Development of an Analytical Technique to Predict Aircraft Landing Gear/Soil Interaction," Flight Dynamics Laboratory, Wright-Patterson Air Force Base, AFFDL-TR-74-115, Vol. I and II, January 1975.

5. Crenshaw, B. M., Butterworth, C. K., and Truesdale, W. B., "Aircraft Landing Gear Dynamic Loads from Operation on Clay and Sandy Soil," Flight Dynamics Laboratory, Fright-Patterson Air Force Base, AFFDL-TR-69-51, February 1971.

6. Freitag, D. R., Green, A. J., and Murphy, Jr., N. R., "Normal Stresses at the Tire-Soil Interface in Yielding Soils," U.S. Army Engineer Waterways Experiment Station, Corps of Engineers, Misc. Paper No. 4-629, February 1964.

7. Green, A. J., "Performance of Soils Under Tire Loads, Report 5: Development of Mobility Numbers for Coarse-Grained Soils," Army Engineer Waterways Experimental Station, Corp of Engineers, Technical Report No. 3-666, July 1967.

8. Kraft, D. C., "Analytical Landing Gear-Soil Interaction-Phase I," Flight Dynamics Laboratory Wright-Patterson Air Force Base, AFFDL-TR-68-88, August 1968.

9. Kraft, D. C., Hoppenjans, J. R., and Edelen, Jr., W. F., "Design Procedure for Estimating Aircraft Capability to Operate on Soil Surfaces," Flight Dynamics Laboratory, Wright-Patterson Air Force Base, AFFDL-TR-72-129, December 1972.

10. Kraft, D. C., Luming, H., and Hoppenjans, J. R., "Aircraft Landing Gear-Soils Interaction and Flotation Criteria, Phase II:" Flight Dynamics Laboratory, Wright-Patterson Air Force Base, AFFDL-TR-69-76, November 1969.

11. Kraft, D. C., Luming, H., and Hoppenjans, J. R., "Multiwheel Landing Gear-Soils Interaction and Flotation Criteria-Phase III," Flight Dynamics Laboratory, Wright-Patterson Air Force Base, AFFDL-TR-71-12, May 1971.

12. Ladd, D. W., "Ground Flotation Requirements for Aircraft Landing Gear," Army Engineer Waterways Experiment Station, Corps of Engineers, Miscellaneous Paper No. 4-459, July 1965.

13. Ladd, D., and Ulery, Jr., H., et al, "Aircraft Ground-Flotation Investigation," Parts I-XIX, Flight Dynamics Laboratory, Wright-Patterson Air Force Base, AFFDL-TDR-66-43, Parts I-XIX, August 1967.

14. Leland, T. J. W. and Smith, E. G., "Aircraft Tire Behavior During High Speed Operations in Soil," NASA TN D-6813, August 1972.

15. Richmond, L. D., Brueske, N. W., and DeBord, K. J., et al, "Aircraft Dynamic Loads from Substandard Landing Sites:" Flight Dynamics Laboratory, Wright-Patterson Air Force Base, AFDL-TR-67-145, Parts I-V, September 1968.

16. Sharp, A. L., "Computer Programs for the Prediction of Aircraft Takeoff Performance on Clay and Sand Airfields," Flight Dynamics Laboratory, Wright-Patterson Air Force Base, AFFDL-TR-68-115, April 1969.

17. Truesdale, W. B. and Nelson, R. D., "Aircraft Landing Gear Dynamic Loads Induced by Soil Landing Fields, Vol. II: Soil Tests and Soil Response Studies:" Flight Dynamics Laboratory, Wright-Patterson Air Force Base, AFFDL-TR-70-169, Vol. II, June 1972.

18. Turnage, G. W., and Green, Jr., A. J., "Performance of Soils Under Tire Loads. Analysis of Tests in Sand from September 1962 Through November 1963," U.S. Army Engineer Waterways Experiment Station, Corps of Engineers, Technical Report No. 3-666, Report 4, February 1966.

19. Van Deusen, B. D., "A Statistical Technique for the Dynamic Analysis of Vehicles Traversing Rough Yielding and Non-Yielding Surfaces:" NASA CR-659, March 1967.

20. Eiband, A. M., Simpkinson, S. H., and Black, D. O., "Accelerations and Passenger Harness Loads Measured in Full-Scale, Light-Airplane Crashes:" NACA TN 2991, August 1953.

21. Wignot, J. E., et al, "Aircraft Dynamic Wheel Load Effects on Airport Pavements," Lockheed-California Company, Federal Aviation Administration, FAA-RD-70-19, May 1970.

22. Preston, G. M. and Pesman, G. J., "Accelerations in Transport-Airplane Crashes:" NACA TN 4158, February 1958.

23. Reed, W. H., et al, "Full-Scale Dynamic Crash Test of a Lockheed Constellation Model 1649 Aircraft," Aviation Safety Engineering and Research, Federal Aviation Agency, FAA-ADS-38, October 1965.

24. Reed, W. H., et al, "Full Scale Dynamic Crash Test of a Douglas DC-7 Aircraft," Aviation Safety Engineering and Research, FAA Technical Report ADS-37, Federal Aviation Administration, Washington, D.C., April 1965, AD 624051.

25. Sela, A. D., and Ehrlich, I. R., "Load Support Capacity of Flat Plates of Various Shapes in Soil," Automotive Engineering Congress, Society of Automotive Engineers, Paper No. 710178, January 1971.

26. Whitman, R. V., and Healy, K. A., "Shear Strength of Sands During Rapid Loadings," Journal of the Soil Mechanics and Foundations Division, Procedings of the American Society of Civil Engineers, April 1962.

27. Wittlin, G., Gamon, M. A., and LaBarge, W. L., "Full Scale Crash Test Experimental Verification of a Method of Analysis for General Aviation Structural Crashworthiness," FAA-RD-77-188, February 1978.

28. Cheng, R. Y. K., "Soil Analyses and Evaluations at the Impact Dynamics Research Facility for two Full-Scale Aircraft Crash Tests," NASA CR 159199, August 1977.

29. Vaughan, V. Jr. and Hayduk, R. J., "Crash Tests of Four Identical High-Wing Single-Engine Airplanes," NASA TP 1699.

30. Castle, C. B.and Alfaro-Bou, E., "Crash Tests of Three Identical Low-Wing Single-Engine Airplanes," NASA TP-2190, September 1983.

31. Laananen, D. H., et. al., "Aircraft Crash Survival Design Guide, Volume III-Aircraft Structural Crashworthiness," USARTL-TR-79-32C, August 1980.

32. PI, W. S., "A Dynamic Tire/Soil Contact Surface Interaction Model for Aircraft Ground Operations," AIAA Paper 85-0708, 1985.

33. Shanks, D. H., Barnett, R. V., "Performance of Aircraft Pneumatic Tires in Soft Soil," Aeronautical Journal, January 1981.

34. Cassino, V., "Soft Airfield Tests with F-4 Aircraft," ESL-TR-82-18, December 1981.

35. Hay, D. R., "C-141A Ground Flotation Test on Landing Mat and Unsurfaced Runways-Civil Engineering Support," AFW-TR-70-30, 1970.

36. Trafford, J. W., et. al., "Aircraft Tire Behavior During High-Speed Operating in Soil," NASA TN D-6813, August 1972.

37. Turnage, G. W., et. al., "Prediction of Aircraft Ground Performance by Evaluation of Ground Vehicle Rut Depths," AD-775744, February 1974.

38. Tsai, K., "Strength Response Parameters of Natural Soil Surfaces and Their Landing Problem of Aircraft," AF19 (628)-5873 January, 1967.

39. Doyle, Jr., G. R., "A Review of Computer Simulation for Aircraft-Surface Dynamics," Jr. of Aircraft, Vol. 23, No. 4, April 1986.

40. Poor, A. P., "Soil Response of Three Geometric Shapes During Impact," Ph.D. Dissertation, May 1965.

ABSTRACTS

1. Cheng, Robert Y. K., "Effect of Shearing Strain-Rate on the Ultimate Shearing Resistance of Clay," NASA CR-2634, February 1976.

This report describes laboratory tests performed to determine the shearing resistance of cohesive soils subjected to strain rates between 1 and 14 rad/sec. A fast step-loading torque apparatus was used to induce a state of pure shear in a hollow cylindrical soil specimen. The relationship between shearing resistance and rate of shear deformation was established for various soil densities expressed in terms of initial water content.

The results of the tests described in this report show that the shearing resistance increases initially with shearing velocity, but subsequently reaches a terminal value as the shearing velocity increases. The terminal shearing resistance was found to increase as the density of the soil increases.

Mississippi Buckshot Clay was used in all the tests described in this report. This is the same type of clay used in the test beds at the NASA-Langley facility for the measurement of drag loads on aircraft tires during high-speed operations in clay soil.

2. Cook, C. E. and Gargiulo, J. D., "An Investigation of Landing Gear-Soft Soil Interaction Utilizing the OV-10A Aircraft," North American Aviation/Columbus, North American Rockwell; NR 70H-570; January 1971.

This report presents the results of a study to investigate the interaction between the landing gear of the OV-10A airplane and soft soil. Sixteen landing and takeoffs were made by the OV-10A on soft unprepared terrain. Two fifty-channel oscillographs were used to measure time histories of airplane response. Measurements were also taken of the terrain contour and static and dynamic strengths of the soil. Landings were successfully performed with soil penetrometer (static strength) readings as low as 40 (static load of 20 psi) for sink speeds as great as 16 feet per second.

An analytical model of soil is developed by assuming that the static and dynamic strength properties of soil may be represented by a second order differential equation with variable stiffness and damping coefficients. These are determined from experimental data from penetrometer and a specially constructed cylinder drop test vehicle.

An analytical model of a pneumatic tire on soft soil is also developed. The primary inputs to the model are the vertical and drag forces generated by the soil model.

Equations of motion are presented for a mathematical model of the OV-10A landing and taking off from yieldable uneven terrain. This model simulates the soil-tire interactions, landing gear-airplane interactions, and airplane dynamic response. A system of 20 non-linear, coupled second order differential equations are used. Analytical determination of landing gear loads for correlation with experimental data was included in the work to be performed under this contract. However, this task could not be accomplished within the allocated funds.

3. Crenshaw, B. M., "Aircraft Landing Gear Dynamic Loads Induced by Soil Landing Fields, Vol. I: Prediction Model and Wheel Loads," Flight Dynamics Laboratory, Wright-Patterson Air Force Base; AFFDL-TR-70-169, Vol. I; June 1972.

This report presents the results of a study to develop a mathematical model to predict sinkage and the resulting loads for aircraft wheels operating on bare soil together with experimental results using a 29x11 10PR Type III tire. Four primary factors which determine soil rutting and drag have been identified. They consist of the tire spring rate, the soil load deflection relation, a drag inertia force, and a lift inertia force. Soil load deflections are based on the mobility number concept developed by the U.S. Army Corps of Engineers Waterways Experiment Station (WES). Empirical constants obtained from tests conducted at the NASA-Langley Landing Loads Track were used to compute the inertia forces. Comparisons of predicted and measured rut depths and drag loads are made for a clay soil with CBR's ranging from 1.5 to 2.3 and speeds from 0 to 90 knots for tire inflation pressures of 30, 45, and 70 psi. Similar comparisons are made for sand having a surface strength of CBR 1.5. The experimental program included 173 tests with a single wheel and 39 tests with two wheels in tandem on buckshot clay and 24 single wheel tests on sand. Overall average differences between predictions and test data for rut depths were the following: 11% on CBR 1.5, less than 1% on CBR 2.3, and 1.5% on sand. Overall average differences for drag loads were the following: 6% on CBR 1.5, 9% on CBR 2.3, and 12% on sand. Average positive and negative differences were somewhat higher and were between 11% and 36%. An alternate computation using a spring-mass-damper model as used in vibrating foundation studies is also included. This alternate model is not recommended as it does not account for drag load interaction and thus is not representative of the physical system. Methods for improvement of the alternate model are discussed. A computer program is described which incorporates the soil/wheel interaction model with a simulation of the C-130 aircraft during taxi and take-off. Analyses with this program show that moderate roughness has negligible effect on take-off distance for either soft fields or hard surfaces.

4. Crenshaw, B. M., "Development of an Analytical Technique to Predict Aircraft Landing Gear/Soil Interaction," Flight Dynamics Laboratory, Wright-Patterson Air Force Base, AFFDL-TR-74-115, Vol. I and II, January 1975.

This report describes methods and evaluating techniques for determining aircraft takeoff performance, loads, and capabilities for operation on soil surface airfields. In addition to take-off and landing distance evaluations, considerations have also been given to ground operations such as landing impact, taxi, and turning. Calculation procedures have been developed and criteria recommendations made.

A revised soil model has been developed to incorporate soil load deflection curves and to allow for a more meaningful physical representation of the soil response available at the time (1974). The new model includes the horizontal shear effects resulting from "skid sinkage."

A series of computer programs were developed during the course of this program for calculating aircraft loads and dynamic response on unpaved surfaces. For given soil strength and surface roughness, these programs compute rut depth, soil drag loads, aircraft gear loads, and structural accelerations as functions of time and include the dynamic interaction between the aircraft and the flexible soil surface.

5. Crenshaw, B. M., Butterworth, C. K., and Truesdale, W. B., "Aircraft Landing Gear Dynamic Loads from Operation on Clay and Sandy Soil," Flight Dynamics Laboratory, Wright-Patterson Air Force Base; AFFDL-TR-69-51; February 1971.

This report presents results of tests to obtain experimental data on wheel performance on soil over a speed range of 0 to 100 knots. The tests were conducted on three soil strengths, CBR 1.5, 2.3 and 4.4 for buckshot clay and CBR 1.5 for sand. The configuration tested was single 29 x 11-10 8PR tire loaded by 5000 pounds ballast weight. In addition to soil type and strength variations, the test variables were tire pressure and speed. Loads and rut depths were obtained for both free rolling and braking conditions. Free rolling drag ratios (μ) as high as 0.45 were obtained for soils with a CBR of 1.5. The drag ratio for free rolling decreased with increasing soil strengths. During braking, drag ratios as high as 1.0 were obtained for soft soils but approached more conventional values with increasing soil strength. The rut depth was a maximum at zero forward velocity and decreased with increasing forward velocity but reached another maxima in the 30 to 50 knot speed range and then decreased for the higher speeds. Rut depths of about 2.2 inches were obtained on CBR 1.5 and 1.2 inches for CBR 2.3 for speeds greater than zero. Rut depths for static conditions were considerably greater. Similar responses were obtained on the sand surfaces. This program has established that there is a pronounced high speed interaction between a wheel and a soft surface. This interaction is most pronounced for soft surfaces and high tire pressures; it is reduced if either the tire pressure is reduced or if the soil strength is increased. An analog computer program of the C-130 airplane was developed to incorporate the high speed effects found during the tests into a soil-gear interaction model. Results from this computer program compared loads from paved and soft soil runways. Where soil surfaces were considered in the simulation, wing shear loads are smaller because gear vertical loads are attenuated by an effective reduction in profile amplitudes on the yielding surface. This testing has generally verified empirical prediction methods for drag ratios for low speeds but does not agree well for the higher speeds. Wheel drag loads were found to vary linearly with rut depth.

6. Freitag, D. R., Green, A. J., and Murphy, Jr., N. R., "Normal Stresses at the Tire-Soil Interface in Yielding Soils," U.S. Army Engineer Waterways Experiment Station, Corps of Engineers, Misc. Paper No. 4-629, February 1964.

This paper describes the results of tests made to measure the distribution of stresses at the tire-soil interface under some representative test conditions. Two soils, a sand and a clay, carefully placed in a test pit, were used in the program. Each soil was tested at three different levels of strength. A single 11.00 x 20 12PR military tire at one test load was employed. Stresses,

however, were measured at several different inflation pressures. Tests were performed with the wheel powered and with it towed at a constant speed of approximately 0.7 mph.

The results of the test performed indicate that the resultant of the normal stress field at the tire-surface interface passes through the center line of the wheel axle for both towed and powered wheels. These results are restricted to very slow moving vehicles, however.

7. Green, A. J., "Performance of Soils Under Tire Loads, Report 5: Development of Mobility Numbers for Coarse-Grained Soils," Army Engineer Waterways Experimental Station, Corporation of Engineers, Technical Report No. 3-666, July 1967.

This report describes the results of a study to examine the effects of tire deflection, tire geometry, wheel load, and soil strength on the performance of coarse-grained soils subject to moving tire loads. Empirical criteria were developed based on analysis of test results that combine the independent parameters of the soil-vehicle system and relate them to dependent performance characteristics such as sinkage, towed force, etc. A combination of independent parameters called mobility numbers were developed which account for the combined effects of soil strength, tire section width and diameter, wheel load, and tire deflection on wheel performance as measured by performance coefficients. The mobility numbers developed in this study are applicable to single wheels operating on sand at speeds common to surface vehicles.

A multiple-pass analysis was conducted to illustrate that performance on the second and third passes also can be related to the sand mobility number, although the relation was not the same as that for the first pass. It is shown in a similar fashion that the performance of vehicles on coarse-grained sand can be predicted using a relation based on the sand mobility number.

8. Kraft, D. C., "Analytical Landing Gear-Soil Interaction-Phase I," Flight Dynamics Laboratory, Wright-Patterson Air Force Base, AFFDL-TR-68-88, August 1968.

This report describes the results of a study to determine the variables which significantly influence aircraft performance when operating on soil runways.

Analysis of available experimental drag-sinkage-velocity data led to the defining of at least three distinct regions for which the sinkage ratio-velocity relationship shows a distinct response. These velocity regions are 0-5 knots, 5-50 knots, and velocities greater than 50 knots. A drag ratio-sinkage ratio lease square fit was developed for use in the second of these velocity regions. The effects of twin wheel arrangements were analyzed on a preliminary basis. The results of a sinkage study using available (1968) prediction methods indicates that present sinkage analysis accuracy is in the range of $\pm$50% to $\pm$100%.

In order to develop a suitable flotation criteria, an investigation was conducted into a dynamic landing gear contacting element-soil interaction response model, utilizing elastic theory. These results led to the development of a flotation parameter (related to sinkage) and a flotation index (related to drag) in nomographic form, which permits comparative flotation analysis of landing gear systems.

9. Kraft, D. C., Hoppenjans, J. R., and Edelen, Jr., W. F., "Design Procedure for Estimating Aircraft Capability to Operate on Soil Surfaces," Flight Dynamics Laboratory, Wright-Patterson Air Force Base, AFFDL-TR-72-129, December 1972.

This report describes a systematic design procedure for establishing various landing gear combinations of tire size, spacing, and configuration which will minimize rolling drag and satisfy the criteria of 200 non-braking passes for aircraft having take-off/landing weights of 150,000 to 250,000 lbs. and low horizontal speeds (close to or less than 40 knots), operating on a standardized CBR 6 (or equivalent) soil surface. The design procedure presented combines the latest results (1972) of Air Force sponsored landing gear/soil interaction research with previously developed Army Corps of Engineers Waterways Experiment Station (WES) coverage technique.

The procedure is a first attempt to make the research results of existing Air Force Flight Dynamics Laboratory programs available toward the improvement of flotation design capability. The design procedure, subject to certain stated limitations, includes techniques for (1) predicting rolling and braking drags and drag ratios, (2) incorporating multiwheel influences on drag and sinkage, and (3) determining allowable aircraft passes. Additionally, the design procedure has been incorporated in a computer program format for utilization on the CDC 6600 located at Wright-Patterson Air Force Base. The computer program is restricted to aircraft with tricycle type landing gear systems.

10. Kraft, D. C., Luming, H., Hoppenjans, J. R., "Aircraft Landing Gear-Soils Interaction and Flotation Criteria, Phase II," Flight Dynamics Laboratory, Wright-Patterson Air Force Base, AFFDL-TR-69-76, November 1969.

This report describes the results of an investigation directed at defining landing gear-soil interaction and developing flotation criteria to permit comparative evaluation of the relative merits of various landing gear configurations.

A basic aircraft tire-soil interaction equation relating the drag ratio (R/P) to sinkage ratio (Z/D) was developed for the velocity range 5 knots to 40 knots. The influence of high velocity and multiple wheel configurations on flotation performance was determined on a preliminary basis. Empirical sinkage prediction equations were developed for predicting the sinkage of aircraft type tires on cohesive and cohesionless soils with an estimated accuracy of $\pm 40\%$ within the 90% confidence limits. The results of the Single Wheel Verification Tests are reported and used to verify the developed flotation analysis equations.

An analytical approach to sinkage prediction using finite element techniques was developed to give a more rational approach to sinkage analysis. The soil was assumed to be an elastic-perfectly plastic medium. The results of this analytical approach as given by the computer program developed during this study and the results of a test case evaluation are described in detail.

A preliminary Single Wheel Relative Merit Index (RMI) was developed for permitting a comparative evaluation of the flotation characteristics of aircraft tires on soil. The RMI was used to rate the flotation capacity of aircraft tires currently used on cargo, bomber, and fighter aircraft.

11. Kraft, D. C., Luming, H., and Hoppenjans, J. R., "Multiwheel Landing Gear-Soils Interaction and Flotation Criteria-Phase III," Flight Dynamics Laboratory, Wright-Patterson Air Force Base, AFFDL-TR-71-12, May 1971.

This report describes the results of the third phase of a study to analytically define landing gear-soil interaction and to develop a system for rating the relative flotation capacity of landing gear contact elements and landing gear systems during aircraft operation on semi and unprepared soil runways. During this phase, existing data relating drag ratio to multiwheel geometry parameters were collected and summarized. Also, twin plate vertical load tests were performed to determine the sinkage interaction effects produced by adjacent dynamic plate loads as compared to a single isolated plate load under similar test conditions.

A computer program has been developed to study the effects of multiwheel landing gears on the sinkage of tires into soil. The trends shown in these results were consistent with those observed in the twin plate vertical load test.

Based on the results of this study, multiwheel criteria were developed which permit the evaluation of aircraft flotation performance. The criteria also permits aircraft designers to determine optimum landing gear configuration for aircraft leading to drag minimization. Available and proposed flotation/operation criteria are outlined.

12. Ladd, D. W., "Ground Flotation Requirements for Aircraft Landing Gear," Army Engineer Waterways Experiment Station, Corps of Engineers, Miscellaneous Paper No. 4-459, July 1965.

This paper presents a set of design curves which can be used to assist the aircraft designer in designing a landing gear that will support a given aircraft load without overloading an airfield of stated strength. Seven classes of Zone-of-Interior and Theater-of-Operation airfields are defined to which the design curves presented specifically apply. The landing gear design parameters included are number of wheels, spacing of wheels, tire contact area, gear type, and load range.

13. Ladd, D., and Ulery, Jr., H., et al, "Aircraft Ground-Flotation Investigation," Parts I-XIX, Flight Dynamics Laboratory, Wright-Patterson Air Force Base, AFFDL-TDR-66-43, Parts I-XIX, August 1967.

This report summarizes results of an extensive study to develop a method for designing an efficient landing gear configuration for aircraft required to operate on Theater-Of-Operation class airfields. The method was developed from a series of ground-flotation tests conducted on mat-surfaced subgrades and unsurfaced subgrades. Also presented is a discussion of the testing procedures and techniques and of the analysis of all tests conducted in conjunction with the ground flotation investigation, including tracking, drag, and speed tests.

To develop criteria for the efficient design of aircraft landing gears, a series of traffic tests were conducted with numerous wheel configurations, loads, and tire pressures. The configurations varied from a single wheel up to 12 wheels; loading weights varied from 1000 to 273000 pounds; tire pressure ranged from 10 to 250 psi; and wheel spacing varied from 2.0 radii up to 6.8 radii. From data developed from these tests, a generalized single wheel criteria was developed. Speed versus drag relations were obtained from scale model tests in which various speeds, loads, tire pressures and tire sizes were investigated.

14. Leland, T. J. W. and Smith, E. G., "Aircraft Tire Behavior During High-Speed Operations in Soil:" NASA TN D-6813; August 1972.

An investigation to determine aircraft tire behavior and operating problems in soil of different characteristics was conducted at the Langley landing-loads track using a 29 x 11.0-10 SPR Type III tire. Four clay test beds of different moisture content and one sand test bed were used to explore the effects on axle drag loads developed during operation at different tire inflation pressures in free rolling, locked-wheel braking, and yawed (cornering) modes, all at forward speeds up to 95 knots.

The test results indicate that, in general, axle drag loads are highly dependent on forward velocity, with loads initially decreasing from static or low speed and then rising sharply with increasing forward speed to a peak in the velocity range of 40 knots for the configurations tested. Further increases in speed bring about a reduction in drag load by a phenomena not presently understood. In addition, for a given soil strength, the magnitude of the axle drag load is strongly a function of tire inflation pressure with higher inflation Pressures resulting in higher axle drag coefficients.

15. Richmond, L. D., Grueske, N. W., DeBord, K. J., et al, "Aircraft Dynamic Loads from Substandard Landing Sites:" Flight Dynamics Laboratory, Wright-Patterson Air Force Base, AFDL-TR-67-145, Part I-V, September 1986.

This report describes the results of a detailed study of ground-induced dynamic loads resulting from operations on substandard airfields. The study was divided into 5 phases. A mathematical model to study tire-soil interaction effects was developed in Phase I. Phase II was a site selection and field measurement program to obtain field roughness profiles and soil strength information from fields typical of those expected to be found in remote theaters of operations. The information from Phases I and II was used in Phase III to conduct comprehensive airplane ground-load dynamic analyses

and (2) formulate airplane design loads and criteria. The development of the tire-soil model was based on the results of a literature survey and experimental data collected from the 367-80 airplane (707/KC-133 prototype) during high-flotation taxi tests conducted by The Boeing Company at Harper Lake, California, in September 1964. The development resulted in empirical expressions that related soil sinkage and rolling resistance to soil strength, tire vertical force, tire characteristics, and taxi velocity. The original development of the empirical non-dimensional expressions was accomplished by the U.S. Army Corps Engineer Waterways Experiment Station (WES). The results of the literature survey and the tire-soil model development obtained during the phase I study are presented in Part II. A total of 9 substandard sites were selected for field measurements from approximately 27 sites visited. These sites, located throughout the United States were selected on the basis of their availability to the field survey team and their suitability as a forward-area airfield. The profiles on these sites represented various degrees of preparation, from semi-prepared to unprepared, and included a variety of soil types. Soil strength measurements and soil samples were collected at each site and the profile roughness was measured. These measurements are presented in Parts III and IV. Phase III was an analytical study to determine the dynamic loads and degradation in takeoff performance of airplanes operating from substandard airfields. Digital and analog computer models simulating the 367-80 airplane in a high flotation configuration were used to conduct the landing impact, taxi, and landing-and-takeoff-distance analysis. The effects of soil strength and profile roughness were included. Parametric variations of tire pressure, gross weight, and taxi velocity were also examined. Prior to the dynamic analysis, a statistical analysis of the profile data was performed. From this data, artificial profiles and sets of discrete one-minus-cosine bumps representative of one of the measured profiles were generated. The dynamic loads resulting from excitation due to the artificial profile and the discrete bumps were compared to the loads from the actual profile. The landing impact analysis was performed using a model similar to the taxi-analysis model except that soil flexibility was not included. A smooth, rigid surface was used in determining the maximum gear and airplane loads developed during landing impact. The takeoff-and-landing-distance performance analysis was performed using a structurally rigid model operating on a smooth, soft soil surface. The effects of changes in the soil strength, tire inflation pressure, and gross weight on takeoff distances were examined. The variation in landing distance with braking coefficient was investigated.

From the results of this study, it was concluded that the simplified soil representation was satisfactory for the taxi analysis because of the relatively small influence that the soil strength has on dynamic loads. The effects of surface roughness were most pronounced on the dynamic loads. For analysis purposes, the discrete excitation will give peak loads that are conservative, while the artificial runways will give results that are unconservative. The results indicate that this class of airplane could successfully operate from semi-prepared sites with only minor modifications to current criteria and operating procedures. It does not seem feasible to operate this class of airplane from the unprepared sites examined in this study.

16. Sharp, A. L., "Computer Programs for the Prediction of Aircraft Takeoff: Performance on Clay and Sand Airfields," Flight Dynamics Laboratory, Wright-Patterson Air Force Base, AFFDL-TR-68-115, April 1969.

This report describes a prediction method for estimating wheel sinkage, landing gear drag, and aircraft take-off performance on clay and sand airfields of various bearing strengths. The method is based on a method developed by Boeing (AFFDL-TR-67-145) which uses modified Mobility Numbers developed by the Army Waterways Experiment Station (WES). Estimates of take-off distance, wheel drag to vertical force ratios for the full ground velocity range, and the wheel sinkage into the soils are prepared for the C-5 and C-141 aircraft.

Three FORTRAN IV computer programs were developed based on the methods generated by Boeing and WES. The first of these is used to calculate drag and sinkage for wheels attached to one strut while taxiing at constant speed. The second considers the complete aircraft taxiing at constant velocity and the third calculates takeoff performance of a complete aircraft on hard surface (paved runways) and on clay and sandy soils. The computer programs were tested for accuracy by analyzing conditions which were identical to those used by Boeing and comparing the results with Boeing's full scale airplane tests.

17. Truesdale, W. B. and Nelson, R. D., "Aircraft Landing Gear Dynamic Loads Induced by Soil Landing Fields, Vol. II: Soil Tests and Soil Response Studies:" Flight Dynamics Laboratory, Wright-Patterson Air Force Base, AFFDL-TR-70-169, Vol. II, June 1972.

This report contains a description of the construction and maintenance of the buckshot clay test bed used for tandem and single wheel high speed landing gear tests conducted at the NASA Langley Landing Loads Track. The test bed was constructed to a CBR strength of 2.7, moisture content of 32.5 percent, dry density of 86.0 pcf, degree of saturation of 91.7 percent, and airfield penetration resistance of 1.7 to 1.8. Analysis of dynamic soil behavior indicated that wave propagation velocities in the soil and soil inertia effects become significant at forward velocities greater than 60 knots. Strain-rate effects are significant at all velocities for buckshot clay and cause 50 to 60 percent increases of shear strength at a forward velocity of 50 knots. Strain-rate effects on sand are insignificant except when pore pressures are developed. The wheel will "outrun" the bow wave or shear wave propagating ahead of the wheel at forward velocities greater than the 150 to 250 knot velocity of the soil shear wave. A series of dynamic plate bearing tests conducted with a controlled rate of loading have shown that the response of a rolling wheel can be duplicated in a dynamic plate test. These tests showed a decrease in soil stiffness in the same velocity range in which increased drag and sinkage were observed to occur in the field tests. The increase in sinkage and drag loads that occurred when brakes were applied can be accounted for by the passive earth pressure theories and the change in stress distribution on the soil-wheel interface.

18. Turnage, G. W., and Green, Jr., A. J., "Performance of Soils Under Tire Loads. Analysis of Tests in Sand from September 1962 Through November 1963," U.S. Army Engineer Waterways Experiment Station, Corps of Engineers, Technical Report No. 3-666, Report 4, February 1966.

This report examines the effects of tire deflection, tread, carcass stiffness, construction, speed, and slip on tire performance in a dry sand. Tests were performed using both Yuma (desert) and mortar sand. Test speeds varied from approximately 0.3 mph to 12 mph.

The test results indicate that for best performance in a dry sand, a tire should be highly deflected, smooth, and of diagonal-ply construction. Variations in carcass stiffness have negligible effects on tire performance when comparisons are made at equal loads and deflections. Performance of pneumatic tires in sand is affected by speed; however, the extent of this influence was not wholly determined.

19. Van Deusen, B. D., "A Statistical Technique for the Dynamic Analysis of Vehicles Traversing Rough Yielding and Non-Yielding Surfaces:" NASA CR-659, March 1967.

This report describes a statistical analysis technique for the classification of virgin terrestrial and extraterrestrial surfaces. A method is devised whereby a single parameter is used to completely specify the surface roughness in a statistical sense.

A dynamic nonlinear yielding surface model was developed from existing information of soil mechanics. The model includes hysteresis due to initial soil compaction and effects of vehicle speed and loading area.

An analogue computer program, capable of predicting the dynamic response of typical lunar vehicles traversing yielding and nonyielding surfaces, was developed. A technique is included which allows a random surface profile to be introduced between the vehicle model and the yielding surface model and allows vehicle-surface separation.

20. Eiband, A. M., Simpkinson, S. H., and Black, D. O., "Accelerations and Passenger Harness Loads Measured in Full-Scale, Light-Airplane Crashes:" NACA TN 2991, August 1953.

Full-scale, light-airplane crashes simulating stall-spin accidents were conducted to determine the decelerations to which occupants are exposed and the resulting harness forces encountered in this type of accident. Crashes at impact speeds from 42 to 60 miles per hour were studied. The airplanes used were of the familiar steel-tube, fabric-covered, tandem, two-seat type.

In crashes up to an impact speed of 60 miles per hour, crumpling of the forward fuselage structure prevented the maximum deceleration at the rear-seat location from exceeding 26 to 33g. This maximum g value appeared independent of the impact speed. Restraining forces in the seat-belt/shoulder-harness combination reached 5800 pounds. The rear-seat occupant can survive crashes of the type studied at impact speeds up to 60 miles per hour,

if body movement is restrained by an adequate seat-belt/shoulder-harness combination so as to prevent injurious contact with obstacles normally present in the cabin. Inwardly collapsing cabin structure, however, is a potential hazard in the higher-speed crashes.

21. Wignot, J. E., et al, "Aircraft Dynamic Wheel Load Effects on Airport Pavements," Lockheed-California Company; Federal Aviation Administration, FAA-RD-70-19, May 1970.

This report describes the results of a problem which included scaled pavement tests, analysis to determine airplane imposed loads on pavement and pavement response, correlation between empirical data and analyses and a literature review. Based on the results of the program, it was concluded that airplane dynamic wheel loads have significant effects on portions of airport pavement.

The results of the investigation indicate that the two distinguishable effects that influence the stress the pavement experiences are (1) airplane induced loads and (2) moving load phenomenon. For a given level of runway unevenness, the loads that will be imposed on the pavement can be accurately defined for various ground operations performed. However, the pavement response to a moving load can vary substantially depending upon the kinds of materials and types of construction used. To obtain proper assessment of moving load effects, full scale pavement tests are considered necessary to provide needed data.

Two test plans are presented. One approach involves "Operational Statistical Tests" and depends upon a heavy statistical sample of data. The alternate approach involves "Moving Load Track Tests" and provides data for point-by-point correlation using analytical data under carefully controlled conditions and configurations.

22. Preston, G. M. and Pesman, G. J., "Accelerations in Transport-Airplane Crashes:" NACA TN 4158; February 1958.

Full-scale transport airplanes were crashed experimentally to determine the crash loads that result from a variety of crash events. It was concluded that pressurized transport airplanes can withstand high-impact-angle crashes and still maintain survivable areas within the fuselage. During unflared-landing crashes, greater fuselage crushing occurred with high-wing than with low-wing airplanes. Airplanes with strong fuselage structures that do not deform and produce sharp, well-supported plowing edges will have relatively low longitudinal acceleration during crashes similar to those studied. Normal accelerations exceeding human tolerance can occur in crashes in which modest fuselage damage occurs. Within the structural range represent by the airplanes crashed, the configuration of the airplane had little effect on the normal acceleration.

23. Reed, W. H., et al, "Full-scale Dynamic Crash Test of a Lockheed Constellation Model 1649 Aircraft," Aviation Safety Engineering and Research, Federal Aviation Agency, FAA-ADS-38, October 1965.

This report provides the details of a full-scale crash test of a large transport aircraft. The purpose of the test was to obtain crash environment data of the test aircraft and the various experiments installed aboard the aircraft.

The Federal Aviation Agency sponsored the test program with the participation of several other organizations who provided data recording equipment and special experiments on board the test aircraft. The participating organizations included the U.S. Navy, the U.S. Army, the U.S. Air Force, the Society of Automotive Engineers and the Flight Safety Foundation which conducted the test under contract to and with the guidance of the FAA. The special experiments consisted of military crew and commercial passenger seats, cargo restraint systems, postcrash locator beacons, baby and child restraint systems, radioactive material containers, a military litter system, and provisions for emergency lighting.

The test involved a Lockheed Constellation Model 1649A aircraft, which was guided into a series of crash barriers with a monorail nose gear guidance system. The aircraft was accelerated under its own power by remote control for a distance of 4,000 feet, reaching a velocity of 112 knots. Initial impact occurred against barriers which removed the landing gear, permitting the airplane to become airborne until the moment of impact with the wing and fuselage crash barriers.

The wing fuel tanks were ripped open by the wing barriers, allowing simulated fuel to spill out in a heavy mist during the crash sequence. The fuselage was broken in two places during the crash, just aft of the cockpit between fuselage stations 370 and 380 and just aft of the galley between fuselage stations 1020 and 1030. Peak longitudinal accelerations on the order of 25G's were measured at the cockpit floor when the aircraft impacted the 20 degree slope. Most of the onboard experiments remained in their relative locations throughout the test.

24. Reed, W. H., at el, "Full Scale Dynamic Crash Test of a Douglas DC-7 Aircraft," Aviation Safety Engineering and Research, FAA Technical Report ADS-37, Federal Aviation Administration, Washington, D.C., April 1965, AD 624051.

This report describes a test program designed to obtain crash environment data regarding fuel containment and to collect data on the behavior of various components and equipment aboard the aircraft, using a DC-7 as the test vehicle.

The test involved a DC-7 aircraft which was guided into a series of crash barriers with a monorail nose gear guidance system. The aircraft was accelerated under its own power by remote control for a distance of 4000 feet, reaching a velocity of 110 knots. At the end of this acceleration run, the aircraft impacted against a specially designed barrier which removed the landing gear, permitting the aircraft to become airborne until the moment of impact with wing and fuselage crash barriers.

The wing and fuselage barriers were designed to provide the following crash sequence: The left wing was to impact against an earthen mound shaped to produce a simulated wing-low accident. Simultaneously, the right wing was to impact telephone poles implanted vertically to simulate trees. Next, the main fuselage was to impact against an 8-degree slope. The slope was designed so that the aircraft could become airborne after sliding a short distance along the ground. Finally, the aircraft was to impact against a 20-degree slope to simulate a crash with a steeper angle of impact.

The test occurred as planned except that the aircraft, instead of coming to rest on the 20-degree slope, bounced over the hill on which the slope was formed and landed at the base of the backside of the hill. A failure of the voltage control regulator, in the data recording system, prevented the program from reaching all its objectives.

25. Sela, A. D., and Ehrlich, I. R., "Load Support Capacity of Flat Plates of Various Shapes in Soil," Automotive Engineering Congress, Society of Automotive Engineers; Paper No. 710178; January 1971.

This paper reports the results of a study to develop a general theory of plate sinkage which is applicable to a wide variety of soils, sinkages, plate sizes, and plate shapes.

The plate sinkage model developed in this study was verified, using available soil test results. The soils considered in these tests were air dry mason sand, buckshot clay, very fine grained Yuma sand, Michigan loam, and Ohio sand. No CBR numbers were given for these soils. The analytical model was found to correlate with all the experimental results included in the paper. The model has two regions of application--a "transition" region which is between 0 and 1 inch of sinkage and the region greater than 1" sinkage.

26. Whitman, R. V. and Healy, K. A., "Shear Strength of Sands During Rapid Loadings," Journal of the Soil Mechanics and Foundations Division, Proceedings of the American Society of Civil Engineers, April 1962.

Triaxial tests with times-to-failure from 5 minutes to 5 milliseconds have been used to investigate the effect of strain-rate on the strength of dry and saturated sands. New techniques were developed for applying strains rapidly, and for measuring the resultant stresses and pore pressures. It was necessary to give careful attention to the possible influence of testing errors, of inertia forces, and of the membrane effect.

The peak friction angles of the sands that were tested were substantially independent of failure-time. However, the excess pore pressures generated within saturated loose sands, did, for certain conditions, vary with failure-time. For these conditions the compressive strengths were correspondingly time-dependent. A tentative hypothesis has been advanced to explain this behavior. One loose saturated sand exhibited a pronounced yield point at low strains, and the yield point stress decreased as the rapidity of load application increased.

27. Wittlin, G., Gamon, M. A., and LaBarge, W. L., "Full Scale Crash Test Experimental Verification of a Method of Analysis for General Aviation Structural Crashworthiness," FAA-RD-77-188, February 1978.

The results of the Task II effort to experimentally verify a method of analysis of the structural dynamics response of general aviation airplanes subjected to a crash environment are presented.

Included in this report is a description of the preparation for the performance of four instrumented full-scale crash tests involving a single-engine, high wing type airplane. All crash testing was performed at the NASA Langley Impact Dynamics Research Facility (IDRF). The crash tests involved a wide range of impact attitudes and included one impact into a soil covered terrain.

Program KRASH, refined for general aviation airplane application during TASK I, is used to mathematically model the single-engine, high-wing type airplane for each of the crash tests. An analysis of each crash condition is performed and the results with regard to post-crash sequence, cg velocity, energy distribution, cabin deformation, member deflections, structure failures, and floor, occupant and engine mass accelerations are presented. Correlation between analysis and test results in presented for each crash test. Comparisons of analytical and test results are presented for the composite of all four crash tests. The analytical results are shown to be in agreement with test results. Conclusions are presented following the summary of results. Appendices A, B, C and D are included and contain soil test data, literature survey and evaluation results, test data, and structural model data, respectively.

A three volume KRASH User's Manual is described in a separate document.

28. Cheng, R. Y. K., "Soil Analyses and Evaluations at the Impact Dynamics Research Facility for Two Full-Scale Aircraft Crash Tests," NASA CR 159199, August 1977.

An investigation to determine the aircraft structural crash behavior and occupant survivability for aircraft crashes on a soil surface was conducted at the Impact Dynamics and Research Facility at NASA Langley Research Center. This report contains the results of placement, compaction, and maintenance of two soil test beds, and a description of the craters formed by the aircraft after each test.

29. Vaughan, V., Jr. and Hayduk, R. J., "Crash Tests of Four Identical High-Wing Single-Engine Airplanes," NASA TP 1699.

Four identical four-place, high-wing, single-engine airplane specimens with nominal masses of 1043 kg were crash tested at the Langley Impact Dynamics Research Facility under controlled free-flight conditions. These tests were conducted with nominal velocities of 25 m/sec along the flight path at various flight-path angles, ground-contact pitch angles, and roll angles. Three of the airplane specimens were crashed on a concrete surface; one was crashed on soil.

Crash tests revealed that on a hard landing, the main landing gear absorbed about twice the energy for which the gear was designed but sprang back, tending to tip the airplane up to its nose. On concrete surfaces, the airplane impacted and remained in the impact attitude. On soil, the airplane flipped over on its back. The crash impact on the nose of the airplane, whether on soil or concrete, caused massive structural crushing of the forward fuselage. The livable volume was maintained in both the hard-landing and the nose-down specimens but was not maintained in the roll-impact and nose-down-on-soil specimens. The pilot and copilot dummies impacted the instrument panel in the airplane specimens that lost cabin volume. Peak accelerations on the cabin floor were generally under -25g; for the nose-down-on-soil specimen, however, they were as high as -45g. The highest accelerations in the dummies' pelvises were in the normal direction and peaked as high as -65g in the nose-down-on-soil test. The dummies' heads that impacted the structure experienced accelerations as high as -60g, while non-impact accelerations were about -20g.

30. Castle, C. B. and Alfaro-Bou, E., "Crash Tests of Three Identical Low-Wing Single-Engine Airplanes," NASA TP-2190, September 1983.

Three identical four-place, low-wing single-engine airplane specimens with nominal masses of 1043 kg were crash-tested at the Langley Impact Dynamics Research Facility under controlled free-flight conditions. The tests were conducted at the same nominal impact velocity of 25 m/sec along the flight path. Two airplanes specimens were crashed on a concrete surface (at 10° and -30° pitch angles), and one was crashed on soil (at a -30° pitch angle).

The three tests revealed that the specimen in the -30° test on soil sustained massive structural damage in the engine compartment and fire wall. Severe damage, but of lesser magnitude, occurred in the -30° test on concrete, and the least structural damage was experienced in the 10° test on concrete.

An average longitudinal cabin-floor acceleration of -26g occurred in the -30° test on soil. An average normal cabin floor acceleration of -29g occurred in the -30° test on concrete. Accelerations in the 10" test on concrete were the lowest for the three tests. In the -30° test on soil, the longitudinal acceleration on the pilot's pelvis was -60g; whereas for the -30° test on concrete, the acceleration was -23g. The tensions in the pilot's lap belt for the two -30° tests was 3700 N and 200 N, respectively. The normal acceleration in the pilot's seat pan was -8g and -37g, respectively. The 10° test on concrete produced a longitudinal pelvis acceleration of -6g, negligible lap-belt tension, and a normal seat-pan acceleration of -14g.

31. Laananen, D. H., et al, "Aircraft Crash Survival Design Guide, Volume III Aircraft Structural Crashworthiness," USARTL-TR-79-32C, August 1980.

This volume (Volume III) contains information on the design of aircraft structures and structural elements for improved crash survivability. Current requirements for structural design of U.S. Army aircraft pertaining to crashworthiness are discussed. Principles for crashworthy design are presented in detail for the landing gear and fuselage subject to a range of

crash conditions, including impacts that are primarily longitudinal, vertical, or lateral in nature and those that involve more complicated dynamic conditions, such as rollover. Analytical methods for evaluating structural crashworthiness are described. Contains a discussion of fuselage airframe design principles and concepts. In particular the material on energy absorption, earth plowing reduction of aircraft mass and design concepts for improved crashworthiness provides data pertinent to soil penetration studies.

32. PI, W. S., "A Dynamic Tire/Soil Contact Surface Interaction Model for Aircraft Ground Operations," AIAA Paper 85-0708, 1985.

This paper describes a dynamic tire/soil contact surface interaction model for aircraft ground operations. The formulation uses a finite element kernel function approach. It is based on the concept of the quasi-steady motion of a tired-wheel rolling at a constant speed on a linear viscoelastic layer (soil). In the soil model, the Young's modulus, Poisson's ratio, and shear modulus are treated as three independent parameters, and the inertia and viscous damping effects are included. The model thus developed can be utilized to predict the contact pressure distribution, soil deformation pattern, and tire footprint area shape developed beneath the moving tired-wheel. Numerical examples were given to correlate the experimental results from a high flotation test program. In general, the predicted drag ratio versus the speed results compare well with the test data trend for soils with various strengths. The analyses indicate that the high drag force and severe rutting occur when the wheel forward speed is near the shear wave velocity of the soil. Furthermore, the numerical results show that all soil parameters used in the model play significant roles in determining the soil strength and the responses. These parameters should be retained in a comprehensive analysis on aircraft tire/soil interaction.

33. Shanks, D. H. and Garnett, R. V., "Performance of Aircraft Pneumatic Tires in Soft Soil," Aeronautical Journal, January 1981.

This paper is concerned with the rolling resistance, or drag, of an unpowered pneumatic-tyred wheel rolling at high velocities in soft soil. Its applications to undercarriage design for aircraft intended to operate from unsurfaced airfields, and to the inverse problem of predicting the performance of existing aircraft in such conditions. New data from wheel tests are given, used to test, for the first time, a proposed predictive method. An attempt is then made to show how a more satisfactory method could be devised, using a very simple rheological model for clay.

34. Cassino, V., "Soft Airfield Tests with F-4 Aircraft," ESL-TR-82-18, December 1981.

Tests were conducted to investigate the interaction of soil surfaces with the landing gear of F-4E aircraft to validate computer prediction routines. Site selection and soil tests are described. In-place soil tests were conducted, and aircraft ground performance was measured during towed and powered taxi operations. Soil strength was adequate to support the aircraft for the two loadings used. Laboratory tests were performed to further identify the soil

strength parameters. Aircraft location while operating on the test area was determined by a ground survey system and a laser tracking system.

35. Hay, D. R., "C-141A Ground Flotation Test on Landing Mat and Unsurfaced Runways-Civil Engineering Support," AFW-TR-70-30.

The Air Force Weapons Laboratory, Civil Engineering Division (AFWL-WLCT), provided civil engineering support for the C-141A Ground Flotation Test on a landing mat runway and an unsurfaced runway. The flight tests were conducted by the Lockheed-Georgia Company. The primary objectives of the test program were to determine the capability of the C-141A aircraft to operate from landing mat runways and to demonstrate the capability to operate on an unsurfaced runway. The support provided included soil strength measurements on the runways, elevation profiles on the runways, and evaluation of the effects of the C-141A on the unsurfaced and landing mat runways. The data collected during the test program are presented and discussed. Approximately 370 takeoffs, landings, and taxis were conducted on the landing mat runway without any major operational problems. Fourteen C-141A operations were successfully conducted on an unsurfaced runway with soil strengths ranging from CBR 2 to CBR 20.

36. Trafford, J. W., et al, "Aircraft Tire Behavior During High-Speed Operations in Soil," NASA TN D-6813, August 1972.

An investigation to determine aircraft tire behavior and operating problems in soil of different characteristics was conducted at the Langley landing-loads track with a 29 x 11.0-10, 8-ply-rating, type III tire. Four clay test beds of different moisture content and one sand test bed were used to explore the effects on axle drag loads developed during operation at different tire inflation pressures in free rolling, locked-wheel braking, and yawed (cornering) modes, all at forward speeds up to 95 knots. The test results indicated a complicated drag-load-velocity relationship, with a peak in the drag-load curve occurring near 40 knots for most test conditions. The magnitude of this peak was found to vary with tire inflation pressure and soil character and, in certain cases, might prove large enough to make take-off hazardous.

37. Turnage, G. W., et al, "Prediction of Aircraft Ground Performance by Evaluation of Ground Vehicle Rut Depths," AD775744, February 1974.

Two single aircraft tires (20-20, 22-PR and 49-17, 26-PR) and three standard military trucks (M715, 1-1/4-ton; M35A2, 2-1/2 ton; and M51, 5-ton) were tested under towed (nonpowered, nonbraked) and self-powered conditions, respectively, in buckshot clay test beds whose strengths ranged from about 110 to 600 cone index. Tests included multiple passes over the prepared test beds (usually 100 passes for the aircraft tires, 10 for the trucks) at low speeds. Only single-wheel configurations were examined (i.e., outer second- and third-axle wheels of the M35A2 and M51 were removed). Curves were developed to allow soil strength (airfield index) to be estimated directly from the rut produced by single or multiple passes of any of the three trucks. These curves were developed through use of a dimensionless prediction term (tire-clay numeric N_C) that allows pneumatic tire performance to be scaled over a

wide range of soil strengths, wheel loads, and tire size, shape, and deflection conditions. The same numeric was shown to be capable of describing multipass rut depth and towed coefficients for the aircraft tires, as well as multipass rut depth for the trucks. Examples illustrate how airfield index (AI) estimated from truck rut depth can easily be used with curves that describe the N_c versus rut depth and towed force coefficient relations for aircraft tires to predict multipass aircraft tire performance. Appendix A shows that values of AI estimated from truck rut depth can be converted to California Bearing Ratio values and used as input for a nomograph description of Aircraft operation on unsurfaced soils.

Relates cone index (CI) to moisture content and density. Also relate Airfield Cone Pentrometer Measurement (AI) to CBR and CI.

38. TSAI, K., "Strength Response Parameters of Natural Soil Surfaces and Their Landing Problem of Aircraft," AF19 (628)-5873, January, 1967.

A suitable rheological model is found to represent the soil deformations under impact loads. The parameters of the model are evaluated from the deceleration history curves of the Princeton impact petetrometer tests.

From the soil parameters obtained, the soil responses under the airplane landing load are estimated. Extensive applications to the dynamical soil problems, such as soft landing of spacecraft, will be possible.

39. Doyle, Jr., G. R., "A Review of Computer Simulation for Aircraft-Surface Dynamics," Jr. of Aircraft, Vol. 23, No. 4, April 1986.

The objectives of this study were to review the literature concerning aircraft-surface dynamic simulation techniques: 1) to establish a historical view of the improvement in the state of the art, 2) to recognize the individuals and organizations that have played a prominent roll in advancing the state of the art, 3) to develop a knowledge base of physical phenomena that have been simulated, 4) to identify mathematical techniques that have been used, 5) to classify the simulations according to their general purpose, complexity, and accuracy, and 6) to suggest areas in which simulation techniques could be improved, and test could be run to validate the simulations.

The report contains a brief summary of the computer programs written to predict the dynamic displacements and forces resulting from nonflight aircraft operations. The capabilities of each program along with their limitations and numerical techniques are cited.

40. Poor, A. P., "Soil Response of Three Geometric Shapes During Impact," Ph.D. Dissertation, May 1965.

The primary objective of this investigation was to determine the soil response on three geometric shapes during impact loading. As a result of the experimental program, a modulus of deformation was determined for each geometric configuration. This modulus is a function of the impact force and the resulting deformation of the soil system.

Due to these complexities of the entire problem, certain assumptions were made to reduce the unknown parameters. The geometric shapes were considered rigid bodies. The investigation considered only a vertical component of motion with the vehicles striking the soil surface in a normal attitude. The interaction time period was limited from the instant of impact to an at-rest condition, and did not consider the magnitude of plastic deformation and elastic response. The test area was considered as a uniform, homogeneous, and isotropic soil mass to a depth of 15 feet.

Even with the imposed limitations, the interaction relationship between a soil mass and an impacting body comprises unknowns which are indeterminate. From analysis of the test results of this investigation, it was apparent that an extremely complex, intermingled, relationship existed between the modulus of deformation, vehicle mass, impact velocity, vehicle geometry, reactive force exerted by the soil mass, inertial forces, plastic deformation, elastic rebound, and the soil mass properties.

This research program consisted of three major phases, all interrelated and interdependent. The first phase comprised the development of the test vehicles, equipment, instrumentation, and procedures which would allow measurement of the soil response to an impacting vehicle. The second phase consisted of the test area preparation, soil investigation, and the complete testing program. The third phase required determination of the data reduction procedures and analysis of results.

LITERATURE SURVEY SUMMARY

General Discussion

Technical publications were reviewed and their contents categorized to assist in future studies to develop improved structural crashworthiness designs for general aviation airplanes. A review and evaluation of publications are presented here. The literature is reviewed with regards to aircraft structure and flexible ground interaction. Emphasis is placed in the following areas:

Analysis
Analytical Model, Data Correlation, Parametric Studies
Landing Surface (Soil) Characteristics
Material and Roughness Properties, Performance Coefficients
Landing Surface/Gear Interaction Tests
Test Procedures, Data Analysis
Full Scale Aircraft Crash Tests
Test Procedures, Data Analysis, Empirical Criteria
Design
Procedures, Criteria, Design Analysis Tools
(nomographs, computer programs)

For each of the above areas, an evaluation is performed which identifies the literature applicable to that particular subject and the contribution of each report. A composite summary of the pertinent aspects of the literature with regard to structural crashworthiness analysis is also presented.

In addition to the literature survey and evaluation, a summary or abstract of each report, a literature survey subject index and a soil/interaction test parameter index are included. Both of the indices contain a matrix categorization of the contents of the reports and area of application or test parameter. The report reference numbers listed in the indices are applicable to this Appendix only.

Analysis

The bulk of mathematical modeling of flexible ground/aircraft structure deals with tire/wheel/landing gear representations. Reference (2) describes the results of a study to investigate the interaction between the landing gear of the OV-10A airplane (Gross Weight: 9755 to 10547 pounds) and soft soil for landings ranging in sink speed from 8 to 18 ft/sec. An analytical model of the pneumatic tire on soft soil was developed. No correlation between analysis and test was performed. References (3), (4) and (5) describe a series of programs sponsored by the Air Force Flight Dynamics Laboratories (AFFDL) which were conducted primarily to develop methods for evaluating techniques for determining aircraft take-off performance, loads and capabilities. Reference (4) describes computer programs which were developed for calculating loads and dynamic response of aircraft operating on unpaved surfaces. Reference (3) describes a computer program which incorporates the soil/wheel interaction model with a simulation of the C-130 during taxi and takeoff. Reference (5) describes an analog computer program developed to incorporate the high speed effects found during testing into a soil-gear interaction model.

References (8), (10) and (11) describe additional AFFDL sponsored efforts involving landing gear-soil interaction. Reference (8) describes the variables which significantly influence aircraft performance when operating on soil runways. At the time of the referenced report, sinkage analysis accuracy was considered to be between $\pm$50% and $\pm$100%. Reference (10) describes efforts aimed at defining landing-gear soil interaction and developing flotation criteria to be used in comparative evaluation of the relative merits of various landing gear configurations. Empirical sinkage prediction equations were developed for cohesive and cohesionless soils. Reference (10) describes the third phase of a study to analytically define landing gear-soil interaction. The three studies, References (8), (10), (11), cover single and multiple wheel gears operating on clay, sand and mixed soils. Reference (15) describes a study which includes the development of mathematical model to study fire-soil interaction. Empirical expressions were developed which relate soil sinkage and rolling resistance to soil strength, tire vertical force, tire characteristics and taxi velocity. Reference (16) presents a prediction method for estimating wheel sinkage, landing gear drag, and aircraft take-off performance on clay and sand airfields of various bearing strengths. The method is based on using modified mobility numbers developed by the U.S. Army Waterways Experimental Station (WES). Reference (19) presents a statistical analysis technique for the classification of virgin terrestrial and extraterrestrial surface roughness. Semi-empirical relationships are presented in Reference (1) to relate shearing resistance and rate of shear deformation. The data presented in this study are based on laboratory tests in which the strain rate varies up to 13.3 rad/sec. Correlation between analysis and test is presented in References (3), (5), (15) and (16). Figures B-1 and B-2, obtained from Reference (3), present a comparison between analysis and test results for CBR 1.5 Clay.

LANDING SURFACE (SOIL) CHARACTERISTICS

Reference (3), (6), (10), (14), (16), and (21) discuss programs in which the properties of sand and clay soils are considered. Clay soil properties are also discussed in References (1), (4), (5), and (17). Reference (7) provides soil strength performance data for coarse grained sandy soils. Reference (26) describes traixial tests for investigating the effect of strain-rate on the strength of dry and saturated sands. References (3), (4), and (5), while involving soil materials, were performed primarily to develop analytical methods for determining landing gear dynamic loads. An investigation of different soils at different strength levels under very slow ($\leq$1 mph) moving vehicles is described in Reference (6). Reference (10) considers clay, sand and mixed soils for use in the development of sinkage prediction equations. The soil was assumed an elastic, perfectly plastic material in this program. A preliminary Single Wheel Relative Merit Index (RMI) was developed during this program to permit a comparative evaluation of the flotation characteristics of aircraft tires on soil. Reference (13) describes a program in which a series of traffic tests were performed on mat-surfaced and unsurfaced subgrades. Numerous wheel configurations, loads and tire pressures were included. In Reference (14), four clay test beds of different moisture content and one sand bed were used to explore the effects on axle drag loads developed during operation at different tire inflation pressures in free rolling, locked wheel braking and yawed (cornering) modes, all at forward speeds up to 95 knots. Reference (15) summarizes the results of a five-phase program. Phase II included a site selection and field measurement program to obtain field roughness profiles and soil strength information from fields typical of those expected to be found in remote theaters of operation. The sites selected represented various degrees of preparation, from semiprepared to unprepared and included a variety of soil types. Reference (17) contains a description of the construction and maintenance of the buckshot clay test bed used for tandem and single wheel, high speed landing gear tests conducted at the NASA Landing Loads Track. Reference (21) describes a program to determine the effect of aircraft, dynamic wheel loads on airport pavements. Appendices C and F of Reference (11) contain data with regard to soil laboratory tests and wave propagation velocities for paving materials, respectively. Landing surface roughness characteristics are discussed in References (2), (3), (4), (15), (19), and (21).

Landing Surface/Gear Interaction Tests

Reference (1), (3), (5), (6), (11), (14), (17), and (18) describe laboratory tests to define material behavior, facilitate and development of analytical models, define parameter relationships or further the development of criteria. With the exception of References (1) and (11), the references relate landing gear and/or wheel performance to soil strength and/or behavior. Reference (1) describes tests to determine shearing resistance of cohesive soils subject to shear strains applied at various rates. The relationship between shearing resistance and rate of shear deformation was established for various soil densities expressed in terms of initial void ratio or water content (see Figure B-3). Reference (11) presents the results of twinplate vertical load tests to determine sinkage interaction effects produced by adjacent dynamic plate loads (see Figure B-4). Soil and/or landing surface field tests are described in References (2) and (13). The data from Reference (2) are used to

form a representation of soil static and dynamic properties. Figures B-5 and B-6, obtained from Reference (2), illustrate the type of curves that are generated from the test data. The results of laboratory soil and scaled pavement tests are presented in Reference (21) Soil characteristics such as California Bearing Rates (CBR), moisture content, grain size distribution and damping characteristics were determined. Concrete and asphaltic-concrete slab characteristics were also determined. Typical CBR, dry density, moisture content and subsoil modulus relationships are shown in Figures B-7 and B-8. Empirical criteria are presented in References (7), (11) and (13). In Reference (7) independent tire soil and system parameters are related to performance coefficients. A combination of independent parameters called mobility numbers were developed which account for the combined effects of soil strength, tire section width and diameter, wheel load and tire deflection on wheel performance as measured by performance coefficients. The mobility numbers developed in this report are applicable to single wheel landing gears operating on sand at speeds common to surface vehicles. Reference (11) provides criteria applicable to multiwheel landing gears which permit the evaluation of aircraft flotation performances rather than single tire performance. The criteria also permits designers to determine optimum landing gear configurations for aircraft leading to drag minimization. Reference (13) presents single wheel criteria for the efficient design of aircraft landing gears based on testing involving different wheel configurations (1 to 12 wheels), loads (1000 to 273000 pounds), and fire pressures (10 to 250 psi).

The data from each of the six test locations was obtained in a consistent manner. At the initial position of each general test location a penetrometer test and a free fall cylinder drop test (designated Hole 0) were conducted. A second penetrometer test and cylinder drop test with the bungee connected at hole 1 were performed at a position of six inches down field of the initial position. The testing process continued in the safe manner at six inch intervals for each of the five remaining accelerated drop tests. The resulting raw penetrometer data is presented in tabular form on Pages A1-19 and A1-20. The pertinent cylinder drop test displacement, velocity, and acceleration data is presented on Pages A1-23 through A1-45.

The raw soil penetrometer data obtained from all the cylinder drop test sites was plotted as penetrometer pressure versus penetration depth. Nine different curves were apparent and arbitrarily identified as Terrain Hardness Curves A through I. Six of these curves all differ in ultimate hardness and shape and, thus, formed the basis for soil type differentiation. These six plots of penetrometer data are presented on Pages A1-49 through A1-54. The data for curves E, F, and H was scattered and insufficient to uniquely define a curve.

Page A1-57 presents the shifted penetrometer data curves as discussed in paragraph 3.3.2.1. Page A1-61 presents the final static soil pressure curves. These curves are a direct indication of the static load supporting ability of the soil. Corresponding values of static soil pressure and penetrometer reading may be determined for any specific soil element by correlating the selected penetrometer data, presented on Pages A1-49 through A1-54, with the static soil pressure curves, presented on Page A1-61. Consider, for example, the static load supporting ability of the soil surface of Terrain Hardness A which is representative of the softest soil on which the OV-10 operated. The average penetrometer reading over the first inch of penetration was

approximately 40. The corresponding average static soil pressure value is approximately 20 psi. Thus, a surface penetrometer value of 40 is representative of a soil that can support a maximum static load of 20 pounds per square inch with some soil deformation but without vertical shearing.

The load supporting ability of the soil measured in CBR units is not available for the various Terrain Hardnesses. Soil tests to determine CBR values were not conducted and a general method of transformation between penetrometer values and CBR units does not exist.

Full Scale Aircraft Crash Tests

Full scale aircraft crash tests in which a flexible ground surface is included are described in References (20), (22), (23) and (24). Reference (20) describes the results of crash tests of light-airplanes (1200 pounds) into an earthen barrier. Impact speeds of 42, 47 and 60 mph were investigated. To simulate accidents in which the airplane stalls and strikes the ground as it enters a spin, the earthen barrier was shaped and located relative to a guide rail along which the airplane traveled such that the engine, left landing gear and left wing tip struck the barrier simultaneously. The airplanes used were a steel tube, fabric covered, tandem, two-seat type. The report concludes that the occupants of airplanes of the type used in the investigation would not be endangered by deforming cabin structure unless crash impact speeds exceeded 42 mph. Inwardly collapsing cabin structure, however, is a potential hazard in the higher-speed crashes. Reference (22) presents results of a program involving full-scale transport airplanes simulating takeoff and landing accidents for pressurized low-wing, unpressurized low-wing and unpressurized high wing aircraft. The resultant damage was from moderate to severe. The unmanned airplanes were guided along a runway under their own power into a set of obstacles designed to produce a series of crash events. The impact angles varied from 4 to 29 degrees and the impact velocity ranged from 63 to 109 mph. Figure B-9, obtained from Reference (22), shows plots of variation of maximum normal acceleration as a function of impact angle and distance from impact point. The crash site for the tests described in Reference (22) was predominantly clay. The sliding coefficient from aluminum was taken as equal to 0.30. This report contains a discussion in which the relationship between crumpling, plowing and friction forces are treated. The kinetic-energy loss is equated to the work done in collapsing the fuselage structure and compressing the soil. Utilizing the test data obtained during the effort, a general relationship between maximum acceleration and impact angle was developed (Figure B-10). However, it is cautioned that the equations developed during the program and presented in the report should not be used to calculate the magnitude of the acceleration in crashes involving different circumstances and different airplanes. References (23) and (24) describe the results of full scale crash tests of a Lockheed Model 16494 aircraft and Douglas DC-7 aircraft, respectively. The test procedures to obtain desired impact conditions were similar to those described in Reference (22). Initial impact was at 112 knots against barriers which removed the landing gear, permitting the airplane to become airborne until contact with wing and fuselage barriers. The terrain was sloped 20 degrees at the fuselage impact point. No attempt in the program was made to relate responses to the type of flexible ground that was used. With the exception of Reference (22) none of the reports referenced herein discuss the properties of the terrain or

the influence it may have had on the results. Also, with the exception of the brief analysis described in Reference (22), none of the crash tests are supported by analysis of the results from the standpoint of developing analytical models to predict responses, even on an inflexible ground. In general, the responses recorded during the tests are tabulated and related to human tolerance curves.

Design Procedures and Criteria

There are many design procedures and computer programs available for assessing landing gear and aircraft performance during take-off and landing from various types of airfields. Computer programs are available for single wheel (References (3) and (10)) and multiple wheel (References (3), (11), and (15)) landing gears. In addition, design curves or nomographs are also available for single wheel (Reference (13)) and multiple wheel (References (8), (9) and (12)) configurations. Reference (4) contains a series of computer programs to help evaluate various aircraft operations, including airfield capability, landing impact with and without runout, taxi, take-off and turning. Reference (16) provides a digital computer program for use in predicting take-off performance on clay and sand airfields. The prediction of the dynamic response of lunar vehicles which traverse yielding and unyielding surfaces is available from an analog computer program described in Reference (19). Reference (21) presents a digital computer program for predicting the rigid and flexible pavement responses due to moving loads as well as pavement design criteria and procedures. Reference (21) also contains a list of additional literature in its Appendix A (Literature Survey) which may provide additional useful information. Subjects which may be of interest include Airport Pavement Response (Static and Dynamic Analysis), Material Characterization, and Pavement Testing. Several references, including (4), (9), (10), and (13) provide criteria related to aircraft flotation and include the effects of soil interaction.

Summary

The review of available literature attempts to encompass a wide cross section of areas. The emphasis in this literature evaluation is on airfield applications. The test data that are available are generally obtained for the purpose of supporting analyses or for the development of procedures and criteria to evaluate aircraft performance, and not for the purpose of helping predict dynamic responses wherein large deformations occur. Even the full scale crash tests that have previously been performed on flexible ground surfaces have not addressed themselves to the significance of the terrain properties on structure and, ultimately, occupant response. For example, little or no measurements of ground flexibility, moisture, finish, or distribution as a function of depth or space have been made in any of the full scale crash tests reported herein. No measurements have been made to ascertain penetration by airframe or the relationship of penetration to airframe size or shape or to the impact velocities. While the penetration of ground by tires (sinkage) for the landing gear-ground interaction is available, these data do not relate easily to the impact velocity combinations and varied shapes that penetrate a flexible ground during a crash condition.

The research effort with regard to developing analytical models to describe landing gear-soil interaction and provide flotation criteria for aircraft operating from unpaved runways is substantial A heavy reliance is placed on the use of the Mobility Number $(\mathcal{Q}) = \frac{CI(bd)}{F_t}\left(\frac{\delta_t}{h_t}\right)^{1/2}$*

*The above mobility number is for clay soil. Mobility numbers for other types of soil take other forms.

where CI = Cone Index

bd = Tire Print Area

F_t = Tire Force

δ_t = Tire Deflection

h_t = Height of Tire

However, the analytical techniques developed for landing gear-soil interaction use are not directly applicable to structural crashworthiness investigations. Modifications are needed which account for airframe shape, crash attitude, shear flow distribution, structure flexibility, and dynamic load effects.

The analysis of flexible ground-structure interaction during relatively high dynamic impact conditions would benefit from an orderly and concerted effort to accumulate data from typical airframe-terrain interaction tests and supportive laboratory soil tests. As a minimum, spatial and depthwise material properties (CBR, soil strength, moisture content), airframe response in the region of impact, airframe configuration (shape and size), post-impact terrain, penetration (size and depth) for a range of typical airplane impact velocities and attitudes, and soil configuration is needed. The data should be obtained for the purpose of developing curves which relate vertical force to sinkage as a function of CBR, soil shear strength to CBR, and horizontal force to frontal area as a function of shear strength.

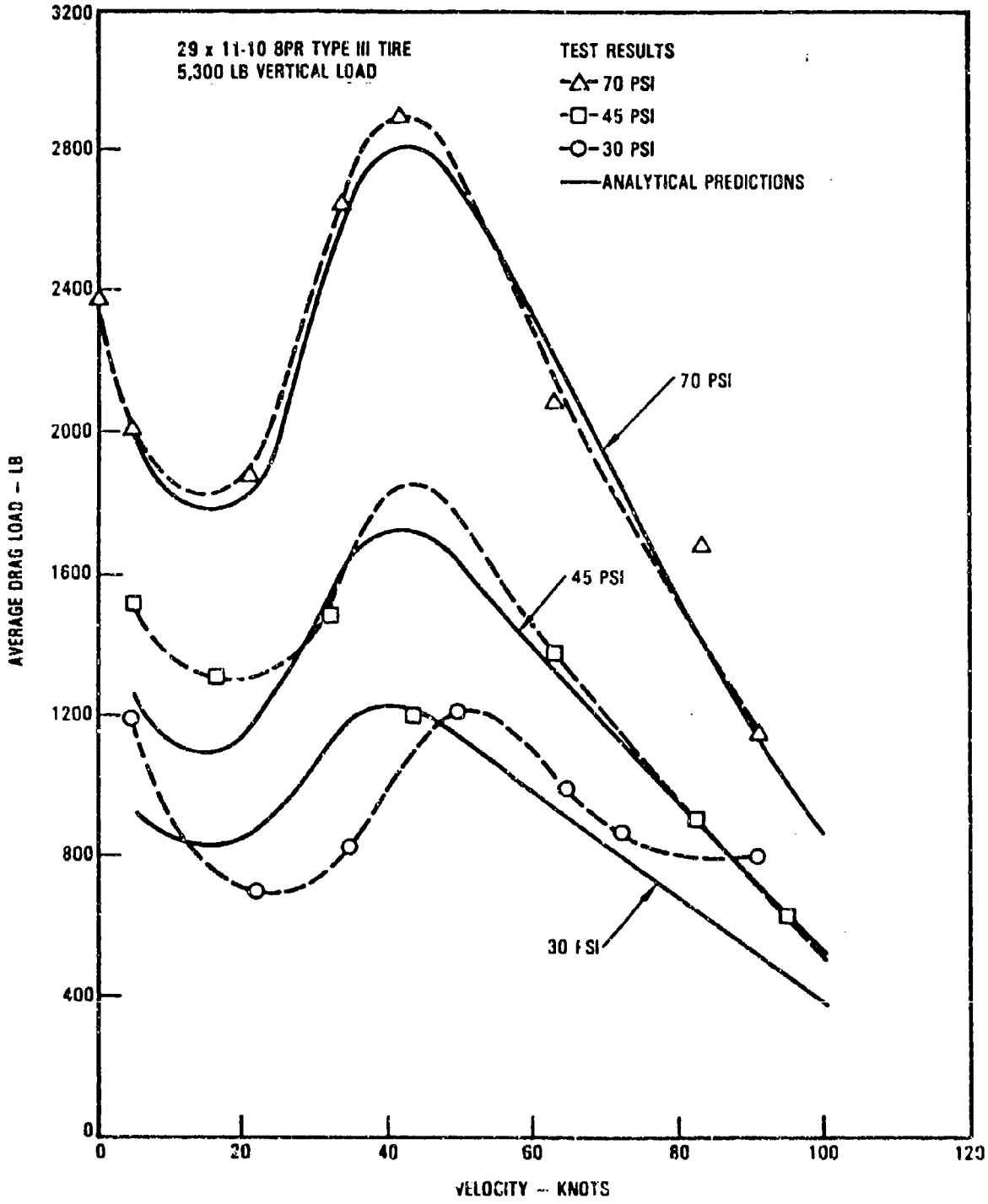

Figure B-1. Comparison of Analytical and Test Drag Loads for CBR 1.5 Clay (Reference 3)

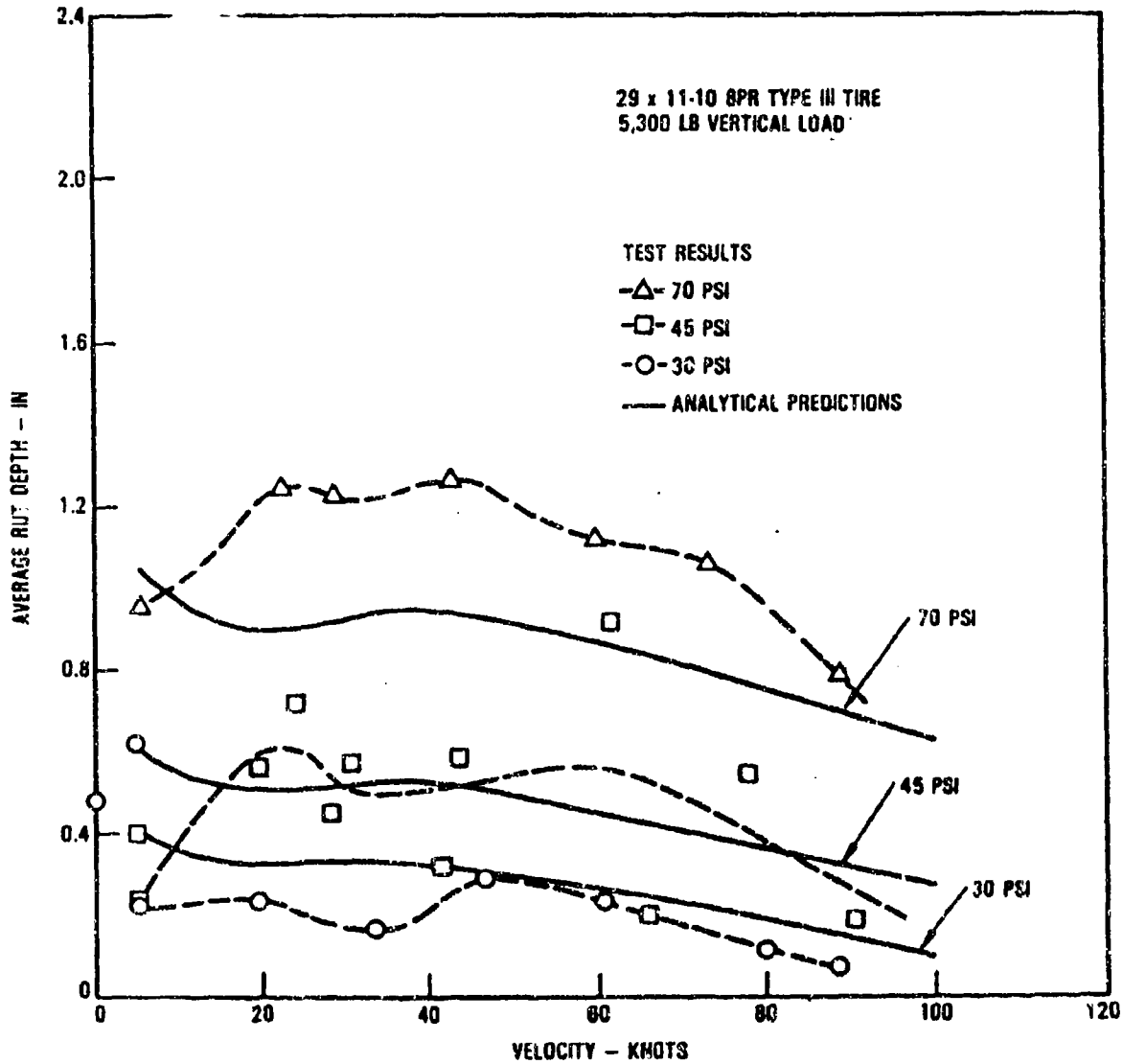

Figure B-2. Comparison of Analytical and Test Rut Depths for CBR 2.3 Clay (Reference 3)

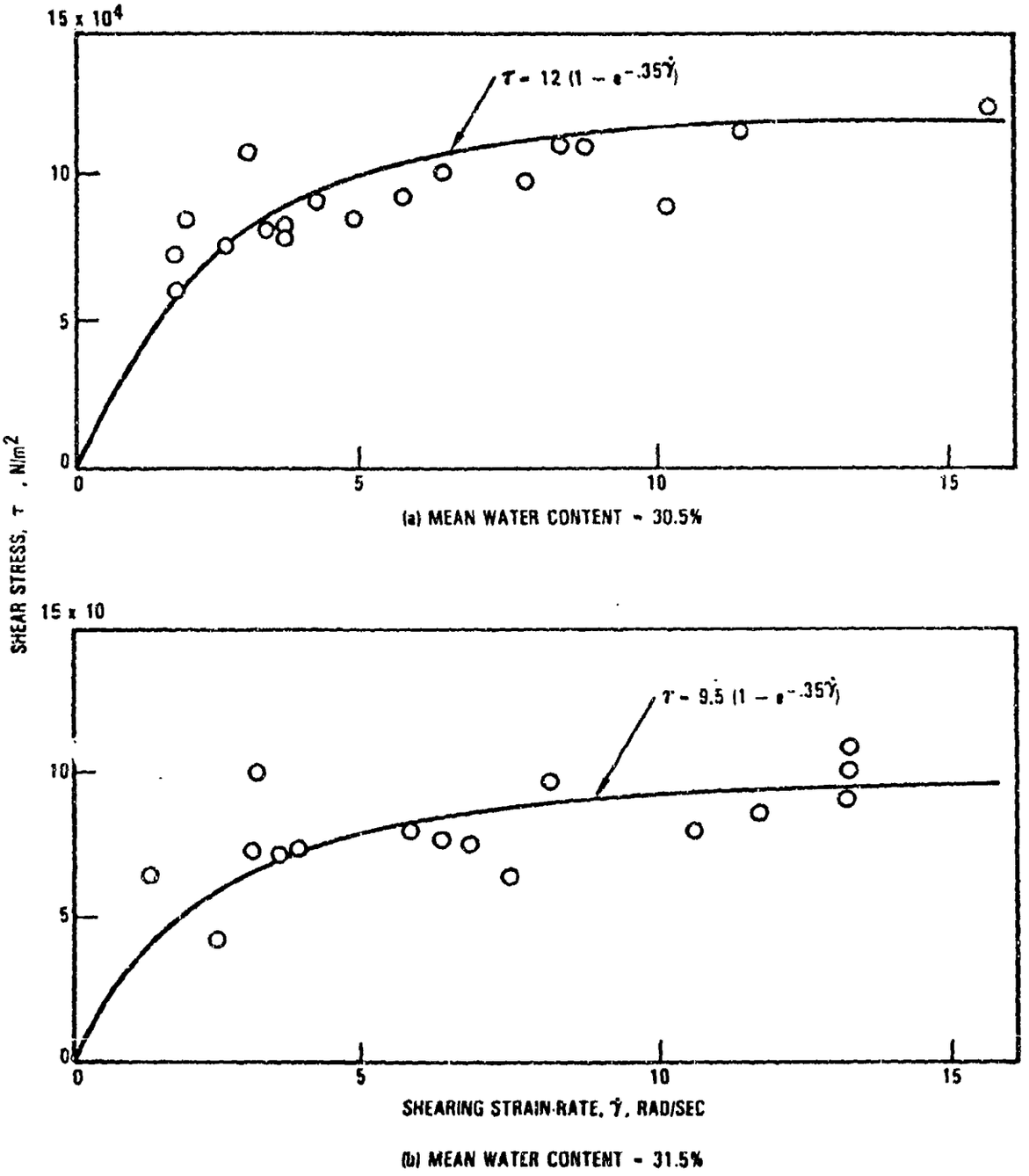

Figure B-3. Plot of Shearing Stress versus Strain Rate (Reference 1)

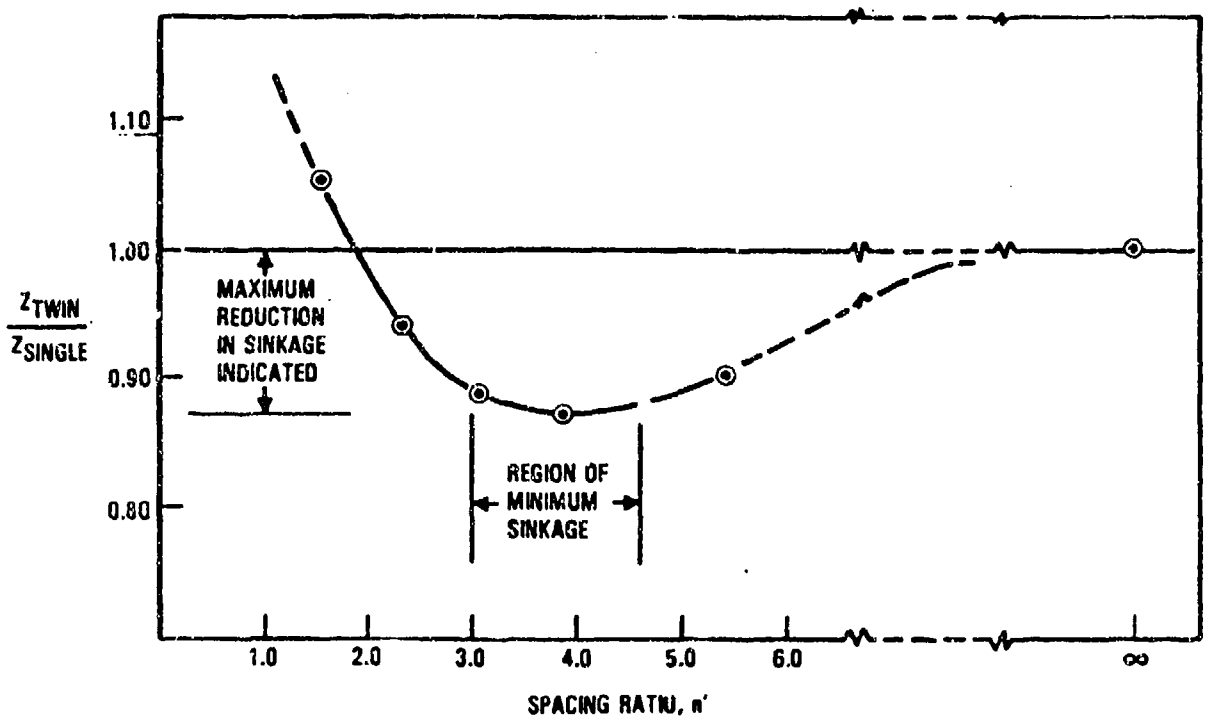

Figure B-4. Z_{Twin}/Z_{Single} vs. Wheel Spacing, Clay Soil (Reference 11)

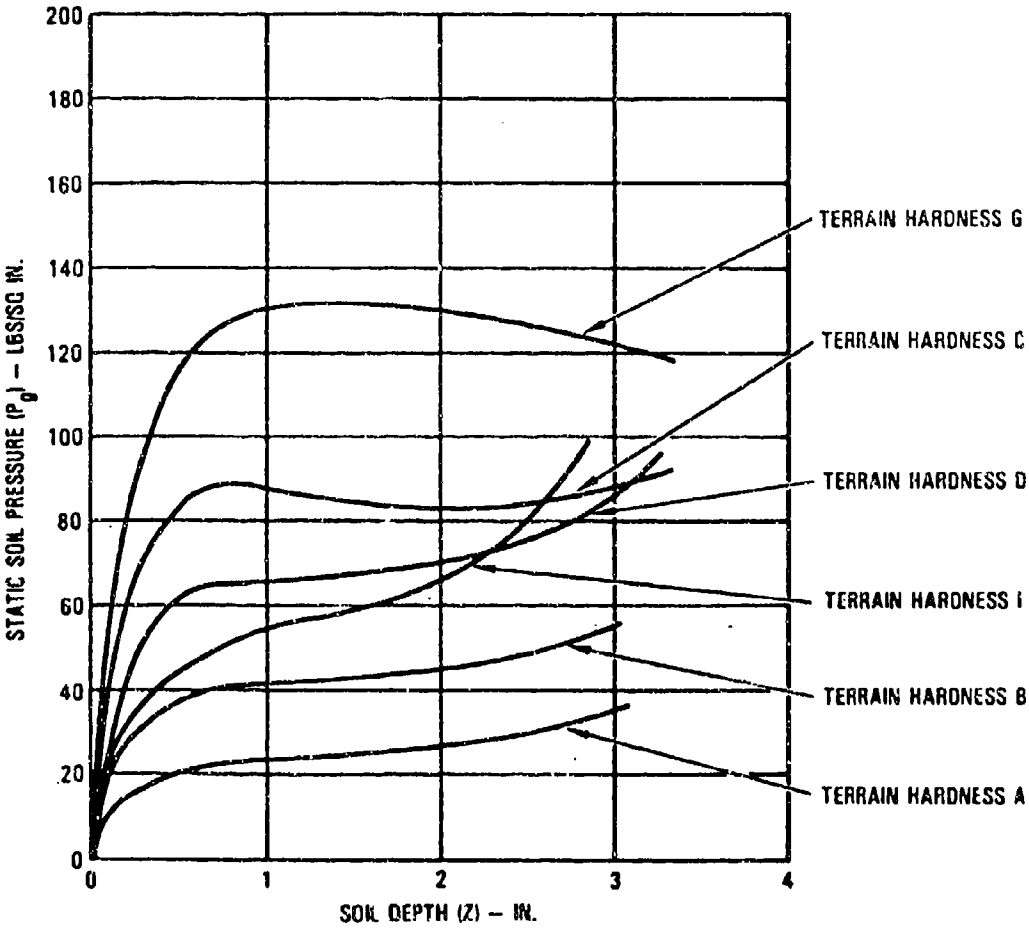

NOTE: THE TERRAIN HARDNESS SCALE IS AN ARBITRARY SCALE ESTABLISHED IN REFERENCE (2). SOIL TESTS TO DETERMINE CBR VALUES WERE NOT CONDUCTED, AND A GENERAL METHOD OF TRANSFORMATION BETWEEN PENETROMETER VALUE WHICH ESTABLISHED THE ABOVE CURVES AND CBR UNITS DOES NOT EXIST

Figure B-5. Static Soil Pressure Curves (Reference 2)

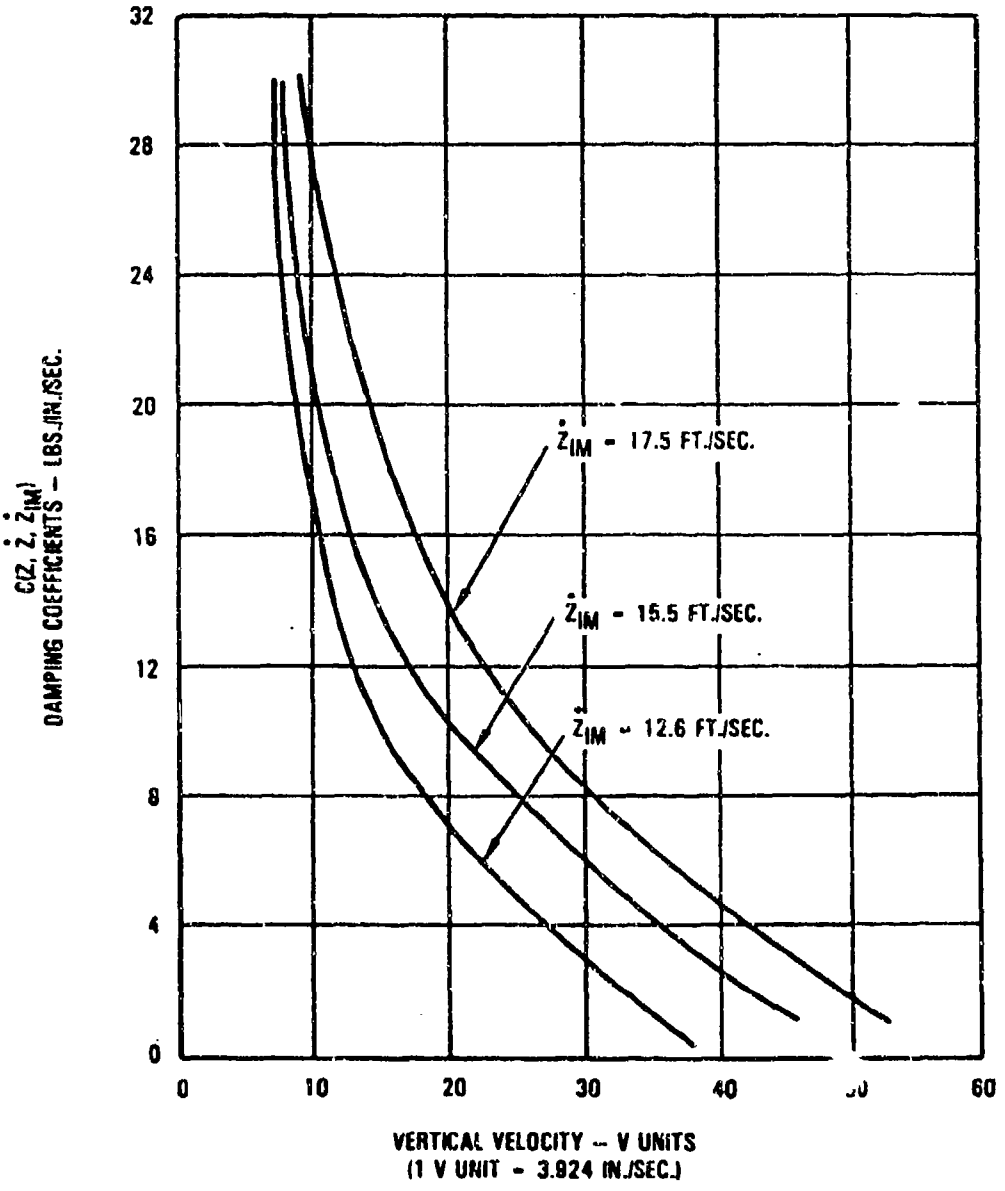

Figure B-6. Soil Dynamic Damping Coefficients for Terrain Hardness B (Reference 2)

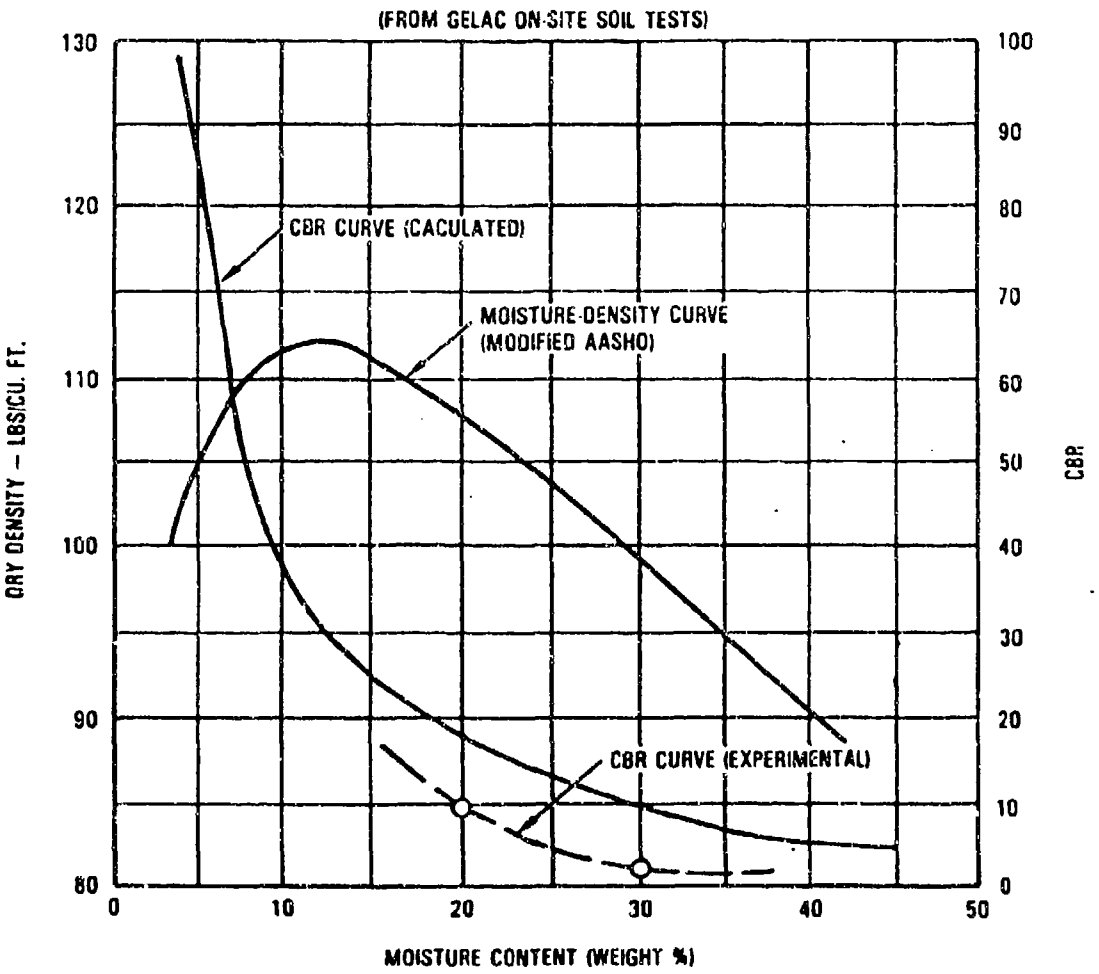

Figure B-7. Subsoil Properties - CBR and Dry Density vs Moisture Content (Reference 27)

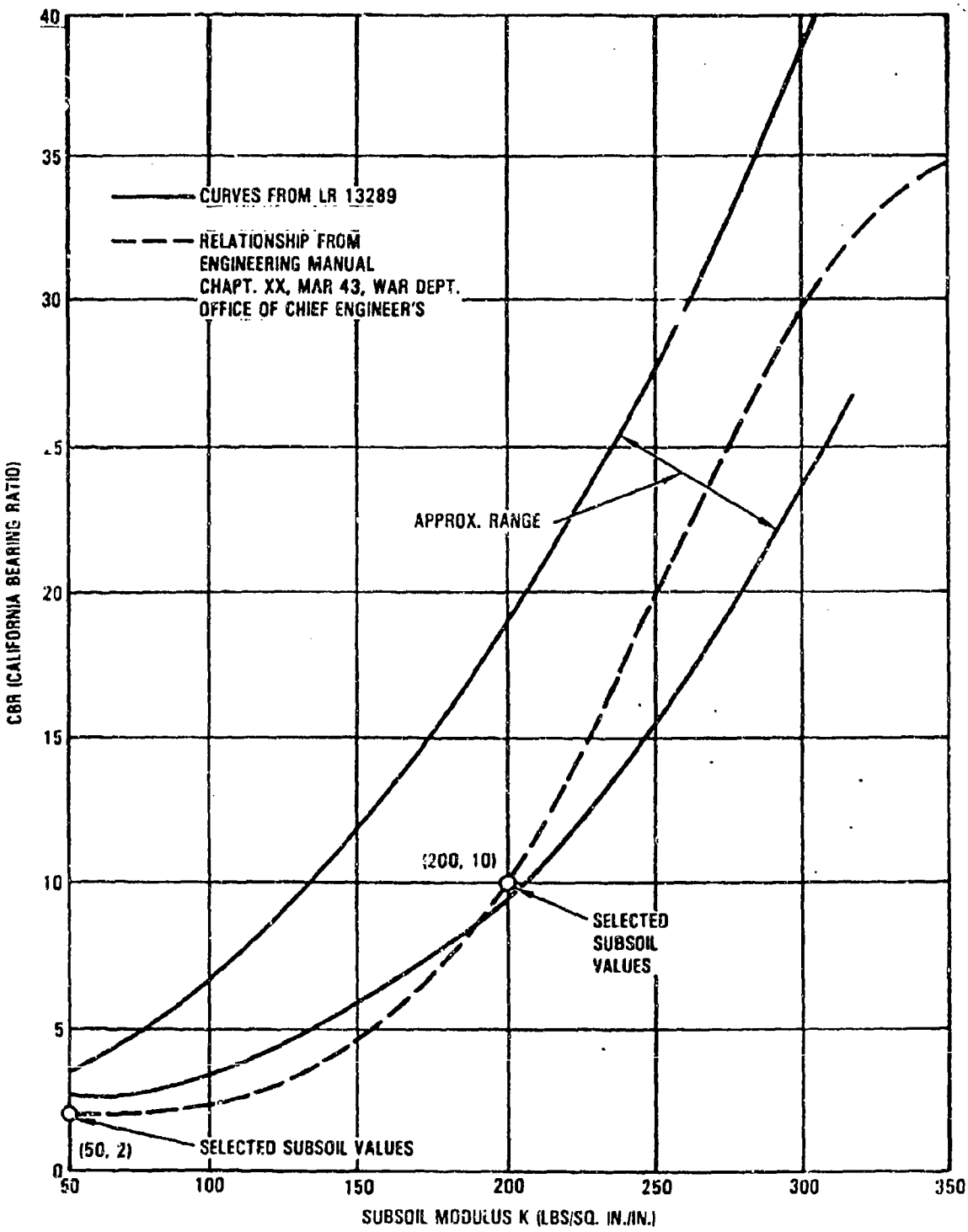

Figure B-8. CBR and Subsoil Modulus Relationship (Reference 27)

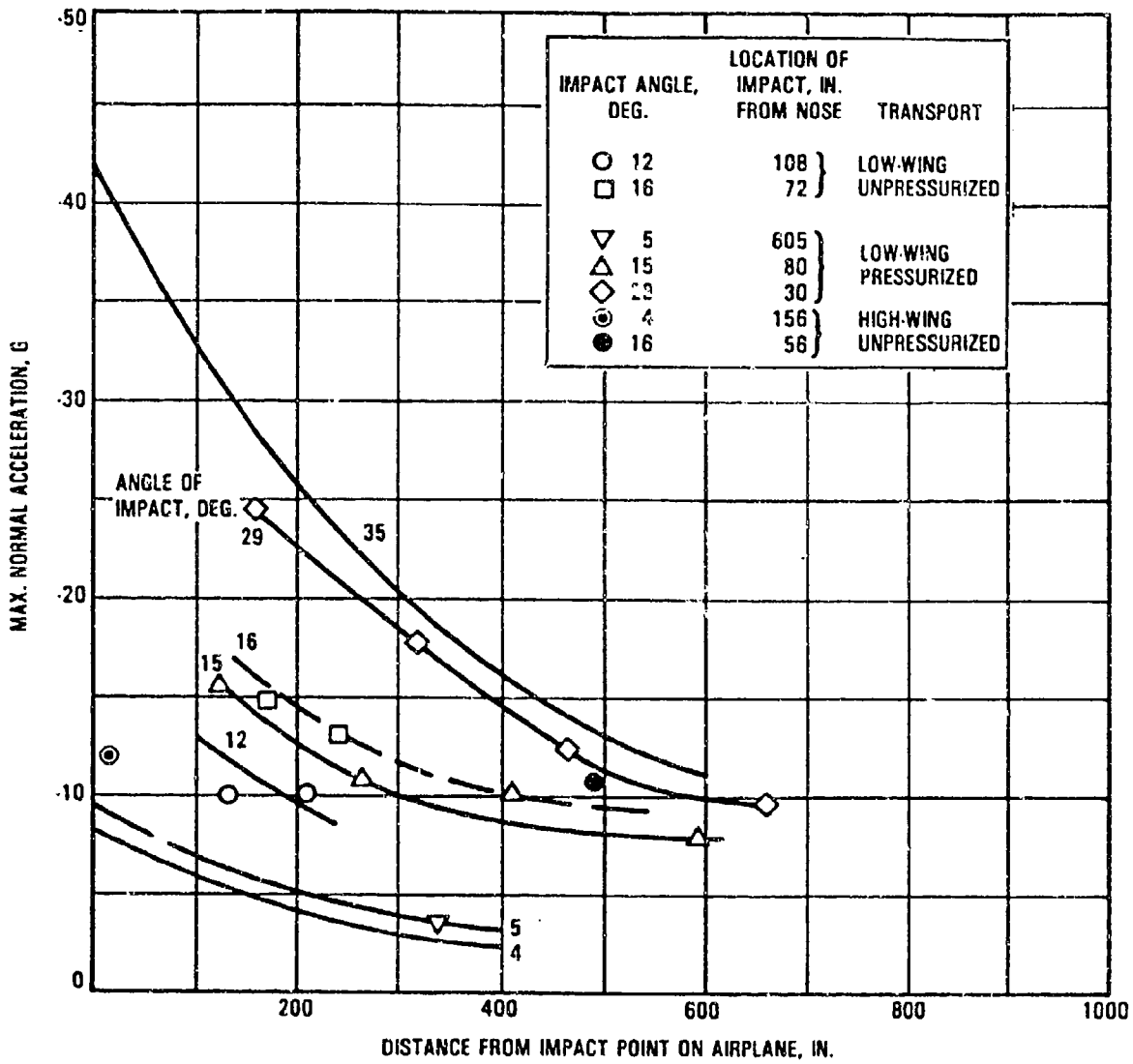

Figure B-9. Effect of Position in Airplane and Airplane Configuration on Maximum Normal Acclerations During Unflared Landing Crases (Impact Velocity Corrected to 95 mph) (Reference 22)

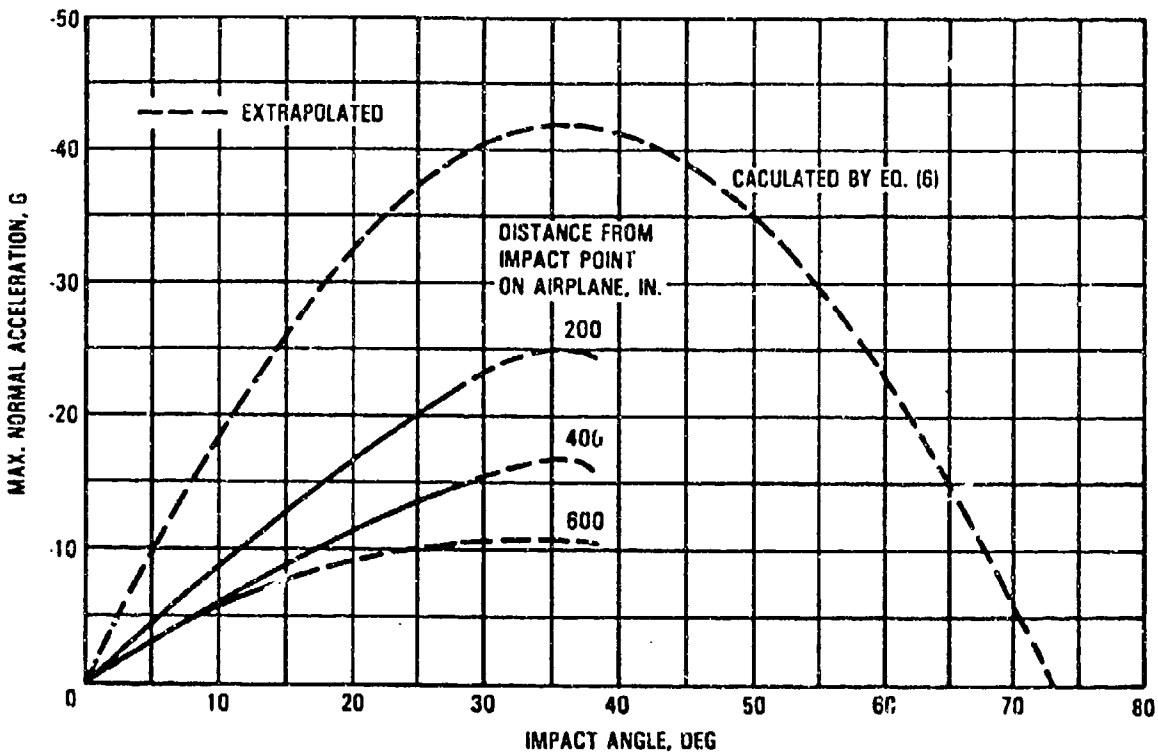

Figure B-10. Comparison of Calculated and Experimental Values for Maximum Normal Acceleration at Various Impact Angles (Impact Speed Corrected to 95 mph). (Reference 22)

☆U.S. GOVERNMENT PRINTING OFFICE: 1993 - 704-078/60211